

About the domino problem in the hyperbolic plane, a new solution.

Maurice Margenstern

---

Publications du LITA, N° 2007-102

Service de reprographie de l'U.F.R. M.I.M., Université de Metz

---

Laboratoire d'Informatique Théorique et Appliquée, EA 3097 Université de Metz  
Directeur de la publication : Maurice Margenstern

# About the domino problem in the hyperbolic plane, a new solution

Maurice Margenstern,  
Université Paul Verlaine – Metz,  
LITA, EA 3097, IUT de Metz,  
Île du Saulcy,  
57045 METZ Cédex, FRANCE,  
*e-mail: margens@univ-metz.fr*

January 23, 2007

## Abstract

In this paper, we improve the approach of the previous paper about the domino problem in the hyperbolic plane[8, 9]. This time, we prove that the general problem of tiling the hyperbolic plane with *à la* Wang tiles is undecidable.

## 1 Introduction

The question, whether it is possible to tile the plane with copies of a fixed set of tiles was raised by Wang, [14] in the late 50's of the previous century. Wang solved the *partial* problem which consists in fixing an initial finite set of tiles: indeed, fixing one tile is enough to entail the undecidability of the problem. The general case, later called the **general problem** in this paper, without condition, in particular with no fixed initial tile, was proved undecidable by Berger in 1964, [1]. Both Wang's and Berger's proofs deal with the problem in the Euclidean plane. In 1971, Robinson found an alternative, simpler proof of the undecidability of the general problem in the Euclidean plane, see [12]. In this 1971 paper, he raises the question of the general problem for the hyperbolic plane. Seven years later, in 1978, he

proved that in the hyperbolic plane, the partial problem is undecidable, see [13]. Up to now, and as far as I know, the general problem remained open.

In this paper, we give a proof that the general problem is also undecidable in the case of the hyperbolic plane. This paper improves a previous paper where the so called "generalized origin-constrained" problem was proved undecidable. In the setting of that paper, the set of origins of computations is infinite but is not dense in the hyperbolic plane, so that it is not the general problem. It is more general than the origin-constrained problem solved by R. Robinson in his 1978 paper, see [13].

Our present proof turns out to have important similarities with the proofs of Berger and Robinson. However, it is more complex for what is the definition of the starting grid which is simply a square grid in the case of the solutions for the Euclidean plane. Our proof combines basic features of both Berger's and Robinson's proof in the grid of the hyperbolic plane which we indicate. For completeness, we also summarise the whole approach of the proof of the undecidability of the general problem.

In this paper, we intensively use the **mantilla**, the grid which we constructed in our first paper, [8, 9]. We refer the reader to these papers, especially to the technical report [9] where the basic properties are proved. This report is available at the following address:

[http://www.lita.sciences.univ-metz.fr/~margens/hyp\\_dominoes.ps.gz](http://www.lita.sciences.univ-metz.fr/~margens/hyp_dominoes.ps.gz)

Here, we simply remember the construction and the properties which we use. Then, in the second section, we introduce new properties which will allow us to define the general construction of infinitely many finite domains of increasing sizes in which computations can be organized. The description of the domains is dealt with in section 3. Section 4 gives the last features needed to organize the computations and gives the proof of the main theorem of this paper:

**Theorem 1** *The general problem of tiling the hyperbolic plane is undecidable.*

## 2 The mantilla and its properties

The starting point of our construction is the **ternary heptagrid** which we introduced in [2]. It is generated by the regular heptagon with vertex angle  $\frac{2\pi}{3}$  by reflections in its edges and, recursively, of the images in their edges. An illustration is given in the left-hand side picture of figure 4, for instance.

Then, we define two kinds of tiles in this grid, inspired by considerations explained in [9].

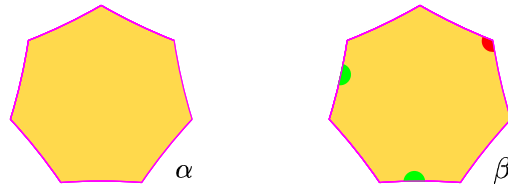


**Figure 1** *The basic tiles of the manitlla.*

## 2.1 The flowers

These tiles can be arranged in special figures which we call **flowers**: they consist in a **centre** which is a tile of the kind ( $\alpha$ ), illustrated by figure 1, and of seven **petals** around the centre, the petals being of the kind ( $\beta$ ), see figure 1. There are several ways to assemble the petals, especially defined by the position of their **red vertex**. We define three kinds of them, called *F*-, *G*- and **8**-flowers, see [9] and figure 2. We remind that the tile ( $\alpha$ ) of figure 1 is prevented to tile the plane by copies of itself only by numbering its sides from 1 to 7, for instance. As no colouring of this kind is possible in the tiling  $\{7, 3\}$ , this gives us a way to fix the assembling of tiles ( $\alpha$ ) and ( $\beta$ ) as flowers, see [9] for an exact description.

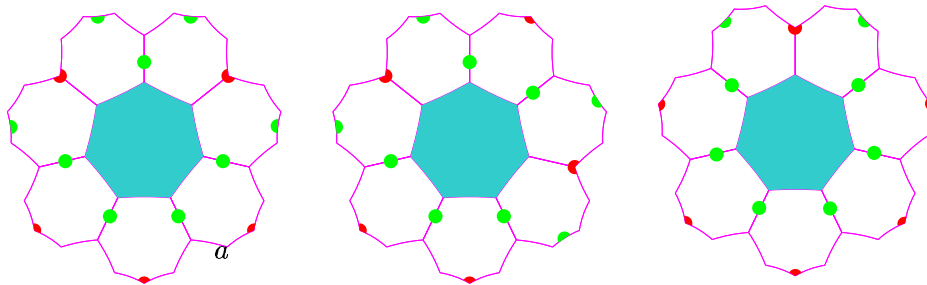


**Figure 2** *From the left to the right: F-, G- and 8 flowers.*

In an **8**-flower, the line of the common edge of two petals sharing the unique red vertex at distance 1 is called the **axis** of the **8**-centre or of the **8**-flower: the reflection in the axis leaves the flower and its centre globally invariant.

From these flowers, we define a splitting of the tiling as suggested by the pictures of figure 3. The splitting is fully described in [9]. Let us remind here

that the domain delimited by the red-vertices of an  $F$ - and  $G$ -flowers define the corresponding  $F$ - and  $G$ -sectors. Such sectors contain the tiles between the two rays starting from the red vertices of their centres, supporting the axes of the closest  $\mathbf{8}$ -centres. By definition, an  $\mathbf{8}$ -sector consists of the four  $F$ -sectors which are adjacent to the five petals around the just mentioned axis.

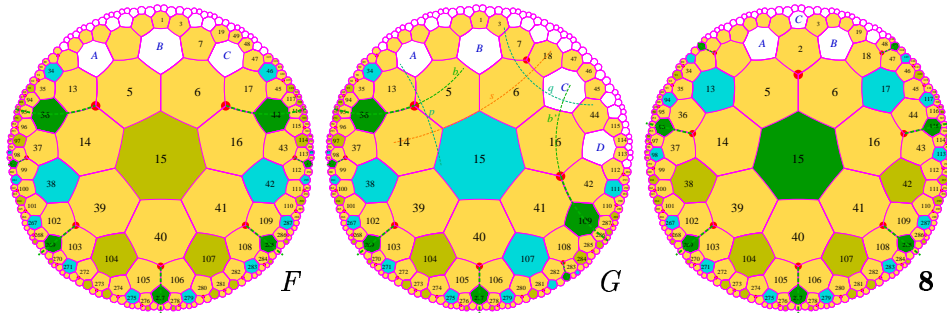


**Figure 3** *Splitting of the sectors defined by the flowers. From left to right: an  $F$ -sector,  $G$ -sector and  $\mathbf{8}$ -sector.*

As proved in detail in [9], there is a finite set of 21 tiles which allows to construct the mantilla.

## 2.2 The trees and the threads

In [9], we introduce trees in the following way. We define the root of such a tree to be an  $F$ -son of a  $G$ -flower: this terminology comes from the splitting. In figure 3, the  $F$ -son of the  $G$ -flower represented in the middle picture of the figure is the yellow centre just below the central  $G$ -centre which is blue. Consider the mid-point  $I$  of the edge  $\sigma$  joining the  $G$ -centre to its  $F$ -son. Let  $K$  be the point of  $\sigma$  in contact with the  $F$ -son. Draw the rays from  $I$  which passes through the mid-points of the two edges which share  $K$  with  $\sigma$ . The edge  $\sigma$  is supported by a line which is an axis of symmetry of the  $F$ -centre. The rays are also symmetric of each other in this axis. Such a tree is represented in the left-hand side picture of figure 4 with a yellow border constituted by the two rays. Later on we shall call them the **trees of the mantilla**, simply, the **trees**. The set of tiles contained or mostly contained between the two rays which define a tree  $T$  is called the **area** of  $T$ , denoted  $ar(T)$ .

As proved in [9], the trees have this important property:

**Lemma 1** *Let  $A$  and  $B$  be two trees of the mantilla. Either both areas are non-intersecting or one of them fully contains the other. By this we mean that the borders of the trees have no common tile.*

We refer the reader to [9] for the proof.

This embedding or independence of the trees allows us to define the notion of **thread**. It consist of a sequence of trees  $\{T_n\}_{n \in \mathbb{N}}$  or  $\{T_n\}_{n \in \mathbb{Z}}$ , such that  $ar(T_{n+1}) \subset ar(T_n)$  for all indices  $n$ , that for any index  $n$ , there is an  $m$  for which  $ar(T_m) \subset ar(T_n)$ , and such that it contains any tree  $T$  of the mantilla for which there are indices  $n$  and  $m$  with  $n < m$  and  $ar(T_n) \subset ar(T) \subset ar(T_m)$ . In all these cases, the inclusion is proper. By proper inclusion, we mean that the borders of  $T_{n+1}$  have no common tile with the borders of  $T_n$ . We say that the thread is an **ultra-thread** when the sequence of indices is  $\mathbb{Z}$ . Consequently, there is no tree of the sequence which contains all the others.

As proved in [9] we have:

**Lemma 2** , *If  $\{T_n\}_{n \in \mathbb{Z}}$  is an ultra-thread, then  $\bigcup_{n \in \mathbb{Z}} ar(T_n)$  is the set of tiles of the whole ternary heptagrid.*

Another lemma proved in [9] says that there is at most one ultra-thread in the mantilla.

As noted in [9] some realizations of the mantilla do not contain an ultra-thread and the others do. In [9] we required the realizations of the mantilla which contain no ultra-thread. Here, we relax this constraint: no hypothesis is put on the realization of the mantilla constructed in the proof.

### 2.3 The harp

Before turning to the new construction, we remind another important structure which we shall adapt for the computation and which was introduced in [8, 9]. It is the **harp** which is used in [8, 9], this figure is used to solve the partial problem with a constrained origin. The problem was proved undecidable by Robinson in [13]. We believe that the solution given in [8, 9] is at least more clear. The harp is defined in an **angular sector** of the ternary heptagrid, see [9, 7] for more details.

The important point to notice with the harp is that it introduces the notion of **verticals** and **horizontal**s. They are important to define the space-time diagram of the execution of the work of a Turing machine on its tape. It is interesting to notice that in the setting considered up to now, this

notion of verticals and horizontals is restricted to the area of a tree. In the following section, we extend this notion to the whole grid.

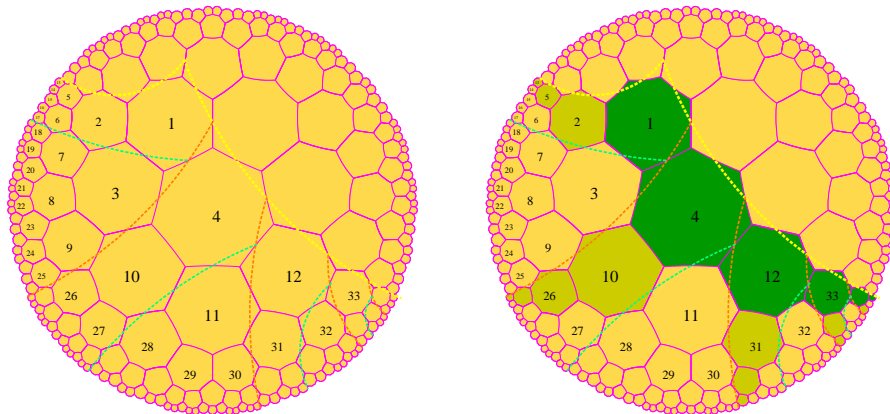


**Figure 4** *The guidelines for the harp.*

### 3 New ingredients

#### 3.1 The levels and the isoclines

In this section, we introduce a new object with respect to [9], the **isoclines**.

In [9], we defined **levels**. Informally, they recursively connect the sons of flowers. By extending the spanning tree of the splitting associated with the flowers we introduced, see [9], it is possible to define a **carpet** structure which is a kind of limit of what we obtain in a tree when the root of the tree is thrown away to infinity. This structure is studied in [7] in the case of the pentagrid and of the heptagrid and we refer the reader to this paper for properties of these tilings and their proofs. As we shall not use these levels, we do not give their formal definition here. Now, the grid admits another notion of **level** induced by the structure of carpet of [7] which comes from the levels of a Fibonacci tree: the set of nodes which are at the same distance from the root, where the distance from the root to a node  $\nu$  is defined by the number of nodes on the path from the root to  $\nu$ .

As noted in [9], these levels are different from those of the mantilla, although they somehow match with them: in particular, applied to a tree of the mantilla, these levels are symmetric as those of the mantilla. But these levels are different: inside a fixed Fibonacci tree, the maximal distance of a level of the mantilla with the Fibonacci level with which it coincides at the borders of the tree is at most linear in the depth of the Fibonacci level



in the tree. However, as defined in [9], these Fibonacci levels have a defect: when we go from a tree to another, the levels do not match, even when the new tree is contained in the other one.

In this paper, we give another construction of the Fibonacci carpet which will solve the problem. If we look at the right-hand side picture of figure 4, we can infer a new splitting of the tree. Considering trees rooted at a black son, call them **black trees**, we can represent an ordinary Fibonacci tree as a stack of black trees. In [9], this decomposition is used to define the **chords** of the harp. Now, if we systematically apply this decomposition, we obtain a sub-family of Fibonacci levels which we call **isoclines** to differentiate them from the general case. Now, the isoclines match from one tree to another: not only when one tree is contained in the other, but also when the areas have no intersection.

The proof of this important property relies on the following statement:

**Lemma 3** *If the  $F$ -son  $\sigma$  of a  $G$ -flower is a black node, all other  $F$ -sons of a  $G$ -flower inside the tree of the mantilla rooted in  $\sigma$  are black nodes. Also, the **8**-centres are always black nodes.*

The proof is obtained by structural induction on the flower structure. It is illustrated by the pictures of figure 5, below.

In the figure, convex arcs cross the tiles. In black nodes, the convex part is turned to the top:  $\frown$ ; and in the white nodes it is turned to the bottom:  $\smile$ . The arcs join mid-points of the concerned edges. In section 4, we shall precisely look at the incidence of figure 5 on the tiles of the mantilla.

An **isocline** is defined as a maximal set of tiles which can be connected by a sequence of such arcs where two consecutive arcs share a common mid-point of an edge.

This proves that the isoclines of different trees match. Indeed, we precisely have:

**Lemma 4** *When an isocline cuts a tree of the mantilla, it cuts its borders at tiles which are equidistant to the root. In particular, the trace of the isoclines inside a tree of the mantilla are the levels of the tree.*

This is clear from the pictures and the lemma in the case of a mantilla with an ultra-thread. In the other case, it is enough to look at the pictures of figure 3. The white  $F$ -centres appear only with **8**-flowers, and the  $F$ -sons of  $F$ -centres, whatever the colour, are again black  $F$ -centres. Moreover, the  $F$ -sons of the same colour, in an  $F$ -flower or in an **8**-flower are on the same isocline.

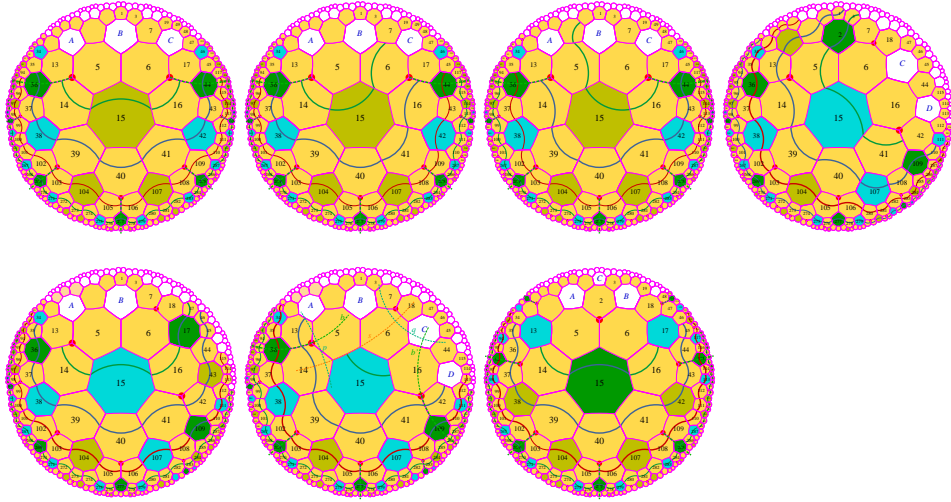


**Figure 5** *The black node property and the levels:  
 first line, from the left to the right: a black  $F$ -centre, two kinds of white  $F$ -centres  
 and a black  $G_r$ -centre;  
 second line: a black  $G_l$ -centre, a white  $G$ -centre and a  $\mathbf{8}$ -centre.*

Now, the isocline have also an important property. Indexing the isoclines in a tree by non-negative integers, the root being on the isocline 0, we have:

**Lemma 5** *Let  $T$  be a tree of the mantilla with its root on the isocline 0. There is an  $F$ -son of a  $G$ -flower on the isocline 5 which is within  $T$ .*

The proof is an easy corollary of the pictures of figures 3 and 5. As a corollary of this important property, we have:

**Lemma 6** *Starting from the isocline 4 of an  $\mathbf{8}$ -centre  $A$  on the isocline 0, there are  $F$ -sons of a  $G$ -flowers on all the isoclines. Moreover, up to the isocline 10, there are such nodes at a distance at most 20 from  $A$ .*

Informally, the isoclines are these horizontals for the whole plane which we need for our construction. The verticals are simply the rays which constitute the border of the trees of the mantilla. This may be surprising as, strictly speaking, the verticals we have just defined are rays, not lines. This is a specific situation of the tiling. There can be such verticals in the hyperbolic plane, for instance the lines issued from a common point at infinity. But in this case, these lines cannot give rise to a continuous set of tiles

because of the diameter of a tile. In fact, in the tiling, the trace of such parallel lines are sets of tiles along a ray, and all these rays converge to a common point. This is also the situation of some ultra-threads. Note that there is a realization of the mantilla in which there is a unique line  $\ell$  joining **8**-centres such that all the axes of these **8**-centres are supported by  $\ell$ .

From now on, we number all the isoclines by indices from 0 to 19, periodically. We agree that the isocline  $n+1$  contains the sons of the nodes of the isocline  $n$  for all  $n$ 's and that the sons of an isocline 19 are on an isocline 0. This defines a direction on the isoclines which goes downwards as the indices increase.

Also from now on, due to lemma 5, we give a special rôle to the isoclines with the numbers 0, 5, 10 and 15 which we shall call the **rows of the mantilla**, simply the **rows**. The definition of tiles to perform this organization raises no difficulty. It is enough to propagate the numbering using the carpet structure. The edge to the father bears the sign  $i$  while the edges to the son, and only them, bear the sign  $i+1$ .

Now, we define the **seeds** as the  $F$ -sons of a  $G$ -flower which are on a row. When a seed eventually gives rise to a tree, we shall call it **active**. When this is not the case, we call it **silent**. It is important, already now, to notice that not all seeds will be active. However, anticipating on section 4, we indicate that all seeds of the isoclines 0 are active. For the trees emanating from active seeds, all the properties we have seen for the threads and ultra-threads are true for them, provided the set of all trees is restricted to them.

As an important corollary of lemma 6 and the study of the parental tiles for each kind of flower of [9], we have:

**Corollary 1** *For any tile  $\tau$  of the mantilla, there is an active seed within a ball of radius 30 around  $\tau$ .*

Now, we turn to the basic process of the construction. This process is also used by Berger and by Robinson in their respective proofs. However, the process, although different, is more explicit in Berger's presentation where it is one dimensional, while Robinson directly deals with the two-dimensional extension of the same process. To better understand the process, we look at it from an abstract point of view.

### 3.2 A parenthese on brackets

We shall consider this process from two points of view. In a first sub-section we shall consider the case when the process evolves on the whole line. In a second sub-section, we shall look at what happens if we restrict it to a ray.



Now, assume that we superpose the rows of the generations from 0 to  $2n+1$ . In this superposition, we assume that the blanks and the blue letters are transparent. We are interested in counting the number  $f_n$  of letters inside a red active interval of the generation  $2n+1$  which are not contained in a red active interval of a previous generation. This is illustrated in figure 6. Such letters will be called **free**. Note that, from this definition, the letters which are the ends of a red interval cannot be free.

From figure 6, we notice that  $f_n$  is also the number of letters which can be seen inside a silent red interval of the generation  $2n+1$ , which are not contained in a red active interval of a previous generation. Indeed, silent intervals are equal by construction and, as for active intervals, we get the second one from the first one by a shift of the length of the considered interval. But such a shift is a multiple of twice the length of the similar intervals in the row of a previous generation. Consequently, these shifts change nothing for these rows. Now, figures 6 and 7 allow us to make the counting by induction. In a red active interval  $I$  of the generation  $2n+1$ , we have 2 red active intervals of the generation  $2n-1$ . In  $I$ , outside the smaller red active intervals, we have one silent interval of the generation  $2n-1$  and two halves of such an interval without the middle  $M$ . As the ends of the intervals are never free letters, we have:  $f_n = 2f_{n-1} - 1$ . Accordingly, as  $f_1 = 3$ , we obtain that  $f_n = 2^n + 1$ . And so, we proved:

**Lemma 7** *The number of free letters inside a red interval of the generation  $2n-1$  is  $2^n + 1$ .*

But now, we can also ask the same questions for the blue intervals, considering that now, blank and red letters are transparent and we denote by  $g_n$  the number of red or transparent letters which are visible in a blue interval  $I_n$  of the generation  $2n$  which are not contained in a blue interval of a generation before  $2n$ . As this consists in exchanging the rôles of blue and red, the same recurrent equation holds for  $g_n$  with  $n > 1$ :  $g_n = 2g_{n-1} - 1$ , which has no meaning for  $n = 1$  as  $g_0 = 0$ . Now, it is not difficult to see, by direct computation, that  $g_1 = 1$ . Accordingly, we obtain that  $g_n = 1$  for all  $n > 0$ .

**Lemma 8** *The number of free letters inside a blue interval of the generation  $2n$  is 1 for  $n > 0$ .*

The result of lemmas 7 and 8 explain why we shall consider the red intervals in our construction.

The free letters also have another interesting property in the red intervals.

**Lemma 9** *Let  $a_1, \dots, a_{2^{n+1}}$  be the positions of the free letters in a red interval of the generation  $2n+1$ , the first position in such an interval being 1, the ends being not taking into account. Then  $a_{i+1} - a_i \geq 2$  except for  $i = 2^n$  and  $i = 2^n + 1$  for which  $a_{i+1} - a_i = 1$ .*

The proof is done by induction on  $n$ , the property being already true for the generation 1. Note that in the proof of lemma 7, we had to look at halves of intervals of the form  $]BMR[$ . In such intervals, the central  $M$  is never counted as well as the ends. Accordingly, by induction, the contribution of a half consists of isolated free letters.

We can describe the structure of the red active intervals contained in a bigger red active interval and of the free letters with better precision. First, it is not difficult to see that the free letters come from letters which are already present in the generation 0:

**Lemma 10** *Let  $I$  be a red active interval of the generation  $2n+1$ , with  $n > 0$ . Let  $x$  be a letter  $R, M$  or  $B$  belonging to a blue active interval of the generation  $2m$ , with  $0 < m \leq n$ . Then  $x$  cannot be a free letter.*

The proof relies on the fact that, as  $m > 0$ , its ends are generated by two red active intervals of the generation  $m-1$  and so, these ends cannot be visible. Accordingly, neither  $R$  nor  $B$  of this blue interval cannot be a free letter. Now, as  $m \leq n$ ,  $M$  is an end of a red active interval of a generation  $2p+1$  with  $p \leq n$ . And so, this  $M$  also cannot be a free letter.

Second, the positions of the red active intervals and of the free letters contained in a given active interval are given by the following lemma:

**Lemma 11** *Let  $I$  be a red active interval of the generation  $2n+1$ . Then,  $I$  can be split into its ends, its free letters and a finite set of interval which exactly contains  $2^k$  intervals of the generation  $2(n-k)+1$ . Similarly, if  $J$  is a blue active interval of the generation  $2n$ , then  $J$  can be split into its ends, its unique free letter and a finite set of intervals which exactly contains  $2^k$  intervals of the generation  $2(n-k)$ .*

The proof is based on a recurrent relation which we already met and which is true for any active interval. Let  $H_n$  such an interval of the generation  $n$ . It exactly contains two active interval of the generation  $n-2$ , so that, repeating the argument of the proof of lemmas 7 and 8, we obtain:

$$(*) \quad |H_n| = 2|H_{n-2}| - 2 + 2 \frac{|H_{n-2}| - 3}{2} + 3$$

where  $|H_n|$  is the number of letters contained in  $H_n$ . This relation gives the following induction relation:  $|H_n| - 3 = 4(|H_{n-2}| - 3)$ .

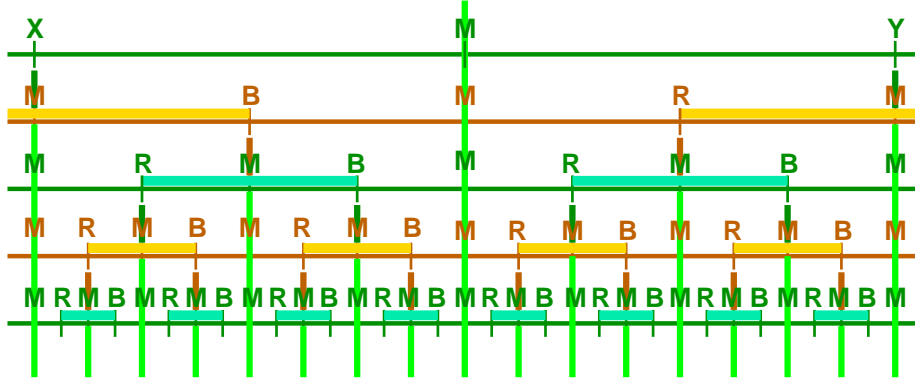


**Figure 7** The silent and active intervals with respect to mid-point lines. The light green vertical signals send the mid-point of the concerned interval to the next generation. The colours are chosen to be easily replaced by red or blue in an opposite way. The ends  $X$  and  $Y$  indicate that the figure can be used to study both active and silent intervals.

For the red active intervals we find  $H_{2n+1} = 4^{n+1} + 1$  and for the blue active ones we find  $H_{2n} = 2 \cdot 4^n + 1$ . But now, we can put again these relations in (\*). In the case of the red active intervals we get:

$$|H_{2n+3}| - 3 = 2(4^{n+1} + 1) + 2(|H_{2n+1}| - 3)$$

From this, by elimination, and taking into account that  $|H_1| = 5$ , we obtain:

$$\boxed{|H_{2n+1}| - 3 = 2^{n+1} + \sum_{k=0}^{n-1} 2^{k+1} (4^{n-k} + 1)},$$

and this gives us the splitting indicated in the statement of the lemma. Using the same argument with blue active intervals, this time we get:

$$\boxed{|H_{2n}| - 3 = 2^{n+1} + \sum_{k=0}^{n-1} 2^{k+1} (2 \cdot 4^{n-1-k} + 1)}.$$

We conclude this sub-section with an additional important information on the silent interval, whose structure is very different from that of the active ones.

Say that a finite sequence  $\{I_k\}_{k \in [0..n]}$  of silent intervals is a **tower** if and only if for each  $k \in [0..n]$ ,  $I_k$  belongs to the generation  $n$  and if the mid-point of these intervals is the same position in  $I_n$  which thus, contains all of

the members of the sequence. Note that if  $\{I_k\}_{k \in [0..n]}$  is a tower, we have  $I_k \subset I_{k+1}$  for all  $k$  with  $0 \leq k < n$ . The common mid-point of the silent intervals of a tower is called the **mid-point** of the tower. The last interval in the tower which contains all of them is called the **area** of the tower.

We have the following lemma:

**Lemma 12** *Let  $I$  be a silent interval of generation  $n$ . The silent intervals which it contains or intersect can be partitioned into finitely many towers. The set of the mid-points of these towers contains the mid-point of  $I$ . For generations  $n \geq 2$ , it also contains the both ends of  $I$ . At last, for the towers which are contained in  $I$  and whose mid-point is not that of  $I$ , their area belong at most to the generation  $n-2$  and their mid-points are ends of proper intervals of  $I$ .*

The proof of this lemma is simply by induction on the generation to which  $I$  belongs. It can be illustrated by figure 7.

This gives a simple algorithm to construct the active and silent intervals generation after generation, considering that each generation is put on another line which we call **layer**.

Initial step:

$n := 0$ ;

the current layer is the layer  $n$ ; the active and silent intervals of this generation are determined.

Induction step:

- i)* The mid-point of the active intervals of the generation  $n$  which are determined on the layer  $n$  send a red signal to the layer  $n+1$ : it is the current **end signal** which consists of two kinds of signal. Each second signal is called  $R$  and the others are called  $B$ , the initial  $R$  being taken at random.
- ii)* The mid-point of the silent intervals of the generation  $n$  send a light green signal to the further layers: it is the current **mid-point signal**.
- iii)* The layer  $n+1$  stops the end signals. The  $R$ -signals define the beginning of an active interval of the generation  $n+1$  and the next  $B$ -signal received on the layer defines the terminal end of the considered active interval. The end signals are absorbed by the layer  $n+1$ . The complement intervals are the silent intervals of the generation  $n+1$ . The current mid-point signals which meet the mid-point of a silent interval go on to the next layer.



The current mid-point signals which reach the mid-point of an active interval will emit the end signal of the next generation.

*iv)  $n := n+1$ ;*

**Algorithm 1** *The algorithm to construct the active and silent intervals, generation after generation.*

We shall go back to this algorithm in the next sub-section.

We conclude this sub-section with a look at the possible realizations of the abstract brackets. From now on, such a realization will be called an **infinite model** of the abstract brackets, **infinite model** for short. At each generation, we have two choices for defining the position of the active intervals of the next generation. Accordingly, this yields continuously many infinite models, even if we take into account that if we fix a position which we call 0, there are countably models which can be obtained from each other by a simple shift with respect to 0. However, the different models do not behave in the same way if, for instance, we look at the towers of silent intervals. In this regard, we have two extremal models. In one of them, 0 is the mid-point of an infinite tower of silent intervals. As this model is symmetric with respect to 0, we call it the **butterfly model**. In another model, 0 is always the mid-point of an active interval of each generation. This model is also symmetric with respect to 0. We call it the **sunset model**.

As we shall later have to deal with the butterfly model, let us sketchily describe it.

To do so, we give numbers to the positions of the letters of the generation 0. We take the mid-point of the infinite tower of silent intervals as position 0. The number of the other positions, call them the **addresses**, are immediately defined in  $\mathbb{Z}$ . We shall define the **size** of an interval as the absolute difference between the addresses of its ends. It is not difficult to check that the size of an interval of the generation  $n$  is  $2^{n+1}$ . Indeed, from the construction of the abstract brackets, the size of an interval at the generation  $n+1$  is twice the size at the generation  $n$ . Now, the  $R$ 's at the generation 0 have addresses  $1+4k$  while the  $B$ 's of the same generation have addresses  $3+4k$ ,  $k \in \mathbb{Z}$ . We notice that the mid-points of active intervals have thus addresses  $2+4k$  while those of silent intervals have addresses  $4+4k$ . Now, let  $a_n$ ,  $b_n$  and  $c_n$  respectively be the addresses of the  $R$ , the  $B$  and the  $M$  of an active interval  $I_n$  of the generation  $n$ . Let  $d_n$  be the address of the  $M$  which follows the  $B$  at the address  $b_n$ . This  $M$  is the mid-point of the silent interval which is the right-hand side neighbour of  $I_n$ . If we denote the size of  $I_n$  by  $\|I_n\|$ , then  $b_n = a_n + \|I_n\|$ ,  $c_n = a_n + \frac{\|I_n\|}{2}$

and  $d_n = c_n + \|I_n\|$ . As  $\|I_n\| = 2^{n+1}$  and  $a_{n+1} = c_n$  in the butterfly model, we get  $a_{n+1} = a_n + 2^n$  which, with the initial condition  $a_0 = 1$ , gives us  $a_n = 2^n + 2^{n+1}k$ ,  $b_n = 3 \cdot 2^n + 2^{n+1}k$ ,  $c_n = 2^{n+1} + 2^{n+1}k$  and  $d_n = 2^{n+2} + 2^{n+1}k$ . In particular, if  $I_{n_1}$  is the active interval of the generation  $n$  for which  $a_n$  is the smallest positive number, we have  $a_{n_1} = 2^n$ ,  $b_{n_1} = 3 \cdot 2^n$ ,  $c_{n_1} = 2^{n+1}$  and  $d_{n_1} = 2^{n+2}$ . Note that  $a_{n_1}$  also gives the address of the left-hand side end of the silent interval with the smallest positive address in the sunset model.

First, we have the following 0-1 property for the infinite models:

**Lemma 13** *Consider an infinite model of the abstract brackets. We have the following alternative: either for any position  $x$ ,  $x$  belongs to finitely many active intervals or, for any  $x$ ,  $x$  belongs to infinitely many active intervals.*

The proof relies on the fact that if  $x$  belongs to finitely many active intervals, there is a layer  $n$  such that if  $x$  belongs to an interval of the generation  $m$  with  $m \geq n$ , then the interval is silent. Let  $I$  be the silent interval of the generation  $n$  which contains  $x$ . Then, it is plain that the tower to which  $I$  belongs is infinite. Otherwise, there would be an active interval containing  $x$  and belonging to a generation  $k$  with  $k > n$ , a contradiction. Now, as an infinite tower is unique when it exists, the property holds for any position.

### 3.2.2 The semi-infinite case

Now, we consider what happens if we cut the result of the previous process, as illustrated by figure 7 at some position.

To simplify things, we take the  $M$  of a silent interval of the generation 0. We imagine a vertical line  $\delta$  starting from  $M$ , the layers being horizontal, and we say that  $\delta$  cuts all the layers. By definition, we forget what happens on the left-hand side of  $\delta$  and we look only at what remains on the right-hand side. Moreover, all active intervals which are cut by  $\delta$  are removed. What remains will be called a **semi-infinite model**

There are a lot of realizations of the semi-infinite model. Say that when a position is contained by an active interval, it is covered by this interval.

Consider an infinite model of the abstract brackets, fix a position  $x$  and focus on the semi-infinite model defined by the cut at  $x$ . Then we have:

**Lemma 14** *Consider an infinite model of the abstract brackets and the position  $x$  of a cut. In the semi-infinite model defined by the cut at  $x$ , for any position  $y$  after  $x$ ,  $y$  is covered by finitely many active intervals.*

The proof is straightforward from the following property:

**Lemma 15** *Consider an infinite model of the abstract brackets and the position  $x$  of a cut. Let  $y$  a position with  $x > y$  and assume that in the model, any position is covered infinitely many often. Then, there is an active interval  $I$  which contains both  $x$  and  $y$ .*

From lemma 15, the proof of lemma 14 is easy: as active intervals of the same colour are either disjoint or imbedded, if an active interval  $I$  contains both  $x$  and  $y$ , this is also the case for any active interval  $I$  which contains  $I$ . This rules out all the active intervals of the same colour and of later generations which contain  $y$ . For the other colour, either all active interval containing  $y$  do not contain  $x$  or at least one of them also contains  $x$  and so, we have the same conclusion for intervals of the other colour. Note that it is not difficult to construct infinite models where 0 is covered by infinitely many blue active intervals and by no red active interval.

Now the proof of lemma 15 is not difficult. From one generation to the next one, the length of an interval gets twice bigger. This means that if  $y \in I_n$ , where  $I_n$  is an active interval of the generation  $n$ , then  $]y - \frac{\|I_n\|}{2}, y + \frac{\|I_n\|}{2}[$  is contained in  $K_{n+1}$ , the interval of the generation  $n+1$  which contains  $y$ . As infinitely many active intervals contain  $y$ , we may assume that  $\|I_n\| > 2|y-x|$ . Accordingly,  $x \in K_{n+1}$ . If  $K_{n+1}$  is active, we are done. If not,  $K_{n+1}$  belongs to a tower of silent intervals which cannot be infinite, by the assumption of the lemma. Now, by construction of the model, the area of a tower is contained in an active interval of the next generation. And so,  $K_{n+1}$  is contained in an active interval which, thus, contains both  $x$  and  $y$ . And so, both lemmas are proved.

Deep results on the space of all these realizations are given by an accurate analysis to be found in [5]. The interested reader should have a look at this paper.

Before describing the computing domains, we shall make another intermediate step: from abstract brackets, we shall construct interwoven triangles which we define in the next sub-section.

We construct these triangles in a kind of tiling in the Euclidean plane with square tiles, all of the same size. Then, we shall see how to define tiles for constructing these triangles. The next step will be to implement these tiles in the heptagrid, which will turn out to be not that trivial. Some tuning will be needed due to specific features involved by the hyperbolic plane and by the mantilla.

### 3.3 Interwoven triangles

In the Euclidean plane, we fix a vertical line which we call the **axis**. Then, we define equidistant lines, perpendicular to the axis which we call the **rows**. We number by the elements of  $\mathbb{Z}$ . By definition, the numbering increases as we go downwards through the rows.

Our goal is to repeat the bracket construction on triangles which will be isoceles. Intervals of the previous sub-section are the projections of the triangles on the axis. There will be blue and red triangles and triangles of the same generation are equal. We want the same connection between triangles as between brackets. We can visualize this as displayed by figure 8.

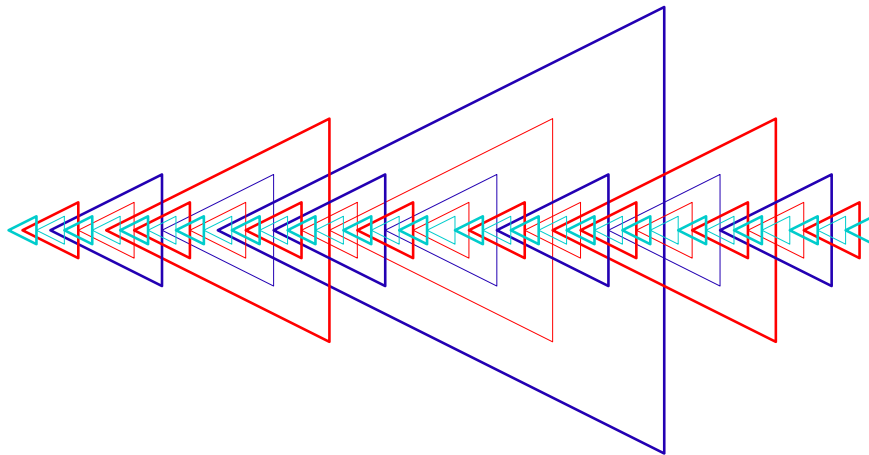


**Figure 8** *An illustration for the interwoven triangles.*

The layers of algorithm 1 can be considered as parallel lines lying in the same plane  $\Pi$ . We can imagine that each layer is the intersection of a plane which is orthogonal to  $\Pi$ . Say that these planes are vertical. Now, we consider that the triangles of a generation are in the vertical plane defined by the layer. In this setting, the intervals on a layer are the projections of the triangles of the plane and the red triangles are projected on the red intervals and the same for the blue triangles with the blue intervals. If we orthogonally project all these planes on the first one, we get the interwoven triangles. Now, note that, here also, we shall distinguish between the triangles whose projection is an active interval and those whose projection is silent. The formers are simply called **triangles** while the latters are called **phantoms**. For properties which are common to both triangles and phantoms, we shall

speak of **trilaterals**. By definition, the **status** of a trilateral indicates whether it is a triangle or a phantom.

We can now transfer the principles of algorithm 1 to this setting in order to obtain another algorithm, allowing to construct the trilaterals. This algorithm will be at the basis of our construction for the solution of the general problem.

Initial step:

- i)* Put the vertex of a blue triangle on the intersection of each line  $4n + 1$ ,  $n \in \mathbb{Z}$ , with the axis. The basis of the corresponding triangles are on the lines  $4n + 3$ , and the height of each triangle lies on the axis. Each triangle is uniquely determined by  $n$ . This is the generation 0 of triangles. The phantoms of the generation 0 are determined by the same lines. But the vertex of a phantom is a line  $4n + 3$  while its basis is on the following line  $4n + 5 = 4(n+1) + 1$ .
- ii)* Call **mid-distance line** the line  $4n+2$  for a triangle and the line  $4n$  for a phantom. Call **mid-point** of an interwoven triangle the intersection of the mid-distance line with the axis. Of course, the mid-point of an interwoven triangle is not its isobarycentre.

Induction step:

- i)* The construction of the trilaterals of the generation  $n$  is completed. In particular, we know the mid-distance line of each of them. The trilaterals of an even generation are blue. Those of an odd generation are red. All trilaterals of the same generation can be generated by taking one of them and shifting it along the axis by repeating an appropriate displacement, say  $d_n$ .
- ii)* Take at random a triangle of the generation  $n$  and denote it by 0. The next triangle of the same generation on the axis, downwards, is denoted by 1 and so on. Similarly, negative numbers are used upwards. The mid-distance lines of the trilaterals of the generation grow outside the trilateral, bearing a green signal. They also grow as a basis of a triangle in the triangles of the generation  $n$  with an odd index, as a basis of a phantom in the triangles of the generation  $n$  with an even index. The mid-point of the triangles with an even index emit legs of the triangles of the generation  $n+1$ . The mid-point of the triangles with an odd index emit legs of the phantoms of the generation  $n+1$ . The legs of the trilaterals of the generation  $n+1$  is parallel to the legs of the trilaterals of the generation  $n$ . The

legs grow until they meet the nearest mid-distance line, bearing a green signal. Afterwards, they grow until they meet the nearest basis. When the legs meet the green signal, they stop it if they are legs of a triangle and they let it grow outside the trilateral which they define when they are legs of a phantom. In all cases, the basis signal which accompanies a green signal goes on after meeting the legs.

iii)  $n := n+1$ ;

**Algorithm 2** *The algorithm to construct the trilaterals.*

Note that the trilaterals are constructed as isocetes triangles, with their heights supported by the axis and with their legs, parallel to the legs of the trilaterals of the generation  $n$ . We also notice that the distance between two consecutive trilaterals of the generation  $n+1$  and of the same kind is now  $d_{n+1} = 2d_n$ . By definition, the trilaterals of the generation  $n+1$  have a colour which is opposite to the colour of the trilaterals of the generation  $n$ . By definition, red and blue are opposite of each other. Also note that the mid-distance signals of the generation  $n$  whose green part is stopped by a triangle of the generation  $n+1$  grow outside this triangle: either as a basis of a triangle or a phantom of the generation  $n+2$ .

Now, we note the following property:

**Lemma 16** *The triangles of the generation  $n+2$  do not meet the triangles of the generation  $n$ . Accordingly the area of a triangle of the generation  $n$  is contained in the area of some triangle of the generation  $n+2$ .*

The proof comes from the same property for the active intervals. If the triangles would meet, their intersection would produce an intersection of the projections.

Note that the property does not hold for the phantoms. For the phantoms, we can collect them into towers, exactly as this was done for the silent intervals. We have:

**Lemma 17** *The phantoms of a tower have the same mid-point. This mid-point may be the vertex of a triangle or the mid-point of a basis of a triangle. In a tower, the colours of the phantoms it contains alternate.*

Note that the green-signal of the mid-distance line of a phantom goes on outside the phantom as long as it meets legs of phantoms. It can be stopped only by the legs of a triangle. There can be realizations of the trilaterals

where such a line never meet the legs of a triangle. This corresponds to the butterfly model in terms of the intervals obtained by projection of the triangles on the axis. If this is the case, this happens for one mid-distance line only, and so there is a unique realization with this property, up to the colour of the basis which accompanies the green signal.

It does not follow from lemma 16 that the triangles cannot meet. In fact triangles of different colours may meet. From the very construction given by algorithm 2, a given triangle  $T$  meets at least two triangles of the opposite colour and which belong to the previous generation: one around its vertex, the other crossing its basis. For this second triangle, its mid-point is the mid-point of the basis of  $T$ .

Now, the same triangle may meet another one: if its mid-point is the vertex of a triangle  $T_1$  of the next generation,  $T_1$  will meet the basis of  $T$ . Now, if its mid-point is the vertex of a phantom  $P$ , then the mid-distance line of  $T$  also supports the basis of a triangle  $T_1$  of the next generation and this basis meets the legs of  $T$ . And so, a triangle always meets three triangles: two of the previous generation and one of the next one. Note that from the definitions, all the triangles met by  $T$  are of the opposite colour.

And so, when the basis of a **triangle** cuts the legs of another **triangle**, the intersection occurs at the mid-point  $M$  of the legs or at the mid-point between the vertex and  $M$ .

Now, the situation with the phantoms is different as we already noticed. The abstract bracket may help us in this regard. Note that the order from the left to the right corresponds to an inclusion order for the angles associated to the trilaterals attached to the intervals. Namely, if  $x$  and  $y$  respectively are two left-hand side ends of two intervals  $I$  and  $J$ ,  $x$  and  $y$  are associated to vertices  $X$  and  $Y$  of trilaterals  $F_X$  and  $F_Y$  and the angle at  $X$  contains the angle at  $Y$ , provided that  $x < y$ . Of course, this does not mean an inclusion between  $F_X$  and  $F_Y$ . This depends on the relative positions of the other ends of  $I$  and  $J$ , say  $u$  and  $v$  respectively. The connections between the trilaterals are summarized by table 1, below, also see figure 8.

From the tower structure and the position of the mid-points of the towers and the above remark, we can conclude that the phantoms of a tower around the vertex  $V$  of a triangle meet the triangle: the bases of these phantoms will cut the legs of the triangle. But the legs of these phantoms will also meet the basis of the phantom whose mid-point is  $V$ . If the mid-point of the tower is the mid-point  $M$  of the basis of a triangle, we have a dual situation: the legs of the phantoms will cut the basis of the triangle but also the bases of these phantoms will cut the phantom with vertex  $M$ . For the towers inside a given triangle or phantom, we have the same relations with triangles and

phantoms of an older generation due to the position of the mid-point of a tower.

Note that contrary to what happens with triangles, when the basis of a phantom cuts the legs of a triangle, this does not occur at the two points which we noticed. As it can easily be inferred from table 1 and from the proof of lemma 7, see also figure 7, this occurs inside the **first half** of the legs, *i.e.* the part which goes from the vertex of the triangle to the mid-point of the leg. More precisely, it occurs between the vertex and the mid-point of this first half. The same property is also true for a phantom, as the greatest member of a tower might be replaced by a triangle. We may summarize this study by lemmas 18 and 19, below.

$u < y$	$ar(F_X) \cap ar(F_Y) = \emptyset$
$y < u < v$	the basis of $F_X$ cuts the legs of $F_Y$
$v < u$	$ar(F_Y) \subset ar(F_X)$

**Table 1** *The connections between the trilaterals according to the relations between their projections. Remember that  $ar(F)$  is the area of the trilateral  $F$  and that we assume that  $x < y$ .*

**Lemma 18** *Between trilaterals, the crossings occur between legs for one figure and the basis for the other figure.*

**Lemma 19** *A leg of a trilateral is never cut inside the open interval delimited by the mid-distance line and the basis of the trilateral.*

The goal of the next sub-section is to prove the following result:

**Lemma 20** *The interwoven triangles can be obtained by a tiling of the plane which is finitely generated and submitted to the constraint that rotations and symmetries of the prototiles are ruled out.*

### 3.4 Tiles for the interwoven triangles

#### 3.4.1 The background

Our tiles are square tiles, but they are not placed by tessellation. We may imagine them as put in isometric rows and then, we shift all odd rows by half the side of the square.



It is not difficult to imagine tiles forcing this property. We can take copies of the tile of figure 9 as the basic tiles.

In the rows defined by this tiling, each second one will be passive: it will simply transmit signals unchanged in order to define simply the slope of the legs of the triangles. It is not difficult to append a signal to the basic squares in order to recognize the passive rows. Figure 10 indicates a way to obtain this result.

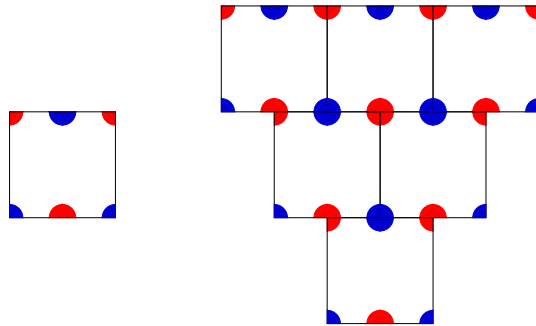


**Figure 9** *An example of a tile forcing the expected display of the squares.*

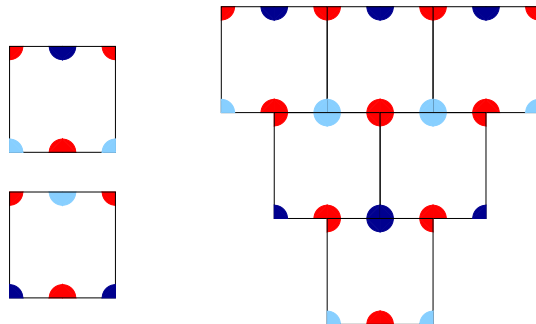


**Figure 10** *An example of a tile forcing the expected display of the squares with a difference between odd and even rows.*

### 3.4.2 Implementation of algorithm 2

Now, we have to translate the construction ruled by algorithm 2 into the tiles we have just introduced in this sub-section. Figures 11, 12, 13 and 14 display the tiles which we propose for the implementation of algorithm 2. The display of the tiles is organized in the following way. First, in figure 11, we display the passive tiles. The tiles are displayed in the following order:

first, triangles and then phantoms. Within both kinds of figures, we order them by colour: first, the first colour blue, which will later be called blue 0, then the second colour blue which will later be called simple blue and then red. This order will also be followed in all the other figures. Also note that triangles give rise to thick signals for their legs and their bases while phantoms give rise to thin signals for the corresponding constituents.

In our study of the interwoven triangles, we remember that we mainly had **horizontal** signals on one hand and **vertical** signals on the other hand. Accordingly, our tiles will have the same property. They will consist in signals, vertical and horizontal ones. The vertical signals are constituents of legs of a trilateral, from the vertices to the corners. Besides the vertices which are realized by bilateral tiles which contain both a left-hand side and a right-hand signal, all other tiles contain at most a single one sided vertical signal. This is why, except for the vertices, tiles with a vertical signal will be presented by pairs: there is a tile with the left-hand side signal and a matching tile with the right-hand side signal. Now, we can look at the different figures, from figure 11 to 14 which present the tiles according to the above indicated grouping and, inside each grouping, according to the order of colours.

The passive tiles convey only vertical signals and they are displayed in section I, in figure 11. The horizontal gray line of the tile is here to remember that it is a passive tile and has no connection with horizontal signals involved by the construction of the triangles. The signal conveyed by a passive tile is always a part of a leg. As there are three colours, two parts for a leg, two sides and two kinds of trilaterals, we have 24 tiles.

The active tiles are displayed in all the figures which we indicated. The display also follows a structural order. The tiles are gathered with respect to the different parts of a trilateral as stemming from lemmas 18 and 19 as well as 16. This is why the grouping of tiles concerns the vertex, the first half of a leg, the mid-point, the second half and, finally the basis in which the corners are distinguished.

Besides the colours of the constituents of the trilaterals, we have four horizontal signals. There is a **green** one to denote the mid-distance lines inside a trilateral. There is a **yellow** one to denote the **free rows** inside a red triangle. There are also a **left-hand side** and a **right-hand side** red signal. These last three signals, the yellow and the two horizontal red ones are used for the detection and the marking of the **free rows**. They concern red triangles only. Red phantoms do not emit such signals. The free rows are also defined by their projections on the axis: they are exactly the free letters of a red active interval. In terms of the tiling itself, this means that

inside a red triangle  $T$ , a free row never meets a red signal, except the legs of  $T$  itself.

Now, let us look at each section of the figures 11 to 14. To facilitate things, we shall number the tiles by the number of its section or sub-section, the number of the line and then the number of the column.

*Tiles for the vertices*

These tiles take into account that a vertex also belongs to the basis of another trilateral. The vertex of a triangle belongs to the basis of a phantom and the vertex of a phantom lies on the basis of a triangle. Now, we have to take into account that the vertex of a trilateral arises on the mid-distance line of a triangle. This line bears a green signal as defined in the previous section. In a red triangle, such a line is also a free row and, accordingly, it also bears a yellow signal.

Now, the triangles of the generation 0 are exceptional, in this regard, as the first generation. This is why we have no green signal with them. Now, as noted in lemma 10, a free row always passes through either the vertex or the basis of a blue triangle of the generation 0. But, of course, the converse is not true: many vertices and bases of triangles of the generation 0 cannot bear a yellow signal as contained in a red triangle of the generation 1. This is why, in figure 11, there are vertices of a blue 0 trilateral with a yellow signal and similar vertices without such a signal.

*Tiles for the first part of the legs*

These tiles correspond to section II*b*, split into section II*b*1 in figure 11, for triangles, and II*b*2 in figure 12, for phantoms.

As noted by lemma 19, these tiles are concerned by the intersections between trilaterals. From lemmas 18 and 16, we know that this part of a leg only is concerned by possible meetings with a basis. Now, we distinguished between the halves of a leg by hues in the same colour. We shall say that there is a **dark** hue of the colour and a **light** one. We associate dark blue 0 and dark simple blue to the first part of a leg of a blue trilaterals, blue 0 being reserved for the generation 0, the light blue 0 and light simple blue are associated to the second half. We associate light red to the first half of a leg of a red trilateral and dark red to the second half.

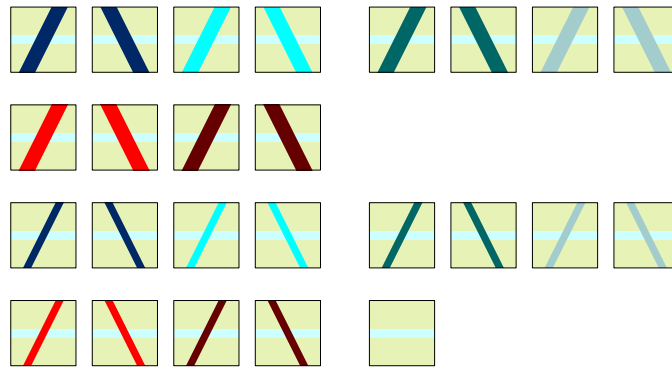
This gives the possibilities displayed by table 2.

The reader may easily check that the tiles of section II*b* gives these possibilities and only them.

However, there are additional properties which have to be fulfilled. When a thick dark blue leg meets a thick red basis, there is no additional signal.

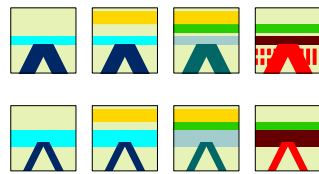
Indeed, this happens within the basis of the corresponding red triangle. Somewhere, this basis gives rise to a phantom, but as a phantom raises no horizontal signal, the intersection does not contain other signals.

I - the passive tiles:



II - the active tiles:

*a* - vertex:



*b* - legs, first part, then mid-distance point, then second part:

*b*<sub>1</sub> - first part of the legs, for triangles:

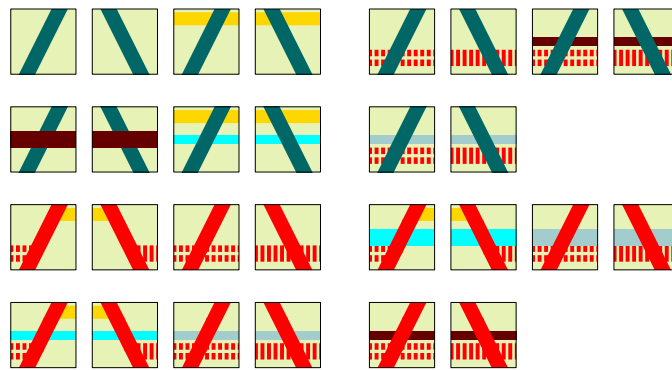
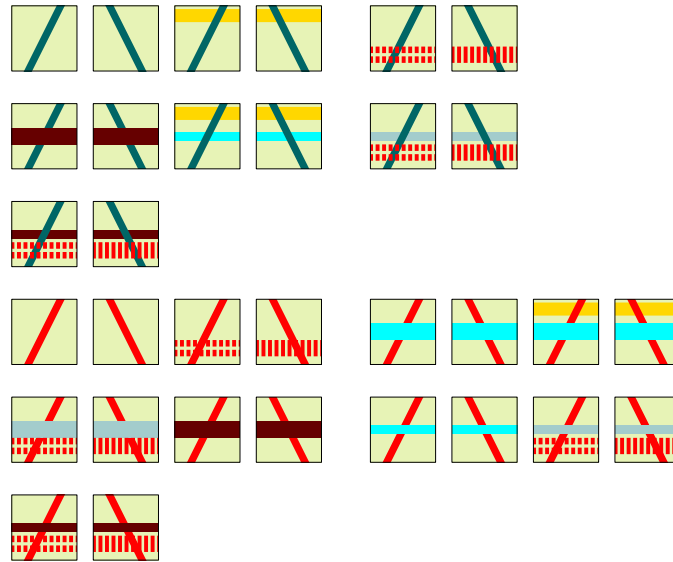


**Figure 11** *The Euclidean tiles for the trilaterals, first part.*

of a red triangle which, by construction, emits red signals, the intersection

contains the trace of the signal. The left-hand side intersection contains

*b2* - first part of the legs, for phantoms:



*c* - mid-point of the legs:

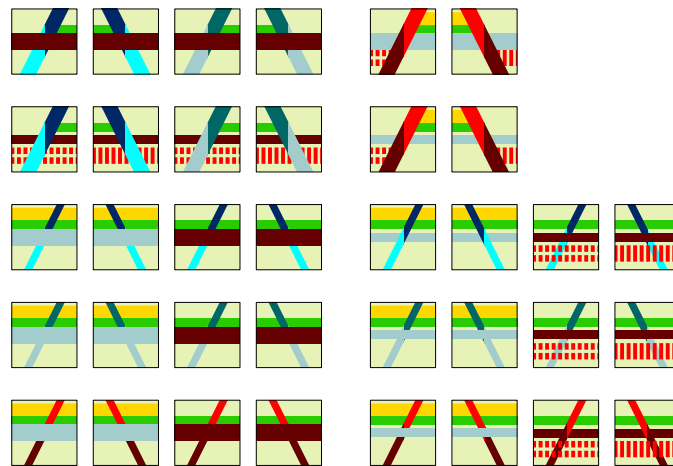


**Figure 12** *The Euclidean tiles for the trilaterals, second part.*

When a thick dark blue leg meets a thin red basis, this means that it

meets the basis of a phantom. As at the mid-point, the basis raises the vertex the left-hand side horizontal red signal and the right-hand side intersection contains the right-hand side horizontal red signal.

main	leg	basis
blue triangle	thick dark	thick dark red any thin
red triangle	thick light	thick light blue any thin
blue phantom	thin dark	any
red phantom	thin light	any

**Table 2** Table of the possible cuts of a the first part of a leg by a basis. In the table, main indicates the trilateral to which the leg signal belongs.

For the intersection of a thick dark blue leg with the basis of a blue phantom, we have to distinguish between the case of blue 0 and simple blue.

In the case of a simple blue, let  $P$  denote the phantom and let  $p$  be its generation. Clearly,  $p > 0$  as  $P$  is simply blue. Now, the basis of  $P$  is generated by a red triangle  $T$  of generation  $p-1$ . As the basis of  $P$  cuts the blue legs, say of a blue triangle  $B$ , the generation  $q$  of  $B$  is greater than that of  $P$ . Now,  $B$  itself is generated by a red triangle  $T_0$  of generation  $q-1$ . Looking at the active intervals which are the projections of the triangles, we have that necessarily  $T$  is contained in  $T_0$  as  $T_0$  contains the first part of the legs of  $P$  and, consequently, the mid-point of the basis of  $P$  which is inside  $T$ . Accordingly, the legs of  $T$  emit a horizontal red signal outside  $T$  on each side of the basis and these horizontal red signals accompany the light blue horizontal signal of the basis of the phantom.

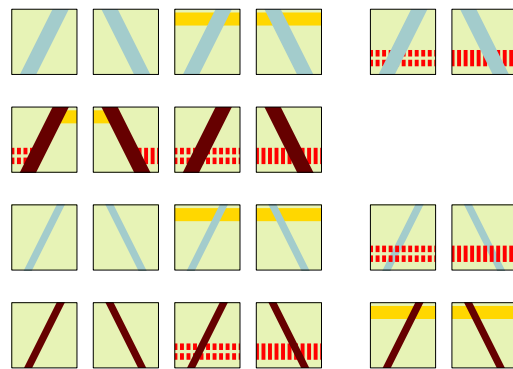
In the case of a blue 0 phantom, this means that the vertex of the blue triangle  $B$  is at the mid-point of the phantom. Accordingly, the corresponding mid-distance line meets a red triangle which generates  $B$ . From lemma 9, the mid-distance line  $\mu$  of a red triangle is a free row and so, this is also the case of the row below  $\mu$  which is the row of the basis of the blue 0 phantom. Hence the corresponding tiles of section IIb.

At last, for the first part of the legs of blue triangles, they may also meet horizontal signals emitted by red triangles: either inside, yellow or red signals or outside, red signals. The first part of the legs may also meet

nothing on a given row, this is why this case has also to be foreseen by the tiling.

For the red triangles, we have similar conclusions for what is the meeting with triangles, blue 0 or simply blue, or phantoms, again of any colour. We already know the reasons for which a blue basis is accompanied with a red horizontal signal. For a red phantom, the above explanation also explain the tiles indicated for section IIb1.

*d* - second part of the legs: for triangles and phantoms



*e* - basis of a triangle or a phantom

*e1* - corners:

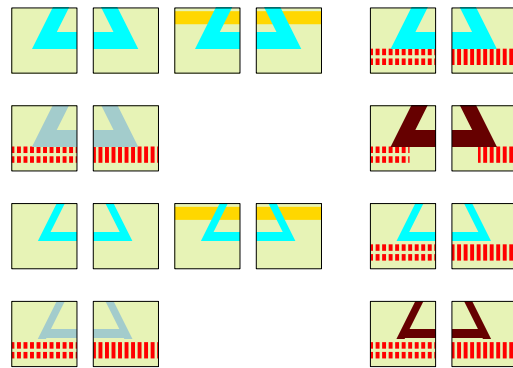


**Figure 13** *The Euclidean tiles for the trilaterals, third part.*

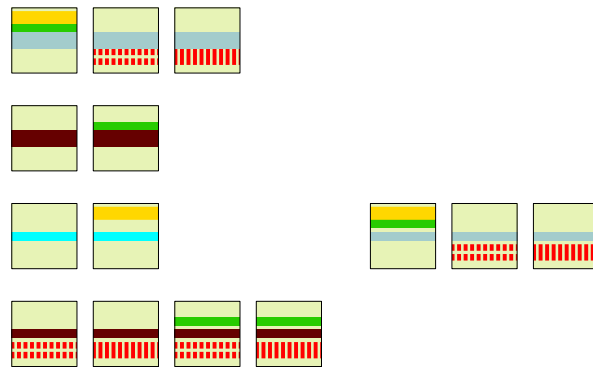
We have to explain the case of a blue 0 trilateral. For a triangle, this

means that the basis belongs to a triangle of the generation 0 and, consequently, that the red triangle belongs to the generation 1 where all the internal rows are free, hence the indicated tiles, both for a triangle and a phantom.

Before turning to the specificities of red triangles, we note that trilaterals in blue 0 colour are not concerned by the cuts which we considered: for them the mid-point only is concerned. This is why we distinguish a colour blue 0, as the generation 0 must follow its pattern which is not yet fixed, contrary to what occurs for the other generations.

Now, the other tiles of the first half of a leg of a red triangle  $T$  are devoted to the detection of the free rows inside  $T$ .

$e_2$  - basis:



$e_3$  - pure communication tiles:

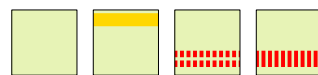


**Figure 14** *The Euclidean tiles for the trilaterals, last part.*

The detection is based on the following principle. The legs of the red triangles and only them, emit a horizontal red signal as already mentioned. This is the rôle of the last two rows in section II.b1, in figure 11. The emitted signals appear in all further sections of figures 12, 13 and 14. For a reason which will soon appear, there are left-hand side red signals, as already mentioned, emitted by a left-hand side leg and right-hand side red signals,



emitted by a right-hand side leg. Once emitted, the signals go out of the triangles which contain them as they are relayed by the legs of red triangles, as indicated by the corresponding tiles. Here, the leg of a triangle contains the vertex and one tile of the basis of the triangle. Accordingly, there will be a tile emitting both signals in the correct direction: it is the tile which contains the vertex of a red triangle. And it will be the single tile with this property.

On another hand, there will be a horizontal free signal, the signal which we already called **yellow**, which is non-oriented and which will run inside the red triangle, along a free row, from its left-hand side leg to its right-hand side one.

It is easy to see that the free signal and the red signals cannot occur simultaneously on a given row inside a triangle. Indeed, if there is a red triangle  $T$  inside the considered triangle  $T_0$ , the vertex, the legs and the basis of  $T$  emit a left-hand side red signal to the left and a right-hand side one to the right. And so, as we rule out tiles combining the yellow signal with a red one, there cannot be both signals.

Now, if there is no part of a red triangle on a given row, there will be no horizontal red signal. But, as there is no third choice, the yellow signal must be drawn. Conversely, if there is a red object on the row, it emits a horizontal red signal, so that the red signalization which will occur on both sides by symmetry of our triangles is forced in this case.

Accordingly, this strategy makes it possible to detect the free rows during the construction of the triangles.

Now, we can deal briefly with the tiles where the vertical signal belongs to the first half of the leg of a phantom. The tiles given in the section IIb2 give all possible cases for the colours, taken into account that blue 0 phantoms do not cut blue 0 triangles: we have simply that the vertices of the ones are on the bases of the others. We note that sometimes a yellow signal accompanies a blue or blue 0 basis, sometimes it is a red horizontal signal. The reason of this configuration has above been explained with the case of the first half of a leg of a blue triangle. The red phantoms give rise to the same discussion: they meet all possible bases. We note that the yellow signal accompanies a basis of a blue 0 triangle but not of a blue 0 phantom: indeed, this means that the red phantom has its vertex inside the blue 0 phantom. The blue 0 phantom is thus inside a tower of phantoms, and its mid-point is also the mid-point of the tower: accordingly, there is no yellow nor red horizontal signal at this level, hence the tiles given in section IIb2.

And so, the tiles of figure 11 and of the section IIb2 of figure 12 allow

all the crossings permitted by lemmas 18, 19 and 16 and only them. In particular, no tile allows a thick dark blue vertical signal to cut a thick light blue horizontal one or a thick light red vertical signal to cut a thick dark red horizontal one.

*Tiles for the mid-points of the legs*

Figure 12 displays the tiles for the mid-points of the legs of the trilaterals: section IIc.

First, we have the case of the triangles. We know that they may give rise to triangles or phantoms. We notice that the red triangles give rise to simple blue trilaterals, never to blue-0 ones as the corresponding tiles do not exist.

For the phantoms, we note the red signals attached to the basis of a red phantom, a situation which we already explained. We also notice the green and yellow signals for a red triangle as the mid-distance row is free.

The second part of section IIc is devoted to the mid-point of the legs of phantoms.

We can see that a blue-0 phantom which crosses a simple blue triangle  $T$  does this at its mid-point and as the mid-point  $M$  of the basis of  $T$  is also the mid-point of a red triangle of the previous generation with respect to  $T$ , the row of  $M$  contains a yellow and a green side inside the red triangle. Now, the mid-point of the red triangle is also the mid-point of the blue-0 phantom, see figures 8 and also 22, whence the tiles. This argument can be repeated *mutatis mutandis* for the case of the mid-point in a simple blue phantom and of a red one.

*Tiles for the second part of the legs*

This part is illustrated by section IIId, in figure 13. It is easier than the first part. Indeed, from lemma 19, we know that the second part of the legs of a trilateral meets no other basis except the one which constitutes the corner of the trilateral with this leg.

Accordingly, we have three pairs of tiles for the simple blue triangles, corresponding to the tiles of the first half which are not concerned by the meeting of a basis. And we have two pairs of tiles for the red triangles: those which are needed for the detection of the free row. From lemmas 7 and 11, we know that in a red triangle, there are as many free rows under the mid-distance row as above. Also, in terms of rows, they are placed in a symmetrical way with respect to the mid-distance row.

The situation for the phantoms is very similar. For the red tiles, there is the case of a leg with no other signal as in the first half of a red phantom.

### *Tiles for the bases: corners and internal part*

Now, we arrive to the bases of the trilaterals. The corresponding tiles are displayed in section IIe in figure 13, for the corners, and in figure 14 for the remaining part of the bases which we call the **internal part** of the bases.

The corners for simple blue trilaterals always bear a horizontal red signal. This is the consequence of the fact that the basis is raised in the mid-point of a red triangle and that the basis goes outside its generating triangle. Accordingly, the signals emitted by the legs of the triangle outside itself accompany the basis. For blue-0 trilaterals, this may occur and this may not. This happens when a blue-0 triangle gives rise to a red triangle of the generation 1. The red signals accompany the blue-0 basis of a phantom in the case of a red triangle of the generation 1 whose vertex is at the mid-point of the phantom, see figure 8. For a red triangle, the tile of the corners are the starting point of the horizontal red signals on the corresponding rows. For the red phantoms, we already know that its basis is always accompanied by a horizontal red signal.

Finally, we arrive to the internal part of the bases. There are two such tiles for blue-0 trilaterals: they are on each side of the vertex of a red trilateral.

For a simple blue triangle, there are two cases: inside the red triangle and then, the tile bears a green and a yellow signals; outside the red triangle and then, the tile bears a horizontal red signal. There are similar cases for a red triangle: inside, there is a horizontal green signal and outside, there is no other signal.

For a blue-0 phantom, it may be on a yellow row, it may be not. The same for a simple blue phantom. When it is with a yellow signal, it is on the mid-distance line, hence it also has a green signal. If it is outside the triangle, it bears the horizontal red signals: one different signal on each side of the red triangle.

Similarly, the red phantoms have always the horizontal red signals as already mentioned several times. Inside the blue triangles which raise their bases, they are on a mid-distance line and so, they bear a green signal.

For completeness, section IIe2 also displays a tile with no signal which is very often used in the tiling of the interwoven triangles, call it the **empty tile**. As already noted, the empty tile alone may tile the plane.

### *A formula representation of the tiles*

Before turning to the proof of lemma 20, we introduce a tool to handle a

huge number of tiles. In section 4, we shall see that the number of prototiles is much number than the number we have in this Euclidean setting. In some sense, the Euclidean situation offers us a school exercise to get convince of the efficiency of the tool, as the figures we have in this section, figures 11, 12, 13 and 14, give us a way to control the validity of the tool.

The tool consists in replacing the graphic representation by formulas which will allow us to control a vast number of tiles. It is not very difficult to see that the tiles we have constructed consist in superposing several patterns, say **elementary patterns** which can be easily defined. These patterns are presented below by figures 15, 16, 17 and 18. In order to represent by formulas the various way with which we assemble these patterns, we give them **names**. As an example, the names for the patterns of the legs, represented by figure 15, are as follows:

$Lb_0tul$   $Lb_0tur$   $Lb_0tbl$   $Lb_0tbr$   $Lb_0\varphi ul$   $Lb_0\varphi ur$   $Lb_0\varphi bl$   $Lb_0\varphi br$   
 $Lb_n tul$   $Lb_n tur$   $Lb_n tll$   $Lb_n tlr$   $Lb_n \varphi ul$   $Lb_n \varphi ur$   $Lb_n \varphi ll$   $Lb_n \varphi lr$   
 $Lrtul$   $Lrtur$   $Lrtll$   $Lrtlr$   $Lr\varphi ul$   $Lr\varphi ur$   $Lr\varphi ll$   $Lr\varphi lr$

a. leg patterns:

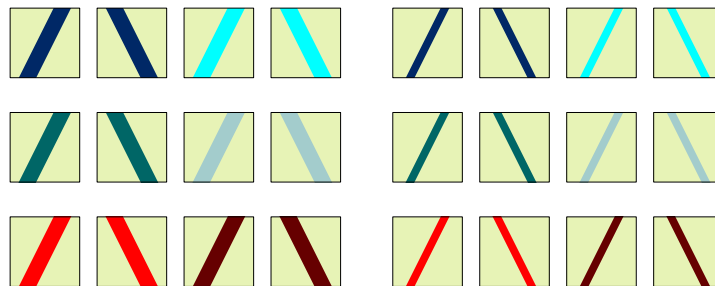


**Figure 15** The elementary patterns to define the legs of triangles and phantoms according to their colour and also taking into account the important difference between the first and the second half of legs.

Similarly, the bases, represented by figure 16, have the following names:

$Bb_nt$   $Bb_n\varphi$   $Bb_0t$   $Bb_0\varphi$   $Brt$   $Br\varphi$

b. basis patterns:

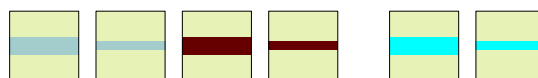


**Figure 16** The elementary patterns for the bases.

Next, we have patterns for joining signals, named as follows and displayed in figure 17.

$V_{b_0t}$	$V_{b_0\varphi}$	$V_{b_nt}$	$V_{b_n\varphi}$	$V_{rt}$	$V_{r\varphi}$
$M_{b_0tl}$	$M_{b_0tr}$	$M_{b_ntl}$	$M_{b_ntr}$	$M_{rtl}$	$M_{rtr}$
$M_{b_0\phi l}$	$M_{b_0\phi r}$	$M_{b_n\phi l}$	$M_{b_n\phi r}$	$M_{r\phi l}$	$M_{r\phi r}$
$C_{b_0tl}$	$C_{b_0tr}$	$C_{b_ntl}$	$C_{b_ntr}$	$C_{rtl}$	$C_{rtr}$
$C_{b_0\phi l}$	$C_{b_0\phi r}$	$C_{b_n\phi l}$	$C_{b_n\phi r}$	$C_{r\phi l}$	$C_{r\phi r}$

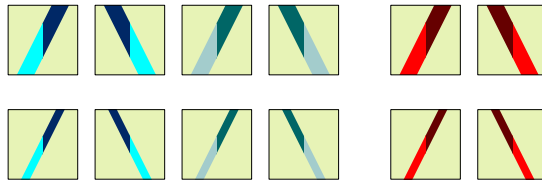
The join group is also important and it introduces a new situation.

d. join patterns:

the vertices:



the mid-points:



the corners:

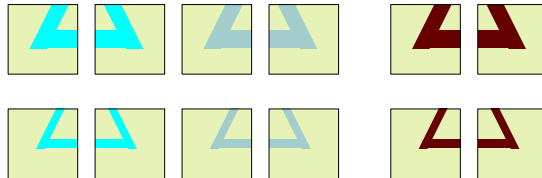


**Figure 17** The elementary patterns for the vertices, for the mid-point of the legs and for the corners.

The patterns of this group can be obtained from the previous ones by means of **operators** which we now define. We introduce four such operators called **masking** operators, denoted by  $\mu_L$ ,  $\mu_R$ ,  $\mu_B$  and  $\mu_T$ , the subscripts meaning *left*, *right*, *bottom* and *top* respectively. The result of  $\mu_X(T)$  is to show the part of the tile  $T$  defined by  $X$ . In this way,  $L$  defines the left-hand

half of  $T$ ,  $R$ , its right-hand half,  $B$  its lower half and  $T$  its upper one. All tiles can be obtained by composition of these operators to the previous signals and an operation of **superposition** of the results. We consider the patterns as opaque under the superposition. In principle, this makes this operation non-commutative. However, in the situations we consider in this report, the difference between  $A + B$  and  $B + A$  is not meaningful. Accordingly, we shall consider the superposition as commutative and, with this convention, it is also associative.

As an example of such a possibility, it is not difficult to see that we can write  $V\gamma\tau = \mu_B(\mu_L(L\gamma\tau ul) + \mu_R(L\gamma\tau ur))$ , where  $A + B$  denotes the superposition of the two tiles  $A$  and  $B$ . In some sense, we can see the names  $V\gamma\tau$  as useful shortcuts for much longer expressions.

We can see that the tiles consist in various ways to assemble vertical and horizontal signals. Most often, the horizontal signals involve a basis. The formulas which we shall soon define indicate which signals may accompany a basis.

c. info patterns:



**Figure 18** *The elementary patterns for the horizontal signals used in the construction.*

Indeed. Consider a basis  $\beta$ . We have a first distinction according to the colour: we know that only blue-0 basis may be accompanied by a yellow signal and that they are never accompanied by a green one. Other bases may be or not accompanied by a horizontal signal. If this is the case, there may be a yellow signal and also a green one, or they are accompanied by a horizontal red signal.

We shall represent these conditions by formulas indicating superpositions. Let  $A$  and  $B$  denote tiles possibly obtained by superposition. We define  $\epsilon_a.A + \epsilon_b.B$  as a superposition whose result may be nothing,  $A$ ,  $B$  or  $A + B$  depending on whether  $\epsilon_a$  or  $\epsilon_b$  are 1 or 0. The tile  $A$ , respectively  $B$ , is present in the superposition if and only if  $\epsilon_a = 1$ , respectively  $\epsilon_b = 1$ . We shall often write  $\epsilon_\alpha$ , for  $\alpha \in \{a, b\}$  as  $\mathbf{1}_{Cond}$  where  $Cond$  is a formula expressing a condition. Note that such a representation can also be used to count how many tiles this produces. Let  $|A|$ ,  $|B|$  be the number of prototiles defined by  $A$ ,  $B$  respectively. Let  $n_a$ ,  $n_b$  and  $n_{a \cap b}$  be the number of cases when  $\epsilon_a = 1$ ,  $\epsilon_b = 1$  and  $\epsilon_a + \epsilon_b = 2$ , respectively. Then, we have

that  $\epsilon_a.A + \epsilon_b.B$  produces  $(n_a - n_{a \cap b}) \times |A| + (n_b - n_{a \cap b})|B| + n_{a \cap b} \times (|A| \times |B|)$  prototiles. Of course, when the conditions are independent, *i.e.*  $n_{a \cap b} = 0$ ,  $\epsilon_a.A + \epsilon_b.B$  produces  $n_a \times |A| + n_b \times |B|$  prototiles. Conformally to this definition, we interpret  $A + \alpha.B$  as  $u.A + \alpha.B$  where  $u$  is always 1.

Now, let us turn to the formulas.

As a very simple exercise, note that the passive tiles convey only vertical signals and that they are simply obtained by the formula  $L\gamma\tau\xi + p$ . We remark that we have 24 tiles.

Next, we define the various configurations of a basis as it may be accompanied by various horizontal signals.

$$(B) \quad B\gamma\tau + \mathbf{1}_{\{\gamma=b_0\}} \cdot \mathbf{1}_{\{\tau=\varphi\}} \cdot \epsilon_y \cdot Hy \\ + \mathbf{1}_{\{\gamma=b_n\}} \cdot (\epsilon_g \cdot (Hg + Hy) + \overline{\epsilon}_g \cdot (\epsilon_y \cdot Hrl + \overline{\epsilon}_y \cdot Hrr)) \\ + \mathbf{1}_{\{\gamma=r\}} \cdot (\epsilon_a \cdot Hg + \mathbf{1}_{\{\tau=\varphi\}} \cdot (\epsilon_l \cdot Hrl + \overline{\epsilon}_l \cdot Hrr))$$

The parameters of this formula are  $\gamma$ ,  $\tau$ ,  $\epsilon_g$ ,  $\epsilon_l$  and  $\epsilon_y$  which are independent. Intuitively, we could define  $\epsilon_g$ ,  $\epsilon_l$  and  $\epsilon_y$  by:  $\epsilon_g = \mathbf{1}_{\{\text{green signal}\}}$ ,  $\epsilon_l = \mathbf{1}_{\{\text{left-hand side}\}}$  and  $\epsilon_y = \mathbf{1}_{\{\text{yellow signal}\}}$ , but they also can be seen as purely formal and independent parameters. Accordingly, we find 14 tiles.

Next, we define the vertices by:

$$(V) \quad V\gamma\tau + B\gamma\overline{\tau} + \mathbf{1}_{\{\gamma=b_0\}} \cdot \epsilon_y \cdot Hy + \mathbf{1}_{\{\gamma=b_n\}} \cdot (Hg + Hy) \\ + \mathbf{1}_{\{\gamma=r\}} \cdot (Hg + Hy + \mathbf{1}_{\{\tau=\varphi\}} \cdot (\mu_L(Hrl) + \mu_R(Hrr)))$$

where  $\overline{\tau}$  is the status, opposite to that of  $\tau$ . Note that  $\epsilon_y$  has the same meaning as in formula (B). In the case of the vertices, we remark that we have three parameters:  $\gamma$ ,  $\tau$  and  $\epsilon_y$ ,  $\epsilon_y$  occurring only when  $\gamma = b_0$ . This gives us 8 tiles.

Then, we define the mid-point tiles of the legs. From the algorithm, we know that the first half of the legs of a triangle meet only a basis of a triangle of the opposite colour. We also know from lemma 17 that the legs of a phantom may meet bases of trilaterals of the same colour, the colour blue-0 being excepted for a basis, as blue-0 trilaterals are not generated by other triangles.

Accordingly, we get the following formula:

$$(M) \quad M\gamma\tau\xi + \mathbf{1}_{\{\tau=t\}} \cdot (B\overline{\gamma}\tau_1 + \mathbf{1}_{\{\gamma \neq r\}} \cdot (Hg + \mathbf{1}_{\{\tau_1=\varphi\}} \cdot Hr\xi) \\ + \mathbf{1}_{\{\gamma=r\}} \cdot (\mu_\xi(Hr\xi) + \mu_{\overline{\xi}}(Hy))) \\ + \mathbf{1}_{\{\tau=\varphi\}} \cdot (B\gamma_1\tau_1 + \mathbf{1}_{\{\gamma_1 \neq r\}} \cdot (Hg + Hy) \\ + \mathbf{1}_{\{\gamma_1=r\}} \cdot (Hg + \mathbf{1}_{\{\tau_1=\varphi\}} \cdot Hr\xi))$$

and, here, we have that the colour of the basis,  $\gamma_1$ , cannot be blue-0.

The counting of the tiles goes as previously. The formula defines 36 tiles.

We define the tiles for the corners in a similar way.

$$(C) \quad C\gamma\tau\xi + \mathbf{1}_{\{\gamma=b_0\}} \cdot \epsilon_a \cdot (\epsilon_y \cdot Hy + \overline{\epsilon_y} \cdot Hr\xi) \\ + \mathbf{1}_{\{\gamma=b_n\}} \cdot Hr\xi + \mathbf{1}_{\{\gamma=r\}} \cdot (\mathbf{1}_{\{\tau=\varphi\}} \cdot Hr\xi + \mathbf{1}_{\{\tau=t\}} \cdot \mu_\xi(Hr\xi))$$

where  $\epsilon_a = \mathbf{1}_{\{\text{accompanying horizontal signal}\}}$ .

The counting of the tiles thanks to the formula gives us 20 tiles.

Next, we turn to the tiles of the legs. In the first half of the legs, we have two kinds of situation: the leg simply meets a horizontal signal, red or yellow, or it meets a basis which leads to several situations, depending on whether the basis belongs to a triangle or a phantom. Note that there is no leg with the colour blue-0. First, we consider the case when the legs belong to a phantom.

$$(L_u\varphi) \quad L\gamma\varphi u\xi + \left( \mathbf{1}_{\{\gamma=b_n\}} \cdot (\epsilon_s \cdot (\alpha \cdot Hy + \beta \cdot Hr\xi) \right. \\ \left. + \overline{\epsilon_s} \cdot (B\gamma_1\tau_1 \right. \\ \left. + \mathbf{1}_{\{\gamma_1=b_0\}} \cdot \mathbf{1}_{\{\tau_1=\varphi\}} \cdot Hy \right. \\ \left. + \mathbf{1}_{\{\gamma_1=b_n\}} \cdot \mathbf{1}_{\{\tau_1=\varphi\}} \cdot Hr\xi \right. \\ \left. + \mathbf{1}_{\{\gamma_1=r\}} \cdot \mathbf{1}_{\{\tau_1=\varphi\}} \cdot Hr\xi)) \right. \\ \left. + \mathbf{1}_{\{\gamma=r\}} \cdot (\epsilon_s \cdot \epsilon_r \cdot Hr\xi \right. \\ \left. + \overline{\epsilon_s} \cdot (B\gamma_1\tau_1 \right. \\ \left. + \mathbf{1}_{\{\gamma_1=b_0\}} \cdot \mathbf{1}_{\{\tau_1=t\}} \cdot \epsilon_y \cdot Hy \right. \\ \left. + \mathbf{1}_{\{\gamma_1=b_n\}} \cdot Hr\xi \right. \\ \left. + \mathbf{1}_{\{\gamma_1=r\}} \cdot \mathbf{1}_{\{\tau_1=\varphi\}} \cdot Hr\xi)) \right)$$

with  $\alpha, \beta \in \{0, 1\}$  and  $\alpha + \beta \leq 1$ . The formula takes into account that a yellow signal exists only on a row where there is the blue-0 basis of a trilateral and that the first half of the leg of a triangle cannot meet a basis of a triangle of the same colour, blue-0 and simple blue being considered as equal under this regard. In this formula, we can interpret  $\epsilon_s$  as  $\epsilon_s = \mathbf{1}_{\{\text{signal only}\}}$  and  $\epsilon_r$  as  $\epsilon_r = \mathbf{1}_{\{\text{red signal}\}}$ , while  $\epsilon_y$  is interpreted as before. We repeat that this is only an interpretation. The rôle of the parameters is simply to differentiate all possible cases. Accordingly, we may consider them as purely formal parameters which take their value independently.

It is not difficult to observe that the counting from the formula gives us 34 tiles. However, with this case, we introduce a tool which we shall more intensively use in section 4. In order to facilitate the counting, we represent the connections between the sub-terms of the formula in a tree-like way, based on the decomposition of the formula in the form  $\alpha \cdot A + \beta \cdot B$ , with  $A$  and  $B$  recursively decomposed in a similar way. The number of leaves of the



tree gives us the number of tiles of this type.

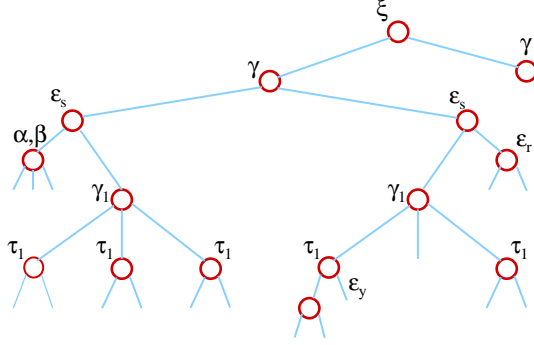


**Figure 19** *The counting for formula  $(L_u\varphi)$ . Remember the conventions: for an  $\epsilon_i$ -node we have 0 to the left and 1 to the right; for  $\tau$ -nodes,  $t$  to the left and  $\varphi$  to the right. For  $\gamma$ , we have  $b_n$  to the left and  $r$  to the right. For  $\gamma_1$ , we have  $b_0$  to the left,  $b_n$  in the middle and  $r$  to the right. The  $\xi$ -node, the root of the tree has two sons, labelled with  $\gamma$ : we have developed only one of them as the second one is identical to it.*

Next, we look at the case when the legs meet the basis of a triangle. The formula takes into account that a yellow signal exists only on a row where there is the blue-0 basis of a trilateral and that the first half of the leg of a triangle cannot meet a basis of a triangle of the same colour, blue-0 and simple blue being considered as equal under this regard. Note that we use the same interpretation of  $\epsilon_s$ ,  $\epsilon_y$  and  $\epsilon_r$  as previously although they work as formal independent parameters.

$$\begin{aligned}
(L_u t) \quad L\gamma t u \xi + & \left( \mathbf{1}_{\{\gamma=b_n\}} \cdot (\epsilon_s \cdot (\alpha \cdot Hy + \beta \cdot Hr\xi) \right. \\
& + \overline{\epsilon_s} \cdot (B\gamma_1\tau_1 \\
& + \mathbf{1}_{\{\gamma_1=b_0\}} \cdot Hy + \mathbf{1}_{\{\gamma_1=b_n\}} \cdot \mathbf{1}_{\{\tau_1=\varphi\}} \cdot Hr\xi \\
& + \mathbf{1}_{\{\gamma_1=r\}} \cdot \mathbf{1}_{\{\tau_1=\varphi\}} \cdot Hr\xi)) \\
& + \mathbf{1}_{\{\gamma=r\}} \cdot (\epsilon_s \cdot (\epsilon_y \cdot (\mu_\xi(Hr\xi) + \mu_{\overline{\xi}}(Hy)) + \overline{\epsilon_y} \cdot Hr\xi) \\
& + \overline{\epsilon_s} \cdot (B\gamma_1\tau_1 \\
& + \mathbf{1}_{\{\gamma_1=b_0\}} \cdot (\mu_\xi(Hr\xi) + \mu_{\overline{\xi}}(Hy)) \\
& + \mathbf{1}_{\{\gamma_1=b_n\}} \cdot \epsilon_r \cdot Hr\xi \\
& \left. + \mathbf{1}_{\{\gamma_1=r\}} \cdot \mathbf{1}_{\{\tau_1=\varphi\}} \cdot Hr\xi)) \right)
\end{aligned}$$

with  $\alpha, \beta \in \{0, 1\}$  and  $\alpha + \beta \leq 1$ . This gives us 28 tiles.

The last case for the legs is given by the second half. There, the situation

is simpler as, from lemma 19, we know that the second half of a trilateral meets horizontal signals only. The signals are the horizontal red signal, of the laterality of the leg, and, for red triangles only, possibly a yellow signal on one side and the horizontal red signal on the other side.

We have the following formula:

$$(L_\ell) \quad L\gamma\tau l\xi + \left( \mathbf{1}_{\{\gamma=b_n\} \vee \{\tau=\varphi\}} \cdot \epsilon_a \cdot (\epsilon_y \cdot Hy + \overline{\epsilon}_y \cdot Hr\xi) \right. \\ \left. + \mathbf{1}_{\{\gamma=r\} \wedge \{\tau=t\}} \cdot (\epsilon_r \cdot Hr\xi + \overline{\epsilon}_r \cdot (\mu_\xi(Hr\xi) + \mu_{\overline{\xi}}(Hy))) \right)$$

where  $\epsilon_a$  can be interpreted as  $\epsilon_a = \mathbf{1}_{\{\text{accompanied}\}}$ .

Here, the counting gives us 22 tiles.

At this point, we may sum up all the countings we have performed. We have 186 tiles, as it can easily be found. To these tiles we have to append all the tiles of figure 18. Accordingly, we find 192 tiles.

Now, we turn to the proof of lemma 20. In this proof, we shall make use of figures 11 to 14. We also make use of the numbering of the tiles introduced in the beginning of section 3.4.2.

#### *Proof of lemma 20*

It is not very difficult to see that the set of tiles which we indicate generates the interwoven triangles. What we have already seen is enough to convince us that this is the case. What is most important is to see that the status of the empty tile being put apart and that of the vertices being fixed a bit later, the set of tiles of figures 11 to 14 forces this tiling and nothing else. In this proof, each time we say "take this tile..." or "place this tile at ...", this means: take a copy of the tile and do what is indicated with the copy. Of course, copy means an image by a shift accepted by the tiling, as mentioned in lemma 20.

In this setting, we consider that the tiles of section IIa, the vertices, can be put along the axis and only at this place. We also assume that tiles of section IIe are forbidden on the axis. We shall assume that we start the construction with the tile *a-1-1*, the vertex of a blue-0 triangle with no yellow signal. From figure 10, we know that the tile necessarily abuts with a passive tile at its lower edge. It is necessarily the tiles *I-1-1* and *I-1-2*, which start the leg of the blue-0 triangle, taking into account that the tiles cannot be rotated nor reflected. Next, we have an active tile, necessarily the first half of a leg and we find *c-1-1* or *c-2-1* for the left-hand side. We shall always denote the left-hand side tiles when describing a leg. This means that here, we decide where will be the triangles of the generation 1.

Let us choose the tile *c-2-1*. This forces the tile *c-2-2* for the right-hand

side leg: otherwise, if we take  $c-1-2$ , the other possible choice, there will be a contradiction with the tile to put between them. And so, with  $c-2-1$  and  $c-2-2$ , the single possibility is  $a-1-4$  as this is the single tile which has a right-hand side and a left hand-side horizontal red signal. Also, it is a tile on the axis, hence a vertex. Now, the passive tiles abut with the light blue as the tiles  $c-2-1$  and  $c-2-2$  are tiles for the mid-distance point. And so, here we must put the tiles  $I-3-3$  and  $I-3-4$ . Later, there is no tile with a light blue-0 colour at the expected position. Again, remember that symmetries and rotations are ruled out: the tiles have an upper side and a lower one and the sides cannot be exchanged. Accordingly, we must put a corner. The choice for the left-hand side is between  $e1-1-1$ ,  $e1-1-3$  or  $e1-1-5$ . To decide this, we have to remember that we already put the vertex of a red triangle on the mid-distance line of the blue-0 triangle which we are constructing. The red vertex allows abutting only on its lower edge and this requires a passive tile, necessarily  $I-2-1$  and  $I-2-2$ .

Next, at the level of the corner we have just put, a new tile should be put which can be taken in sub-section  $b1$ , lines 3 or 4 or in sub-section  $c$ , the tiles  $c-1-5$  or  $c-2-5$  as left-hand side tiles only are indicated. Now, as a mid-distance tile of a red triangle agrees only with a simple blue basis, tiles from  $c$  are ruled out. Now, between the tiles from  $b1$  we have to place, there is a single one on the axis. This must be a vertex, namely the vertex of a blue-0 phantom. And so, there is no horizontal red signal between the tiles from  $b1$ . Accordingly, we must put the tile  $b1-3-5$  as the corner also force a thick horizontal blue-0 signal. But now, due to the presence of this part of the red triangle in the blue-0 one, we know that we must put the corner  $e1-1-5$ . Also, between the tiles  $b1-3-5$  and  $b1-3-6$ , we have to put a vertex, due to the presence of the axis, as already noted, and so, it is necessarily  $a-2-2$ , as we have a thick light blue-0 horizontal signal and a yellow one.

Further, the passive tiles are forced by the legs of the red triangle, and so we put there the tiles  $I-2-1$  and  $I-2-2$ . But, below the corner, as there is no signal, we have an empty passive tile, the tile  $I-4-5$ . Later, we arrive at the mid-point of the phantom: we notice that sub-section  $b2$  does not contain tiles with a vertical blue-0 signal. Only tiles from sub-section  $c$  may match here. Now, we have four possibilities given by the tiles of sub-section  $c$ , line 3, say the tile  $c-3-*$ . Now, as the left-hand side neighbour  $L$  of the tile  $c-3-*$  meets the light red leg coming from the red vertex, and as all tiles  $c-3-*$  contain a green signal, the tile  $L$  must also be taken in sub-section  $c$  and there is only two choices:  $c-1-5$  or  $c-2-5$ . This means that here, we decide the situation of the triangles of the generation 2. And so, if we decide to put here a triangle, we take the tile  $c-3-5$ . Now, this entails

that the red leg will meet the tile  $c-2-5$ . Now, for both trilaterals, the blue-0 phantom and the red triangle, we now may turn to the second half of their legs.

Before going on, we have to look at what happens on the mid-distance row which we just reached. This feature is known because the tile  $c-3-5$  contains the horizontal green signal. Note that any tile  $c-3-*$  contains this signal. Now, between  $c-3-5$  and  $c-3-6$ , there is room for exactly one tile which is again on the axis: hence we have to put a vertex. This is the vertex of the generation 2 induced by the choice at the meeting point of the leg with this mid-distance row. And so, we have to put here the tile  $a-1-3$ .

Now, we can look at what is performed below this mid-distance line.

For the blue-0 phantom, we take the tile  $I-3-3$  and for the triangle, we take the tile  $I-2-1$ . Next, as for a blue-0 triangle, we easily check that the single possibility is to place the corner of a blue-0 phantom. At the same time, the second half of the red leg is the tile  $d-2-1$  as there is no horizontal red signal on the row: the tile required on the axis by the corners is a vertex, hence without red signal at all. Accordingly, the corner is the tile  $e1-3-3$ . Again, the tile between  $e1-3-3$  and  $e1-3-4$  is again a vertex, and it is necessarily  $a-1-2$ : the vertex of a blue-0 triangle.

Now, we know that the construction of the generation 0 is forced by the tiling under the conditions we indicated. Figure 22 illustrates also this point.

Let us look at what happens with the second half of the legs of the red triangle.

After the corner of the blue-0 phantom, we have a passive row, both for the new blue-0 triangle and for the red triangle. As we know from the construction of a blue-0 triangle, after this passive row, we have the mid-distance row. We use a tile  $c-1-1$  or  $c-2-1$ . If we put the tile  $c-2-1$ , we need the tile  $e2-4-1$  until we meet the leg. But a corner cannot connect a thick signal with a thin one. And so, we must put the tile  $c-1-1$  and use the tile  $e2-2-1$  until we can place the corner  $e1-2-5$ . Note that this tile raises a horizontal red signal to the left. Symmetrically, the corner  $e1-2-6$  raises a horizontal red signal to the right. Note that the structure of these two horizontal red signals are different.

Next, we have the construction of a red phantom: the basis of the just constructed red triangle meets the axis at a tile which is necessarily  $a-2-4$ . The construction goes on the same way but it is simpler: there is no free row to delimit inside a phantom and so, we just look at the closest green signal. If we denote by 0 the blue-0 triangle which we have initially constructed and if

we denote by successive integers the blue-0 trilaterals which are successively constructed downwards, we notice that the closest green line is emitted by the blue-0 phantom 4. This green line is again defined by a tile  $c$ -3-\*. As it meets a red phantom, it defines the mid-point of the leg of this phantom but the green signal goes on outside the red phantom as we have here a tile  $c$ -5-\*.

Here, we meet an important point of the construction. The green signal grows until it meets a triangle, whatever the colour, red or simple blue. It may happen that the signal will never meet such a triangle. In this latter case, whatever the tile  $c$ -3-\* defined by the blue-9 phantom 4, the choice induces a unique vertex on the axis for the corresponding row and a trilateral  $\mathcal{T}$  will grow starting from there.

It is not difficult to see that this trilateral grows indefinitely: the first part of its legs will never meet a green signal. Indeed, from the correspondence we studied between vertices of trilaterals and ends of the intervals, we know that if a green line is raised inside  $\mathcal{T}$ , it will be met by a trilateral which is raised by a vertex placed between the vertex of  $\mathcal{T}$  and the green line. This can be checked by the study of the butterfly model, where 0 would be the abscissa of the vertex of  $\mathcal{T}$  on the axis.

As noted, the model which we implement may be not the butterfly model. When this is the case, the green signal will always eventually meet the leg of a triangle. There may be a contradiction between the tile  $c$  which has to be put there and the tile  $e2$  which is involved by the continuation of the green signal in that sense that the colour of the accompanying signal may be different as well as the width of the signal. To solve this contradiction, we fix a rule: the decision of the choice belongs to the leg of the triangle. This means that we may have to change the tiles on this mid-distance line as well as those which depend on the choice performed at the axis. At the considered step of the construction this involves only finitely many tiles and once this is performed, the new tiles will never be changed again. This is why the construction is correct. We simply note that inside a triangle, everything inside the triangle is fixed when the basis of the triangle is constructed as well as the trilaterals of the next generation which it determines. With a phantom, the construction is temporary: it may be changed but once, because at that moment, the part which is changed falls inside a triangle and so, it cannot again be changed.

Now, what we did up to this point can be repeated above the vertex of the blue-0 phantom 0. This allows us to construct blue-0 trilaterals  $-k$ , with  $k \in \mathbb{N}^+$ . But from these trilaterals, we can construct the red triangles of

the generation 1, step by step, upwards. We can even construct them from the basis: the position of the corners must match with legs emanating from the appropriate vertex. The shape of the corner forces a unique solution and it is the right one.

Now, it is not difficult to see that the construction of the further generations obeys the same process. The difference with what we have seen is that, depending on the choices, the towers of phantoms grow more or less. Also, as the red triangles give rise to simple blue trilaterals only, the blue-0 colour is no more in use for the new blue generations. These new features require all the intermediate tiles of sub-sections *b1* and *b2* to handle all possible situations and only them: this is proved by the analysis we previously provided in the description of the tiles. All of this is a consequence of the lemmas 18 and 19.

Accordingly, lemma 20 is proved.

## 4 The proof of the main theorem

In this section, we first implement the isoclines in the mantilla. Then, we turn to the implementation of the tiles for the interwoven triangles in the hyperbolic plane. There, we shall see the new features entailed by the hyperbolic plane and by the mantilla. As a consequence, a new signal will be introduced as well as a few new tiles. Then, in a third subsection, we shall deal with the definition of the computing areas.

### 4.1 Implementation of the isoclines in the mantilla

From [9], we know that the mantilla can be constructed from a set of 21 prototiles. At first glance, as we have two kinds of nodes to define the isoclines, this would require 42 tiles. This is not the case as, for instance in the **8**-flower, there are tiles which are always black nodes. A careful analysis of the configurations displayed in figure 5 shows that other tiles share this property and that also some of them are always white nodes.

This analysis is reported in table 3 where for each tile, we indicate the edges whose mid-points are ends of the arc of the isocline which crosses the tile. The edges are indicated according to their labels in the tile for centres. For petals, when an edge has no label, we indicate its position by two neighbouring edges or, by an edge and the red vertex, which means that the considered mid-point is on an edge whose one end point is the red-vertex.

tile	$st$	edges	relative
$F$	$B$	6-2	6-2
	$W$	6-1	6-1
	$W$	7-2	7-2
$\mathbf{8}$	$B$	$\overline{6-2}$	$\overline{6-2}$
$G_l$	$B$	2- $\overline{6}$	2-6
$G_l$	$W$	1- $\overline{6}$	1- $\overline{6}$
$G_r$	$B$	$\overline{2}$ -6	$\overline{2}$ -6
$G_r$	$W$	$\overline{2}$ -7	$\overline{2}$ -7
2 $\circ$ 77	$B$	((7-2)-(•-))	5-1
2 $\circ$ 77	$W$	(2-(•-))	6-1
1 $\circ$ 1 $\overline{3}$	$B$	((1- $\overline{3}$ )-1)	3-6
1 $\circ$ 1 $\overline{3}$	$W$	((1- $\overline{3}$ )-( $\overline{3}$ -1))	3-5
1 $\overline{4}$ 7 $\circ$	$W$	((1- $\overline{4}$ )-( $\overline{4}$ -7))	3-5
$\overline{5}$ 7 $\circ$ 7	$B$	(7-( $\overline{5}$ -7))	2-5
$\overline{5}$ 7 $\circ$ 7	$W$	(7- $\overline{5}$ )-( $\overline{5}$ -7))	3-5
11 $\circ$ 6	$B$	((-•)-(6-1))	7-3
11 $\circ$ 6	$W$	((-•)-6)	7-2
11 $\circ$ 2	$B$	((-•)-(2-1))	7-3
11 $\circ$ 2	$W$	((-•)-2)	7-2
37 $\circ$ 7	$B$	(7-(3-7))	2-5
37 $\circ$ 7	$W$	((7-3)-(3-7))	3-5
1 $\circ$ 14	$W$	((1-4)-(4-1))	3-5
$\overline{5}$ $\circ$ 77	$B$	((7- $\overline{5}$ )-(•-))	5-1
$\overline{6}$ $\overline{6}$ 7 $\circ$	$W$	( $\overline{6}$ - $\overline{6}$ )	2-4
1 $\overline{2}$ $\overline{2}$ $\circ$	$W$	( $\overline{2}$ - $\overline{2}$ )	4-6
11 $\circ$ $\overline{3}$	$B$	((-•)-( $\overline{3}$ -1))	7-3
47 $\circ$ 7	$W$	((7-4)-(4-7))	3-5
1 $\circ$ 15	$B$	((1-5)-1)	3-6
1 $\circ$ 15	$W$	((1-5)-(5-1))	3-5
6 $\circ$ 77	$B$	((7-6)-(•-))	5-1
6 $\circ$ 77	$W$	(6-(•-))	6-1
137 $\circ$	$B$	((1-3)-7)	3-6
157 $\circ$	$B$	(1-(5-7))	2-5

**Table 3** Table of the centres and petals equipped with the isoclines.

Again for the petals, we also give local numbers to the edges. By definition, the red vertex is between 1 and 7 and the numbers are increasing while clockwise turning around the tile. Further, figure 20 displays the 34 tiles of the mantilla, equipped with the isoclines. We simply draw the arcs which we symbolized by the symbol  $\frown$  for black nodes and the symbol  $\smile$  for white nodes in section 3.1. We notice that the arcs are oriented in different ways with respect to the local numbering which is defined with respect to the red vertex whose position is the same in all the tiles of figure 20. Table 3 indicates the exact location of the signal with respect to the edges of tile in terms of intrinsic properties of the tiles.

There is a simpler way to locate the arcs at the price of a global property. We know that the isoclines induce the structure of a Fibonacci carpet. This

means that any tile has a father. In a white node, the edge to the father is the single edge delimited by the ends of the edges joined by the isocline. In a black node, the ends of the edges joined by the isocline define two consecutive edges. If we see these edges as the upper part of the tile, the edge to the father is the right-hand side edge. Now, give the number 1 to the edge to the father and number the other edges by consecutive numbers from 2 to 7 while counter-clockwise turing around the tile. The isocline signal goes from the edge 3 to the edge 7 in the case of a black node, and it goes from the edge 2 to the edge 7 in the case of a white node. Call such coordinates of an edge **paternal**.

We notice that 5 tiles are always black:  $\mathbf{8}$ ,  $\overline{5\circ 77}$ ,  $11\circ\overline{3}$ ,  $137\circ$  and  $157\circ$ . Also, 5 tiles are always white:  $\overline{147\circ}$ ,  $11\circ 4$ ,  $\overline{667\circ}$ ,  $\overline{122\circ}$  and  $47\circ 7$ . Next, 10 tiles have a black version and a white one:  $G_\ell$ ,  $G_r$ ,  $2\circ 77$ ,  $1\circ\overline{13}$ ,  $\overline{57\circ 7}$ ,  $11\circ 6$ ,  $11\circ 2$ ,  $3\circ 77$ ,  $1\circ 15$  and  $6\circ 77$ . At last, the tile  $F$  has three versions: a black one and two white ones.

Note that we also indicate the petals of a  $G$ -centre which are also parental petals of an  $F$ -centre. As not all black  $F$ -centre are in this situation, we have to mark those which are. Note that in each case, as a  $G$ -centre exists in two versions, black and white ones, this induces for each one three petals as one of them has a single version and the other has two ones.

Namely, the petals are  $47\circ 7$  and  $1\circ 15$  for a  $G_\ell$ -flower with  $47\circ 7$  always white. They are  $37\circ 7$  and  $1\circ 14$  for a  $G_r$ -flower, with  $1\circ 14$  always white. Now, there is an important difference with [9] where the tiling was also divided so that realizations of the mantilla with an ultra-thread were ruled out. Here we do not exclude such realizations and, more other we have to identify all possible trees of the mantilla. This is why the just mentioned petals are present in the set of tiles with the mark only.

On another hand, we impose that the seeds are among the roots of a tree of the mantilla which belongs to an isocline 0, 5, 10 or 15: in sub-section 3.1, we have indicated that the seeds contains at least all the roots which are on the isoclines 0. We indicate the selection process later. The implementation of the numbering from 0 to 19 on the set of tiles of figure 20 is not difficult. The general pattern is indicated by figure 21, below. We notice an important consequence of the isoclines and of the numbering.

By themselves, together with the structure of the mantilla, the isoclines prevent to turn a tile: this would entail contradictions between the arcs of the isoclines. Note that we already know from [9] that the structure of the mantilla itself rule out such a possibility. Now, the numbering, even if it is only periodic, allows to define the directions up and down. Also, the isoclines themselves allow to define what are the directions left and right.



However, this does not exactly correspond to what we define by the same words in the Euclidean plane.

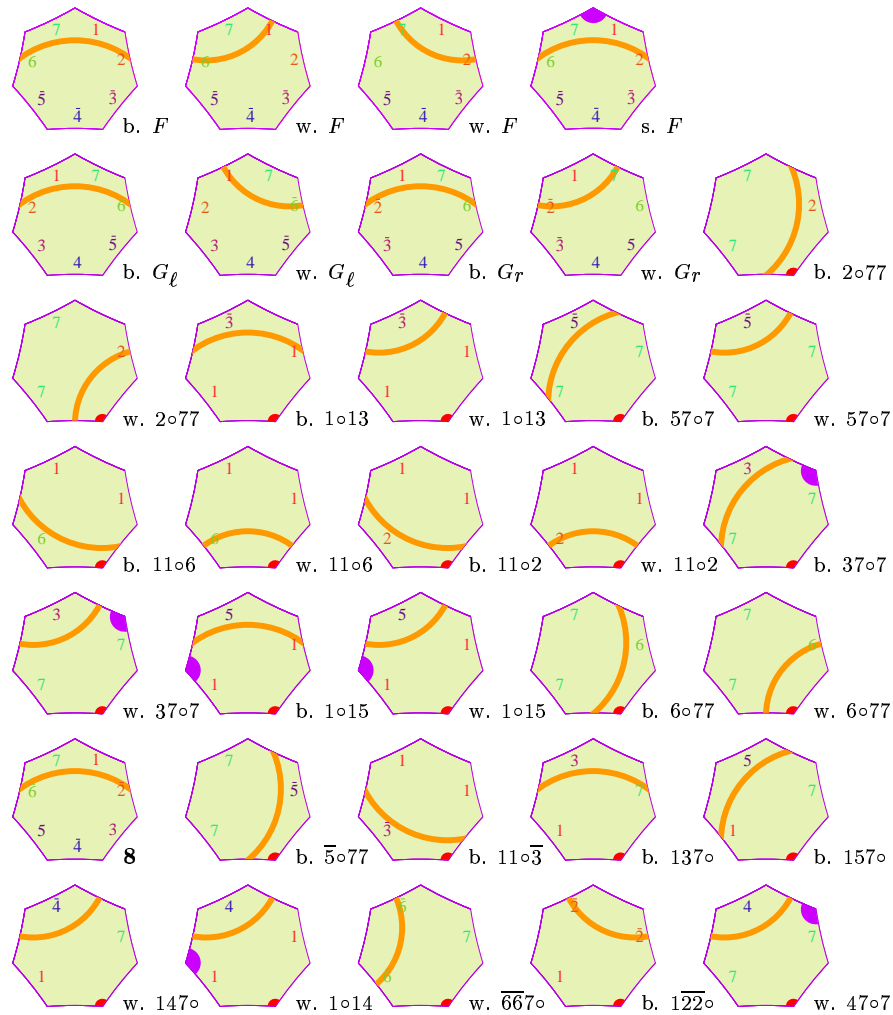


**Figure 20** *The tiles for the mantilla, equipped with the isoclines. The first row is devoted to  $F$ -centres as there are four versions of them. The following four rows display the 20 tiles corresponding to the 10 tiles of the mantilla which have a black and a white version. The sixth row displays the tiles which have only a black version. The last row displays those which have only a white version. Note the four petals of  $G$ -flowers which allow to detect the  $F$ -son.*

In the sequel, the isoclines 0, 5, 10 and 15, which we already called the rows of the mantilla in the section 3.1, will also be called **active** as they contain the seeds. The other isoclines play a passive rôle. Accordingly, the

isoclines 1 to 4, 6 to 10, 11 to 15 and 16 to 19 can be seen as behaving exactly in the same way as the passive rows of section 3.4. They only convey the vertical signals, the implementation of which is investigated in the next subsection. For this reason, the just indicated groups of isoclines will be called the **passive zones**.

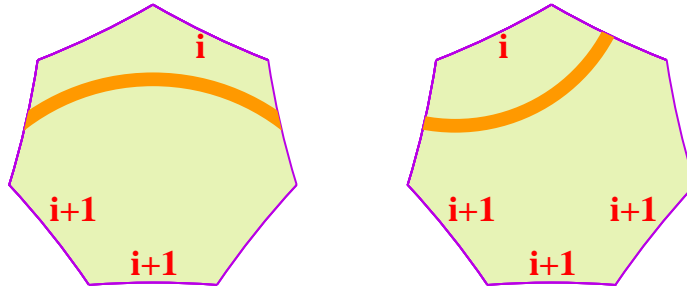


**Figure 21** *The implementation of the numbering of the isoclines.*

It is also not difficult to append marks to the numbering in such a way that the active rows are distinguished from the passive zones. Figure 10 already indicated a possible solution.

## 4.2 Implementation of interwoven triangles in the hyperbolic plane

The set of tiles which we described in section 3.4 which is also displayed by figures 11, 12, 13 and 14 is not, strictly speaking a set of Wang tiles.

However, its implementation in the heptagrid will consist of true *à la* Wang tiles. But for this purpose, we have to first indicate how we implement the trilaterals in the hyperbolic plane.

### 4.2.1 The trilaterals in the hyperbolic plane

In section 4.1, we already implemented an **isocline signal** which defines the isoclines of section 3.1. The rows which we have just defined among them in the previous sub-section are the rows along which we shall construct the bases of the implementation of the trilaterals. These rows will also convey the horizontal signals needed by our construction.

Now, that we know what are the rows, we have to indicate what are the verticals, what is the axis and how to define the legs of the triangles as the notion of slope is meaningless in the hyperbolic plane.

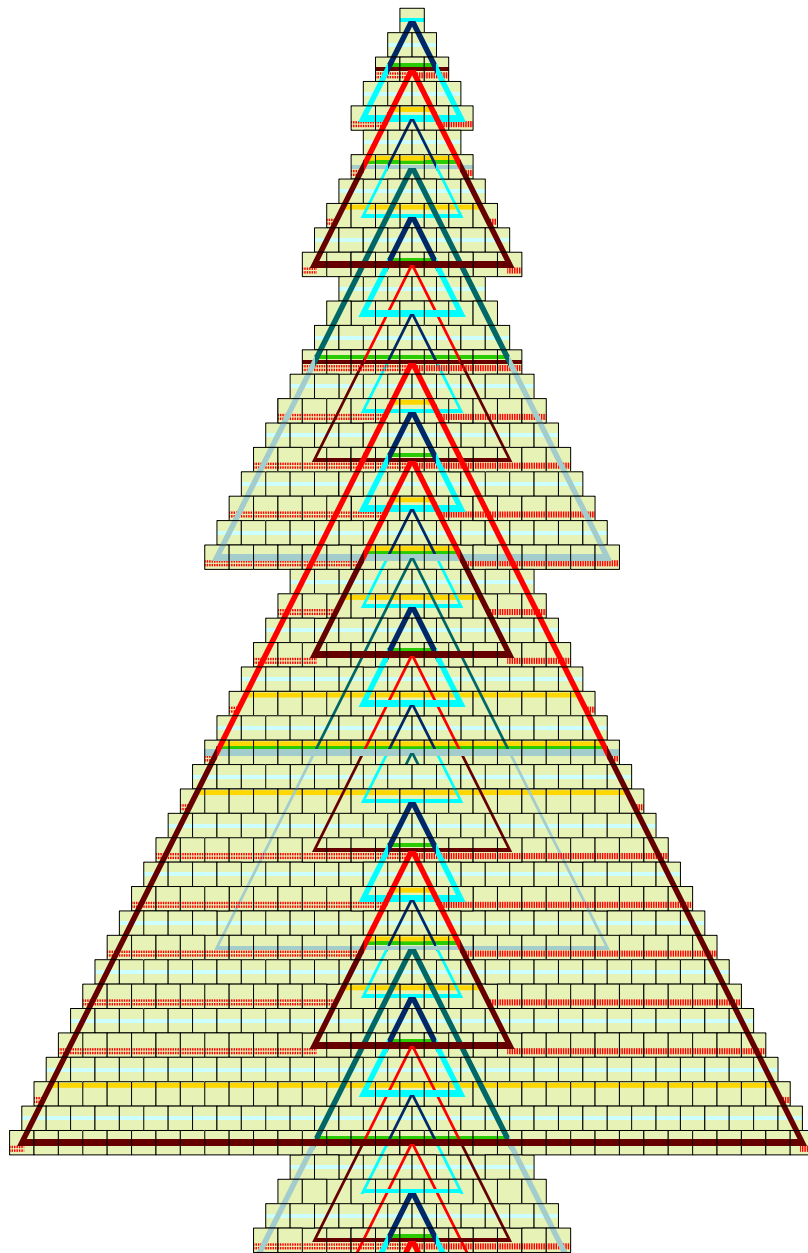


**Figure 22** *Triangles and phantoms up to the generation 3. This involves only the tiles indicated in figures 11, 12, 13 and 13. Note the vertex of the phantom of the generation 3 at the mid-point of the basis of the triangle R of the generation 3. Also note the part of the basis of another phantom of the generation 3 around the vertex of R.*

The legs of the trilaterals will be implemented along the border of the trees of the mantilla rooted at a seed, where the vertex stands. The left-hand side leg goes on the leftmost branch and the right-hand side leg along the rightmost branch. The corners are the intersections of the legs with an isocline which will also support the basis of the trilateral.

Note that the implementation of the Euclidean trilaterals are not triangles of the hyperbolic plane. However, we shall keep the same terms as in the Euclidean case. First, it raises no confusion and, second, it is simpler.

Now, from this definition of the implementation, a lot of questions arise at the level of signals inside and between trilaterals.

The first question is about the verticals and the axis: what are here their implementation?

We may consider the borders of a tree of the mantilla as verticals. In the part devoted to the simulation of a Turing machine, we shall indicate what are the actual verticals but, up to now, we do not need them. The axis is a more urgent question. In fact there is no axis as we had in the Euclidean case. However, the axis has an important rôle in the Euclidean case, as it triggers the positioning of the vertices of the trilaterals. In the hyperbolic case, there is no possible axis and we have to replace it by a procedure which gives the same result. Now, from lemma 5, we can apply the following: each active seed of an isocline 0 dispatches a signal to its sons and grandchildren until it reaches the next isocline 0. Call this signal the **scent**. When the signal reaches an isocline 5, 10 or 15: if it meets a seed, the seed becomes active and the signal goes down further. If it meets a tile which is not a seed, then it stops. Accordingly, not all seeds of an isocline 0 is reached by the scent from a seed of the just upper isocline 15. Note that the property of an active seed to diffuse the scent is not attached to the status nor the colour of the trilateral emitted by this seed.

This mechanism allows to trigger the diffusion of the green signal on the isoclines 15. It is important to remember that, starting from the second generation, any vertex of a trilateral appears within a blue-0 phantom. Accordingly, the starting of all green signals is performed by the phantoms of the generation 0.

From this, it is natural to define the following:

*A **branch** is a sequence of active seeds  $\{\sigma_i\}_{i \in \mathbb{N}}$ , either indexed by  $\mathbb{N}$  or by  $\mathbb{Z}$ , such that the tree of the mantilla rooted at  $\sigma_i$  contains the tree of the mantilla rooted at  $\sigma_{i+1}$  and such that the distance between  $\sigma_i$  and  $\sigma_{i+1}$  in isoclines of the mantilla is 5.*

Note that a branch starting from a vertex of a blue-0 triangle is infinite

and that the scent exactly marks all the branches.

If the mantilla possesses an ultra-thread, there is a branch indexed by  $\mathbb{Z}$  which we shall call a **traversal**. If this is not the case, all branches are indexed by  $\mathbb{N}$ . However, in the case of an ultra-thread, there are also branches only indexed by  $\mathbb{N}$ : the condition on the distance 5 may be not satisfied between an active seed  $\sigma$  and another one  $\xi$  belonging to the tree rooted at  $\sigma$  and such that there is no intermediate tree of the mantilla rooted at an active seed between  $\sigma$  and  $\xi$ . As an example, computer checkings show that in a tree of the mantilla rooted at a seed, say on an isocline 0, there are 6 seeds on the isocline 5 which are inside the tree and 324 seeds on the isocline 10 which are inside the tree. Note that the number of nodes inside the tree on the isocline 5 is 144 and that there are 17,711 nodes inside the tree on the isocline 10. Now, if any seed on the isocline 10 would be a grand-children of a seed on the isocline 5, there would be at most 36 of them. Consequently, the phenomenon which we have described happens very often.

Now, in any case, the trilaterals which are on a branch implement a semi-infinite model of the abstract brackets. We know that such a model is obtained as a cut of an infinite model. Our first condition will be that in each realization of the tiling, the branches implement cuts of the same infinite model. Of course, in the case of an ultra-thread, the traversal will implement the same infinite model.

Clearly, this requires to **synchronize** the choices of the triangles at each generation on different branches as these branches can be independent in a mantilla without ultra-thread. The synchronization is also needed in all the cases as we do not know a priori, whether the realization possesses or not an ultra-thread.

As already mentioned, the basis of a trilateral of the generation 0 is very large. As there are 36 active seeds on it, this means that a single triangle  $B$  of the generation 0 defines 36 phantoms whose vertex is on the basis of the triangle. Now, consider that the isocline 5 which crosses  $B$  gives rise to red triangles. There are 6 of them. And so, we have to define how to manage the horizontal red signals emanating from these triangles. We also have that all these triangles cut the basis of  $B$ .

In order to handle more easily the problem, define the **latitude** of a trilateral as the set of rows of the mantilla from its vertex down to its basis, both included. The length of this set is called the **amplitude** of the zone constituted by the latitude. Of course, trilaterals of a same generation have the same amplitude. The synchronization has, as a consequence that the latitudes of triangles of the same generation from one branch to another

exactly coincide or do not overlap. Consequently, the same also holds for trilaterals.

This induces a problem for the propagation of horizontal red signals. We have defined them with a laterality: left-hand or right-hand side. Up to now, there is a tile which allows to join one laterality with the other: it is the tile of the vertex of a red triangle. But here, the opposite meeting occurs between different laterality, *i.e.* a left-hand side signal coming from the right meets a right-hand side signal coming from the left. For this purpose, we shall just introduce a new tile illustrated in sub-section 4.2.3: its left-hand side half is a red-hand side horizontal red signal and its right-hand side half is a left-hand side horizontal red signal. Call it the **red join tile**.

Coming back to the realization of semi-infinite models, this entails a similar situation connected with missing trilaterals. Remember that, in a semi-infinite model, all active intervals which contain the point where the cut is performed are removed from the model. Depending on the infinite model, this leads to remove either finitely many active intervals or infinitely many of them. In our implementation, we first remember that a seed  $\sigma$  always defines another seed inside the tree of the mantilla rooted at  $\sigma$ , at a distance 5 from  $\sigma$ . This means that once a vertex of a trilateral is present, the whole trilateral is present and, consequently, this is also the case for all its followers, below, of the same generation. However, as the considered seed also generates a basis, it may happen that there is no seed to realize a vertex containing this point of its basis. The basis is still propagated by the seed which cannot foresee this possibility. In some sense, this basis is a lost signal and so, we also have to handle this phenomenon and to prove that this will not disturb the process we used up to now to construct the trilaterals.

#### *Managing lost signals and synchronization*

The implementation of the interwoven triangles in the hyperbolic plane entails a new ingredient to our tiling. In the Euclidean situation, we have horizontal red signals. In the hyperbolic case, we also have blue horizontal signals. This is due to the following problem which did not occur in the Euclidean case as, inside a triangle exactly one trilateral is generated by the mid-distance line of the triangle.

In the hyperbolic case, inside a triangle of a given generation, we have several trilaterals generated on the mid-distance row of this triangle. This is clear from what we have already noticed. But also, within the same latitude, we have infinitely many trilaterals, even if on the branches which are raised within this latitude, there may be missing trilaterals in this latitude. This

second phenomenon is proved by the following lemma:

**Lemma 21** *Within a given latitude corresponding to an interval of the model realized by the tiling, there are infinitely many trilaterals.*

*Proof.* Consider the lowest row  $\beta$  of the latitude. As we know the interval  $I$  corresponding to the considered latitude, we also know the highest row  $\kappa$  of the latitude. Now, fix a tile  $\tau$  on  $\beta$ . There is at least one  $\mathbf{8}$ -centre  $H$  over  $\kappa$  such that the ray  $\rho$  crossing the  $\mathbf{8}$ -centers below  $H$ , look at figure 5, meets the isocline of  $\beta$  on the left-hand side of  $\tau$ . We may assume that there is an isocline  $0$  between  $H$  and  $\kappa$ . Considering a seed  $\sigma$  on this isocline which is on the left-hand side of  $H$ , it is now plain that the tree rooted at  $\sigma$  is on the left-hand side of  $\rho$  and that, as all the triangle of the generation  $0$  starting from  $\sigma$  are present, there is a trilateral associated to  $\beta$  and  $\kappa$  inside the tree rooted at  $\sigma$ . By taking a reflection in  $\rho$  of this construction, we can prove the same property for the right-hand side of the tile  $\tau$ . Now, taking two tiles  $\tau_1$  and  $\tau_2$  with  $\tau_1$  on the left-hand side of  $\tau_2$ , we have a trilateral on the left-hand side of  $\tau_1$  and another one on the right-hand side of  $\tau_2$ . Repeating this argument, we get infinitely many trilaterals. ■

Due to the multiplicity of the trilaterals of the same generation within a given latitude and also due to the occurrence of a lot of bases which cannot find their vertex, it is important to be sure that a leg will distinguish between a lost basis and the basis with which it will make a corner of the trilateral under construction.

Let us look at the case of a lost basis  $\beta$  of a red triangle of the generation  $m$ . It may happen that such a basis occurs not far from a leg of a bigger red triangle, *i.e.* of the generation  $n$  with  $n \geq m+2$ . As a basis of a red triangle whose corner is not yet installed and as phantoms do not emit signals, the basis has no horizontal red signal with it. And so, it seems that there is no difference for this leg of the generation  $n$  between this basis and the expected basis of the generation  $n$ . In fact, there is a difference. The lost basis  $\beta$  is of the generation  $m$  with  $m < n$ . Now, on the latitude of the lost basis, there are infinitely many other bases which are not lost, as proved by lemma 21. And two of them, the closest one to the left and the closest one to the right emit horizontal red signals starting from their corner which are closest to  $\beta$ . As there is no leg to stop this signal,  $\beta$  is accompanied by such a signal. This is not the case for a basis of the generation  $n$ : at the time of its construction, the red signal is not installed at the level of the basis. This gives us a way to distinguish between the two situations.

First, we have to remark that there is still a problem with the basis of a red phantom. Such a basis is accompanied by the horizontal red signal

of a vertex of a red triangle as a basis of a trilateral, inside the triangle which has generated it, which, to its turn, generates trilaterals of the other kind. Now, it seems that there is no difference between a lost basis of a red phantom of the generation  $m$  and a basis of a red phantom the generation  $n$  which looks after the legs of its phantom. In fact, there is a difference. In the tiles which we devised in section 3.4, the horizontal signal is below the basis. It is enough to fix a level in the tile at which the normal horizontal signal travels. We shall call such a signal the **upper** one as we agree to place it above the basis signal on the tile. Then, in the case of a basis of a red phantom, we shall agree that the signal emitted by the vertex of a triangle generated by this basis is **below** the basis. Accordingly, we shall say that it is the **lower** signal. By construction, the lower and upper signals have the same colour as the basis. Their laterality is fixed by elements which give them rise: the corner, for the upper signal, the vertex for the lower. It is plain that between two consecutive elements, both signals can be joined as, in both cases, the right left-hand side signal comes from the left and the left-hand side signal comes from the right. Consequently, a basis of a red phantom of the generation  $m$  will have two horizontal red signals outside the phantom: the upper signal generated by corners of the neighbouring phantoms of the same latitude and the lower signal which is below the basis and which is generated by the vertices of triangles occurring on this row of the mantilla. On the other hand, inside the angle defined by the legs of a red phantom of the generation  $n$ , the expected basis has a single signal, the lower one and so, the legs of the phantom may notice the difference.

From this, we immediately remark that for blue trilaterals, in the present state of the tiles, there is a problem: as they do not emit signals, there is no way to distinguish between a basis which did not find legs and an expected one of a later generation. But the just above analysis points at a solution: let us decide that blue triangles, both blue 0 and simple blue ones will emit horizontal blue signals outside themselves. The signals will be managed exactly as the red ones. We shall have a left-hand side and a right-hand side blue horizontal signal. We have a tile to join signals between triangles lying in the same latitude which we call the **blue join tile**. Also for bases of blue phantoms, the signal induced by the vertices of blue triangles generated by this basis travels below the basis and the upper signal, generated by corners travels at the standard level of the horizontal blue signal, above the basis. In the tiles, this standard level is the same as the standard level of the red signals. As we have dotted signals, the superposition of an upper horizontal blue signal and an upper horizontal red signal on the same row will raise no problem. Note, that this superposition occurs very often as it is the general



case, see figure 23.

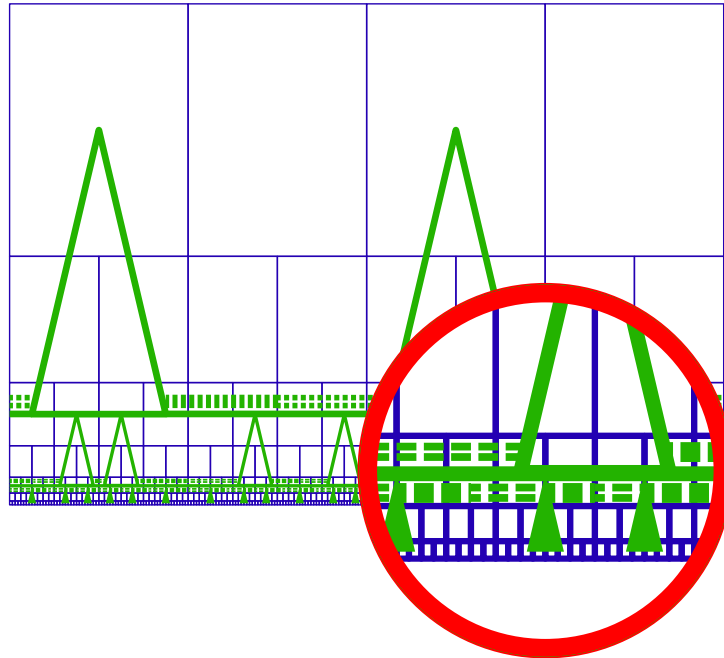


**Figure 23** *Management of the bases as a synchronization signal fro trilaterals of the same latitude.*

And now, there is a good news: lost signals are not that lost. As they travel on the same row as all trilaterals of a given latitude, they may be interpreted as a synchronization signal. Moreover, there is no need to stop them when they meet a corner and we decide that all bases of the same isocline merge. The difference between inside and outside the trilateral is clearly made by the presence or not of an upper horizontal signal of the same colour: if the upper signal is present, this part of the basis is outside the trilateral, if not, this part is inside the trilateral. As suggested by figure 23, the basis which now runs across the whole hyperbolic plane on its isocline, from the left to the right, can be split into intervals of two kinds. In one kind, all the intervals are inside a trilateral. In the other kind, all the intervals are outside any trilateral. Of course, we only consider maximal intervals with this property. Note that this notion of inside and outside is specific to the generation of the basis. Accordingly, an outside interval of a basis may fall inside a trilateral of another generation. In our sequel, we shall speak

of an **open** basis when we consider an interval which is inside a trilateral of the generation of the basis and we shall speak of a **covered** basis when it is outside. Clearly, an open basis has no upper horizontal signal of the same colour while a covered basis is necessarily accompanied by such a signal.

On an outside interval of a basis, there are indeed two horizontal signals of the same colour as the basis. One is a right-hand side signal coming from the left and the other is a left-hand side signal coming from the right. We know that they are joined by an appropriate pattern. Note that such a junction is unique. A similar remark can be made for lower signals. They also merge, being joined by a similar tile when the opposite lateralities come from directions which are opposite to the sense they indicate, and they are joined by a vertex of a triangle when the opposite lateralities come from the sense which they indicate.

At the level of the tiles, the upper horizontal signal of the covered basis merges with the upper horizontal signal of the corner of the same laterality and the same colour.

Repeat that these tiles allow to a right-hand side horizontal signal coming from the left to meet with a left-hand side signal coming from the right. Note that such a tile cannot be used inside a triangle  $T$ : the opposite junction is only made by the presence of another triangle of the same colour inside  $T$ . There is no other possibility as the mantilla and the isoclines prevent to rotate the tiles. And so, appending the above joining tiles does not affect the way we use the horizontal signals inside a triangle.

This new situation fixes what happens in between consecutive trilaterals of the same latitude. It is illustrated by figure 23. In our sequel, we shall only speak of bases.

As we introduced several important changes, we have to pay a new visit to the algorithm. Just after, we shall complete the set of tiles.

#### 4.2.2 The algorithm revisited

First, we construct a realization of the mantilla, see [9].

Then, we draw the isoclines, taking at random an  $F$ -centre which is the son of a  $G$ -flower. While drawing the isoclines, we assign them numbers in  $0..19$ , periodically. By definition, the numbering increases, downwards.

*The step 0*

*Triangles*

The step 0 of the construction is the drawing of the blue-0 trilaterals and its accompanying signals of the generation 0: the blue signals, to the

left and to the right emitted by the legs of the triangles of this generation.

For this purpose, each seed on the isocline 0 is the vertex of a blue-0 triangle whose legs are spread until the next isocline 10. The seed also sends a signal inside the triangle, the **scent** in the conditions we explained in sub-section 4.2.1. As this process is achieved when the construction of the phantoms of the generation 0 is completed, we consider it as independent of the further generations and, accordingly we shall not mention it. It will be implicit when we shall say that the active seeds of a certain generation do this and that. Each seed of the isocline 0 also emits three horizontal signals. One is the basis of a phantom of the generation 0 which is drawn along the whole isocline, from left to right, across the whole hyperbolic plane. The other signals are the horizontal blue signals emitted by the triangle. Due to the presence of the basis, they travel below the basis: they are the lower signals. They meet other lower signals emitted by the neighbouring seeds of the isocline 0 thanks to the blue join tile. And this phenomenon is repeated along the whole isocline.

The scent raises the green line when it reaches the isocline 5 and also, later, when it reaches the isocline 15. This green line is inside the triangle and it grows until it reaches the leg of the triangle where it is stopped. All seeds which are on the green line and which receive the scent become active. They emit legs of a red trilateral. We choose at random one isocline 5 in order to fix those which will generate the triangles of the generation 1. The blue 0 legs of the generation 0 go on until they reach the isocline 10. The seeds of the isocline 5 which are inside a blue-0 triangle are active and they also emit legs of the corresponding trilateral. They emit the basis of red phantoms which will travel on the isocline 5, to both its ends at infinity. They accompany this basis, by horizontal red signals which are placed below the basis. The seeds also similarly emit a scent inside the triangle which reaches the isocline 10. The seeds of the isocline 10 which receive the scent, and only them, become active. They emit legs of the phantoms of the generation 0. They also emit the basis of the blue-0 triangle. The basis signals merge and when they reach the legs of the seed, they form a corner at their intersection. The basis signal travels along the isocline in both directions, until its ends.

Note that the basis meets the legs of red triangles before it meets its expected legs. As there is no red triangle of a previous generation, there cannot be red signals inside a triangle of the generation 1 and so, the legs of the triangle determine a yellow signal on the isocline 10.

Besides the red basis, there is a single horizontal signal inside a triangle of the generation 0: the green signal which is on the isocline 5. The triangle

emits six horizontal blue signals: three on its left-hand side and three on its right-hand side.

Between triangles within the same latitude, these signals meet, using the blue join tile. We may place it wherever we wish, vertices and legs being excepted. Remember that between two consecutive corners of distinct triangles, there can only be one blue join tile. Indeed, the seeds of the isocline 10 are active if and only if they are on a basis of a blue-0 triangle and they receive the scent of a red triangle generated at the isocline 5.

### *Phantoms*

Now, let us look at the construction of the phantoms which are raised by the active seeds of the isoclines 10. Their latitudes are defined by the isoclines 10 up to 19 and the next isocline 0.

Consider an active seed  $\sigma$  of the isocline 10. It emits legs of a phantom and it also emits the basis of a blue-0 triangle. Now, as  $\sigma$  is an active seed of the isocline 10, it is on a branch starting from a seed  $\sigma_0$  of the isocline 0 belonging to the same interval  $[0..19]$  of isoclines as the considered isocline 10. Accordingly, the tree of the mantilla issued from  $\sigma$  is contained in the tree of the mantilla issued from  $\sigma_0$ . Accordingly, the legs issued from  $\sigma$  must meet a basis on the next isocline 0, downwards.

The legs of the phantom go down until they reach the isocline 15. The seed  $\sigma$  also diffuses a scent inside the phantom. When it reaches the isocline 15 it stops on tiles which are not a seed. When it meets a seed, as in the case of a triangle, the seed becomes active and the scent triggers the construction of a green line inside the phantom. But, contrarily to what happens in a triangle, in the case of a phantom, the legs do not stop the green line which goes on outside the legs of the phantom, looking after legs of a triangle which will stop the signal.

In our situation of the step 0, the different green lines which we have inside the legs of each red triangle of the generation 1 meet and, at the same time, they merge. Soon, they meet the legs of each triangle which stop them. At the same time, inside each red triangle, as long as the green line meets a seed which also receives the scent emitted by a the vertex of a phantom, the seed becomes active.

Now, at this moment, it is the starting point of the step 1.

But before looking at this step, we have to see what happens with the bases triggered by the seeds which lie on the isocline 0.

The basis itself goes to infinity in both directions and, consequently, it will serve as a basis for all blue-0 phantom of this latitude. Now, the basis is accompanied by a horizontal blue signal below the basis, a left-hand side

signal to the left of the seed, a right-hand side one to its right.

For these signals, either the basis meet legs of a blue-0 phantom, or they do not. If both signals starting from the seed meet such legs, each one on its side, being inside the blue-0 phantom, they form a corner with the legs, completing the construction of the corresponding blue 0 phantom. We notice that there is no horizontal signal above the basis inside the phantom. Also, at the joining point with the legs, the horizontal signal which is below goes on: as all seeds of the isocline 0 become active, a lot of them which are outside the basis of any phantom will emit the legs of a triangle and, consequently, below the basis of the phantom which we consider, the lower horizontal blue signals. They will join the one we consider thanks to the blue join tiles. Infinitely often, the bases of the isoclines 0 meet the legs of a blue-0 phantom inside the angle determined by the legs and this way, a phantom is constituted. But also infinitely often, much more on any interval of such an isocline than bases which succeed, the basis does not meet such legs. Note that this is known by the seeds of the isocline 0. If a seed of the isocline 0 receives the scent, it knows that it belongs to a branch which starts at least from the previous isocline 0. The branch may even join a traversal, but the seed cannot know it. But if the seed of the isocline 0 receives no scent, it knows that it starts a new branch.

A covered basis goes on on each side of such a corner until it meets a corner, which must happen, as infinitely many phantoms do exist within the considered latitude. When a corner is met, the upper horizontal signal merges with that of the corner and, in the next sub-section, we look at the tiles which implement this junction. Now, as the corners of the triangles emit upper horizontal blue signals, these signals will pass over the bases of the generation 0 which do not find legs to form a blue-0 triangles. The tiles will also bear this indication.

We shall deal with the other bases, those of the blue-0 phantoms and those of the red trilaterals of the generation 1 in the next point devoted to the induction step.

#### *The step $n+1$*

We define the starting point of the step  $n+1$  by the time when, drawing the legs of a triangle of the generation  $2n+1$ , they reach their mid-distance row. The first thing we do is to decide which of the concerned isocline 15 becomes a row of vertices of the simple blue triangles of the generation  $2n+2$ . Note that in this description, we shall never indicate that legs of a triangle emit upper horizontal signals of their laterality and in their colour, outside the triangle. This will be considered as obvious.

As the induction hypothesis, we assume the following:

(i) All trilaterals of the generation  $m$  with  $m < 2n$  are complete. In particular, all the horizontal signals which they emit are drawn. A signal can go out from a triangle of its colour. It enters a triangle  $T$  of its colour if and only if there is a leg of a triangle of its colour inside  $T$  and on this row. A signal crosses the triangles of the other colour which intersect its latitude and it also crosses any phantom which intersects its latitude. However, for trilaterals of their colour, the legs require to be crossed by signals of their laterality. For horizontal signals of another colour than that of the crossed legs, there is no restriction.

(ii) The bases for the generations  $m < 2n$  are completely drawn, up to infinity. The upper horizontal of the same colour accompanies them between consecutive trilaterals within the same latitude. It has the lateralities of the corners which emit them and the opposite lateralities are joined. For phantoms, the lower horizontal signal is everywhere present. Its different lateralities are joined appropriately.

(iii) All triangles of the generation  $2n$  are completed, with the same meaning as in (i).

(iv) All bases of the generation  $2n$  are completely drawn up to infinity. They are covered as required by an upper horizontal blue signal between consecutive trilaterals of the same latitude.

(v) All the vertices of the phantoms of the generation  $2n$  are determined and the legs which they emit are drawn until they meet the first green line of an isocline 15.

(vi) All the active seeds for the triangles of the generation  $2n+1$  are determined and the legs are drawn until they reach the mid-distance row determined by the phantoms of the generation  $2n$ : the isocline 15 found at (v).

Note that for  $n = 0$ , this is exactly the point which we have reached after the step 0.

Now, as the mid-point of the legs of the phantoms of the generation  $2n$  as well as those of the triangles of the generation  $2n+1$  are determined, we go on drawing these lines until they meet their respective bases.

For the legs of the phantom, we are now in their second half, they go on as long as they cross upper horizontal blue signals, whatever the accompanying signal. In particular, the upper horizontal blue signal may be accompanied by a red one.

The bases of the phantoms are emitted by the seeds which are on the mid-distance row of red triangles of the generation  $2n-1$ , this row being the

closest to the row  $\rho$  of the vertices of the considered phantoms, and below  $\rho$ . The bases grow, accompanied by a lower horizontal blue signal, and they travel on their row until they meet the legs. When this happens, if the basis is inside the angle determined by the legs, it cannot be covered by an upper horizontal blue signal. Indeed, a basis of a given generation does not travel on a row which belongs to the latitude of a triangle of its colour and of a previous generation. A horizontal signal of the generation  $2n$  on this row necessarily comes from the vertex of a triangle. Now, the signal can be an upper one only if it was put on this level by the corner of some phantom of the generation  $2n$ . This means that it has met the corresponding legs. Now, if this happens for one phantom, this also happens for the others, and at the same time.

Note that there is not a confusion with a basis which is outside a blue phantom of a previous generation: such a basis has two horizontal blue signals: an upper and a lower one. Now, the upper signal is emitted by a triangle which is inside the phantom. The row at which travels the expected basis is the first one, inside the angle determined by the phantom, on which there is no upper horizontal blue signal. Accordingly, the leg meets its basis on this row, as indicated above. In the next section, we shall see how the tiles force the right choice, thanks to the laterality of the signals, see page 0 in the proof of lemma 23.

This also fixes the row of the basis outside the phantoms of the generation  $2n$ . As indicated before, the basis signal  $\beta$  is drawn along the isocline from left to right across the whole hyperbolic plane. As there are seeds on an isocline 0 at any distance in number of isoclines from a given row and as far as desired from a given point on a row, there are always legs of phantoms of the generation  $2n$  which meet  $\beta$ . Now, the corner of these legs emit upper horizontal blue signals in the direction of their laterality. Consequently, between two consecutive corners belonging to different phantoms, the upper signal go towards each other. The blue join tile allows to perform the meeting. Now,  $\beta$  also crosses seeds which are not inside a phantom. Accordingly, these seeds emit a lower horizontal blue signal. Between two consecutive vertices, the configuration of the signals is the same as the configuration of an upper signal between consecutive corners of different phantoms. And so, the same joining pattern as for the upper signal allows to join two lower signals meeting each other. The exact configuration of the corresponding tiles is given in the next section.

At this point, the trialterals of the generation  $2n$  are completed, including the signals which accompany their bases along the whole row.

Let us now look at what happens with the legs of the triangles of the

generation  $2n+1$ .

They do the same as the legs of the phantoms of the generation  $2n$ . This time they look at the upper horizontal red signals which are interpreted in the same way. However, there is a difference: the legs also mark the free rows inside a triangle with the yellow signal. They perform this task exactly as it is depicted in the Euclidean case. Accordingly, the legs find their bases as the corresponding bases are emitted by the active seeds of the concerned isocline 15. The bases are drawn along the whole isocline, running without interruption from left to right, across the whole hyperbolic plane. Between two triangles of this generation and of the same latitude, the accompanying horizontal red signals make use of the same mechanism as what was just described for the phantom of the generation  $2n$ . Note that here, there is no lower signal as vertices of phantoms do not emit signals.

Accordingly, the red triangles of the generation  $2n+1$  are completed.

Now, we know that the seeds which are on the basis of a triangle of the generation  $2n+1$  and which are also on a green line of a triangle of the generation  $2n$  and which receive the scent of a seed of a blue-0 phantom are active and only them. We also know that they emit legs of phantoms of the generation  $2n+1$ , the issue of the basis of triangles which they emit being already considered.

The legs take into account the horizontal red signals only which emanate from the triangles of the previous generations. We know that in any model of the abstract brackets, a silent interval has the same structure of the intervals it contains as an active one. Accordingly, things happen exactly as it does for the triangles of this generation. The green signal is met at the place where the green line of the phantoms of the generation  $2n$  is. Indeed, this is the mid-distance row for these phantoms. Now, we know that for phantoms, the green signal is not stopped by the legs. Accordingly the signal goes further on both its sides. As this row is free of signals of the previous generations and as it does not contain a lateral signal of the generation  $2n$ , it is also free for the generation  $2n+1$ . Now, the legs of the phantoms of the generation  $2n+1$  also meet this green signal which also crosses their legs. The legs go on again until they meet the bases issued by the next free row, this time free of upper horizontal red signal. Indeed, this time the legs reach a row which is the mid-distance row of a triangle of the generation  $2n$ . We know that the active seeds inside those triangles in this row emit bases of phantoms. The discussion is exactly the same as for the phantoms of the generation  $2n$ .

And so, (i) and (ii) are true for the step  $n+1$ .

Now, while the phantom of the generation  $2n$  and the triangles of the



generation  $2n+1$  achieve their completion, the seeds on the defined rows for the vertices of the triangles of the generation  $2n+2$  have started to emit signals: they are the seeds which are on the just selected isoclines 15 and which receive the scent of a blue-0 phantom and which are on the green line. Accordingly, these seeds are also on a branch.

Let  $T$  be a triangle of the generation  $2n+2$ . Its legs go downwards as long as they meet an upper horizontal blue signal. One of these signals is accompanied by the basis of the triangle  $T_0$  of the generation  $2n+1$  which has generated  $T$ . During their travel, the legs of  $T$  also meet bases of phantoms from the generation 0 until the generation  $2n$ . For what is the blue phantoms, these bases are emitted by the vertices of the blue triangles already present in  $T$ . All these phantoms contain the vertex of  $T$ . Accordingly, as their bases, at this point, did not yet reached their legs, they are open and they are only accompanied by the lower signal only for what is their colour. And so, a blue basis is not accompanied by the upper horizontal blue signal. The leg of  $T$  must not disturb this configuration by introducing an upper horizontal blue signal outside. Consequently, the leg does not emit such a signal in this case. It considers that the lower signal is enough to indicate that the considered row is not free. Note that these signals occur before the legs of  $T$  meet the basis of the triangle  $T_0$ .

Now, there are other basis signal of a phantom which are accompanied by an upper horizontal signal: they concern phantoms which are inside  $T$ . The legs also must not undo such signal. We see, in the next section, in the proof of lemma 23, that the tiles make the difference and do not allow to replace the established situation by the opposite one. For each phantom of such a generation, from the generation 0 until the generation  $2n$ , its basis accompanies the upper horizontal blue signal. Note that these signals occur along the whole way of the legs of  $T$ .

At last, the legs of  $T$  meet the first free row. It is the green signal already met by the phantoms which are generated by the appropriate seeds of the basis of  $T_0$ . Consider  $P$  such a phantom. As the green signal which runs on the mid-distance row of  $P$  is not stopped by the legs of  $P$ , the signal will meet the legs of  $T$  and it will be stopped by these legs. Indeed, the legs go until this row as, from lemma 11, the inside of the half of a blue active interval exactly consists of juxtaposition of the blue active intervals of the previous generations. And so, the free row precisely occurs at this row.

The legs go on, it is now their second part which reacts differently than the first part as some events which happen for the first part cannot happen for them. Again, the legs meet upper horizontal blue signals from the triangles of the previous generations. Then, we have the basis emitted by

the green signal of the triangles of the generation  $2n+1$  which are issued from  $P$ . This basis meets also similar bases produced by red triangles of the generation  $2n+1$ , all contained in the tree of the mantilla which is rooted at the vertex of  $T$ . Accordingly, the basis will meet the legs. As previously, the basis travels on a row which has no horizontal signal. Accordingly, it is clearly identified and it cannot be confused with previous blue bases which are accompanied by a upper horizontal blue signal. We again have the same discussion for what happens with the bases outside the triangle: the corners emit an upper horizontal blue signal which meets a similar signal but of the opposite laterality emitted by the neighbouring corner of another triangle. The blue join tile allows the signal to meet.

Accordingly, the items *(iii)* and *(iv)* are also true at the step  $n+1$ .

Now, the bases of the triangles of the generation  $2n+2$  contain active seeds which emitted them and which now emit the legs of the phantoms of the generation  $2n+2$ . Let  $P_2$  be such a phantom. Its legs go down and thanks to lemma 11, we know that the first occurrence of a free green signal is on the mid-distance row of the phantoms of the generation  $2n+1$  which are inside the triangle  $T_1$  of the generation  $2n+1$  which has generated  $P_2$ . And, as legs of a phantom, the legs of  $P_2$  do not stop the green signal.

Accordingly, the item *(v)* of the induction hypothesis is also true for the step  $n+1$ .

Now, when the triangles of the generation  $2n+2$  have reached their mid-distance row, this has triggered the construction of the trilaterals of the generation  $2n+3$ . At this time, one of the concerned isocline 15 is chosen as a row where all the active seeds generate a triangle of the generation  $2n+3$ . The construction of the legs go as usual, the same phenomena as for the construction of the triangles of the generation  $2n+2$  occur for what regards the crossing of bases of the phantoms of the generations from 0 up to  $2n+1$  which may be accompanied or not by an upper horizontal signal. As in the case of the generation  $2n+2$ , the legs of the triangles of the generation  $2n+3$  do not undo the previous constructions. Now, as red legs, the legs of the triangles of the generation  $2n+3$  detect the free rows inside the triangle by the technique already described for the Euclidean triangles. And the first green signal met by the legs is the one we just describe for the phantom  $P_2$  or one of its copies in the same latitude.

And this proves that the item *(vi)* is also true for the step  $n+1$ .

Consequently, all items of the induction hypothesis are also true for the step  $n+1$ .

This proves that the construction of a tiling implementing the interwoven triangles is possible by using the just described algorithm.

### 4.2.3 The new set of tiles

The implementation of the square tiles of section 3.4.2 in heptagonal tiles does not present major difficulties. It is simply a translation process which we now indicate.

*From the square tiles to the heptagonal ones*

The square tiles of section 3.4 bear two kinds of signals: vertical and horizontal ones.

In the translation of the square tiles into the heptagonal ones, the horizontal signals will follow the route of the isocline signal. For the verticals, the things are not more complex. Going back to the construction of the isoclines and remembering lemma 4, we first notice that we need only to use black nodes for the vertical signals. The route of a left-hand side leg goes along the leftmost branch of a tree of the mantilla. Accordingly, in our black tiles, this route goes from the edge 1 to the edge 4 in paternal coordinates. The route for a right-hand side leg goes along the rightmost branch of a tree of the mantilla. And so, this route goes from the edge 2 to the edge 6 in paternal coordinates: remember that the right-hand side border of a tree of the mantilla consists of the black-nodes whose father is not in this tree.

For this reason, we do not provide the representation of these tiles in their heptagonal setting. Also, we shall keep the Euclidean format to present the new tiles required for the horizontal signals, to manage the new definition of the bases connected with the synchronization. The Euclidean format will also be used for the vertical signals of the construction which we have up to now considered.

*The tiles for the horizontal signals*

We mainly have two kinds of new tiles: the tiles for introducing the horizontal blue signals in our previous setting, *i.e.* for inside the trilaterals and the tiles for joining signals outside the trilaterals, *i.e.* between two consecutive trilaterals of the same latitude.

As already announced in section 3.4, we shall not list pictures of the tiles: there are too many of them. Instead, we shall make use of the tools we introduced in the Euclidean representation of the interwoven triangles. We have just to change a bit the elementary patterns from which we construct the formulas with which we represent the different combinations of patterns leading to the needed prototiles. This will allow us to make up tables which allow to indicate all kinds of tiles. We shall also use the tree-like representation of formulas in order to count the number of prototiles. The total number, which we obtain in a table summing up the partial sums, will

explain why we do not provide pictures of the prototiles.

*The elementary patterns*

In order to facilitate the reading, we repeat the patterns which we already introduced in section 3.4. We present the patterns by groups concerning the information which they convey. The groups have names but, as the situation is much more complex than in the Euclidean situation, the names of certain groups are changed: for example, the names of the horizontal red and blue signals are different, as here we have also blue signals, as we have upper and lower signals. We also have new joining patterns and the corners are modified with respect to the Euclidean tiles in order to take into account that all trilaterals of the same latitude have a common basis.

Remember that the basic signals are the **legs**, the **bases**, the **informations** and the **joins**. They are given **names** which indicate the characteristics which they contain. Such characteristics which may vary from tile to tile inside the same group can be represented by variables which we denote by greek letters. Such a variable will have the same meaning in all the patterns which we shall describe. The letters and their meaning are given by table 4, as well as their possible values.

The legs are vertical patterns. The bases are horizontal patterns. The informations can be vertical or horizontal.

As previously, the legs have 24 elementary patterns, depending on the type, triangle or phantom, the colour, simple blue or red, the half, first or second half of the leg and the laterality: left-hand side or right-hand side. They are represented in figure 24. Note that the colour blue-0 occurs for legs only in the passive zones. And so, for trilaterals of this colour and on active rows of the mantilla, their legs only consists of elementary patterns belonging to the join signals.

$\gamma$	colour of the trilateral	$b_0, b_n, r$
$\tau$	status of the trilateral	$t, \varphi$
$\pi$	position of a horizontal signal	$u, l$
$\xi$	laterality of a signal	$l, r$

**Table 4** *The table for the variables in the names of the patterns*

The names for the legs are those of section 3.4. We remind them here for the conveniency of the reader. The names have the form  $L\gamma\tau\pi\xi$ . They can be listed as follows, corresponding to the usual order inferred from figure 24:

$Lb_0tul$   $Lb_0tur$   $Lb_0tbl$   $Lb_0tbr$   $Lb_0\varphi ul$   $Lb_0\varphi ur$   $Lb_0\varphi bl$   $Lb_0\varphi br$   
 $Lb_ntul$   $Lb_ntur$   $Lb_ntll$   $Lb_ntlr$   $Lb_n\varphi ul$   $Lb_n\varphi ur$   $Lb_n\varphi ll$   $Lb_n\varphi lr$   
 $Lrtul$   $Lrtur$   $Lrtll$   $Lrtlr$   $Lr\varphi ul$   $Lr\varphi ur$   $Lr\varphi ll$   $Lr\varphi lr$

Similarly, we constitute the elementary patterns of the group bases. There are four of them, listed as follows, and defined by their type, triangle or phantom, their colour, red or blue. They are indicated by the following names which follow the pattern  $\boxed{B\gamma\tau}$ :

$Bb_nt$   $Bb_n\varphi$   $Bb_0t$   $Bb_0\varphi$   $Brt$   $Br\varphi$

We notice that this time  $\gamma \in \{b_0, b_n, r\}$  as blue-0 trilaterals have to be taken into account. They are represented in figure 25.

The information signal is more important. It contains horizontal and vertical signals.

For what is about horizontal signals, they concern the following situations. First, we have the horizontal signal emitted by the legs of the triangles: blue and red. We also know that these signals have a laterality: left-hand side and right-hand side. They also have a level in the tile: upper and lower. Accordingly, we have eight of them, listed as follows and illustrated in the first row of figure 26. We have also the yellow signal for the free rows inside red triangles and the green signal which indicates the mid-distance row of a trilateral.

These are the horizontal signals of the group. There is a second subgroup: the vertical signals which are represented by the scent of a trilateral. As already seen, this signal is only attached to an active seed in order to define new active seeds on the isoclines 5, 10 and 15, as we know that all seeds on the isoclines 0 are active. And so, there are two types of signalization,

a. leg patterns:

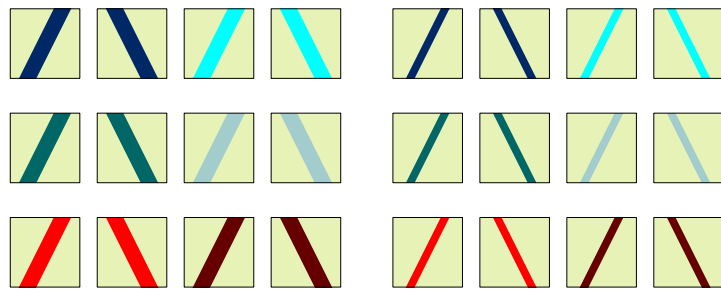


**Figure 24** *The elementary patterns of the legs.*

depending on the node which transmits the signal: either a black node or a white one. In the sub-section 4.2.2, we indicated that the scent does not

concern the nodes which are on the legs of the trilateral. However, in order to reach all nodes which are inside the trilateral zone covered by the scent, it is simpler to also send the signal to the legs: simply, they are not affected by this signal. It will be superposed to that of the legs when it is needed. However, this signal also travels with counting marks: when it reaches the mark 5, the signal stops if it is not a seed and it goes on with the mark 0 if it reaches a seed which, by this fact, becomes active. The corresponding tiles are also indicated in figure 26.

*b.* basis patterns:

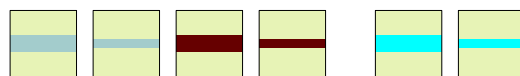


**Figure 25** *The elementary patterns of the bases.*

The names of the patterns have the following syntax:  $\boxed{H\gamma\xi\pi}$ , with  $\gamma$ ,  $\xi$  and  $\pi$  with their usual meaning. Two tiles have the pattern  $\boxed{H\gamma}$ , with  $\gamma \in \{g, y\}$ , as it concerns the green and the yellow signals. For the scent, we have names of the form  $\boxed{S\omega\nu\kappa}$  where  $\omega \in [0..4]$ ,  $\nu \in \{b, w\}$  and  $\kappa \in \{s, c, f\}$ . The index  $\omega$  is the number of the isocline of the tile modulus 5. The letters  $b$  and  $w$  correspond to black and white, the status of the tile as a node in the Fibonacci carpet. The symbols  $s$ ,  $c$  and  $f$  correspond to the start, the continuation or the final point of the signal.

The names are:

$Hblu$     $Hbru$     $Hrlu$     $Hrru$     $Hbll$     $Hbrl$     $Hrll$     $Hrrl$   
 $Hg$     $Hy$

and, for the horizontal red and blue signals and, for the scent they are as follows:

$S0bc$     $S0bs$     $Sibc$     $Siwc$     $S0bf$     $S0wf$

with  $i \in [0..4]$ . The corresponding tiles are displayed by figures 26 and 27.

The join group is also important and it introduces a new situation.

There are four types of join tiles: those for leg signals, those for bases and legs, those for information signals, see below, figure 28.

There are two cases for the join of legs. The first case consists in joining two legs of the same type, colour and place but with different laterlaties: this means the vertex. There are six kinds of vertices. Their names are of the form  $\boxed{V\gamma\tau}$ . Accordingly, we have:

$$Vb_0t \quad Vb_0\varphi \quad Vb_nt \quad Vb_n\varphi \quad Vrt \quad Vr\varphi$$

It is not difficult to see that  $V\gamma\tau = \mu_B(\mu_L(L\gamma\tau ul) + \mu_R(L\gamma\tau ur))$ , where  $A + B$  denotes the superposition of the two tiles  $A$  and  $B$ . In some sense, we can see the names  $V\gamma\tau$  as useful shortcuts for much longer expressions.

c. info patterns:

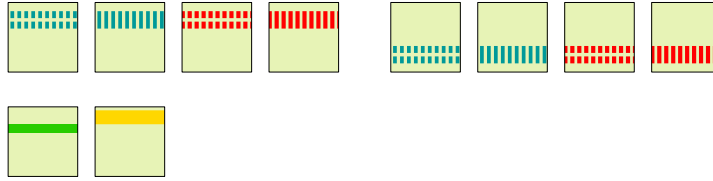


**Figure 26** The elementary patterns for the horizontal signals: red, blue, yellow and green.

The second case of joining legs concerns legs of the same type, the same laterality and the same colour but of different places. This concerns the tile which is placed at the mid-distance row of a trilateral, on one of its legs. There are again twelve kinds of such tiles, again taking into account the blue-0 colour. See also figure 28 for illustration.

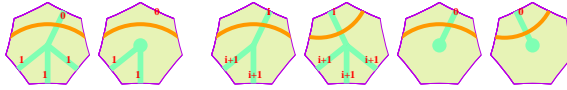


**Figure 27** The elementary patterns for the scent.  
Here we take the heptagonal form as the tree structure is used by the tiles.

The names for this cases are of the form  $\boxed{M\gamma\tau\xi}$ , namely:

$$\begin{array}{cccccc} Mb_0tl & Mb_0tr & Mb_ntl & Mb_ntr & Mrtl & Mrtr \\ Mb_0\varphi l & Mb_0\varphi r & Mb_n\varphi l & Mb_n\varphi r & Mr\varphi l & Mr\varphi r \end{array}$$

It is not difficult to see that  $M\gamma\tau\xi = \mu_L(L\gamma\tau l\xi) + \mu_R(L\gamma\tau u\xi)$ .

Our last group deals with joining bases and legs at the occasion of a corner and the joining of horizontal signals of different lateralities in the acceptable conditions.

There are twelve kinds of corners, again the blue-0 colour being counted. Their name is of the form  $\boxed{C\gamma\tau\xi}$ . We have:

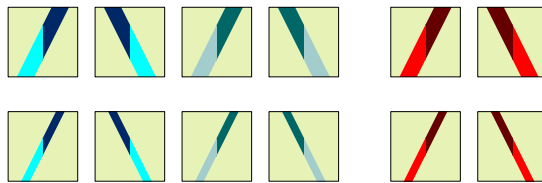
$$\begin{array}{cccccc} Cb_0tl & Cb_0tr & Cb_ntl & Cb_ntr & Crtl & Crtr \\ Cb_0\varphi l & Cb_0\varphi r & Cb_n\varphi l & Cb_n\varphi r & Cr\varphi l & Cr\varphi r \end{array}$$

d. join patterns:

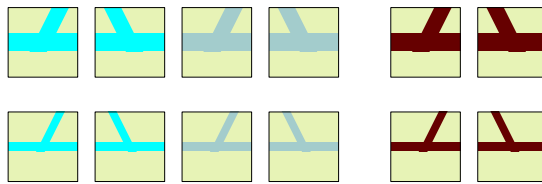
the vertices:



the mid-points:



the corners:



the joining tiles for horizontal signals:

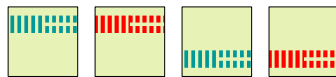


**Figure 28** *The elementary patterns for the join tiles.*

*For the crossing of legs and bases, we have all possible cases for blue and red legs, the blue-0 case being excluded by definition, and also all possible cases for the basis, this time the blue-0 case being taking into account.*

Here also we notice that the join signal is a composed expression. It is rather complex:  $C\gamma\tau\xi = \mu_T((L\gamma\tau u\xi) + B\gamma\tau) + \mu_B(B\gamma\tau)$ . Indeed, in the signals where a basis is involved, we assume that the basis signals stands symmetrically with respect to the horizontal mid-distance line of the tile. Accordingly, the rôle of the second making operator consists in restoring the other part of the basis signal which is cancelled by the pplication of the first one. At last, we have the joining of horizontal signals: a right-hand



side signal coming from the left meets a left-hand side signal coming from the right. Their joining is permitted and so, the corresponding tiles are provided. They are of the form  $\boxed{J\gamma\pi}$ , namely:

$$Jbu \quad Jru \quad Jbl \quad Jrl$$

It is not difficult to see that  $J\gamma\pi = \mu_L(H\gamma r\pi) + \mu_R(H\gamma l\pi)$ .

*Construction of the tables of the tiles*

We define the tiles by grouping them as follows: vertices, first half of the legs, mid-distance points, second half of the legs, corners, bases, horizontal signals. To this purpose, we assemble the previous patterns. To simplify the expressions, we shall make use of the abbreviations which we have just introduced in the previous part of this sub-section.

We shall gather the results of the study into tables which will also allow us to count the prototiles, namely tables 5 and 6 for the description of the prototiles and table 7 for the counting.

Before entering the precise study of each group, let us make a few remarks. As we said, we have mainly two kind of signals: horizontal and verticals.

As indicated in sub-section 4.2.1, the legs go along the borders of a tree of the mantilla. We know that, the vertex being excepted, we have four tiles involved for each side. Remember that the tiles are  $s.F$ ,  $b.1 \circ 1\bar{3}$ ,  $b.11 \circ 2$ ,  $b.G_r$ ,  $b.1 \circ 15$  for the right-hand side leg and  $s.F$ ,  $b.\bar{5}7 \circ 7$ ,  $b.6 \circ 77$ ,  $b.G_\ell$  and  $b.37 \circ 7$  for the left-hand side leg, see figure 20. One tile is used once and it is adjacent to the vertex:  $b.1 \circ 1\bar{3}$  for the right-hand side and  $b.\bar{5}7 \circ 7$  for the left-hand one. The three other tiles are endlessly used in a periodical way. As the vertex stands on a row of the mantilla, as the distance between two rows is 5 in terms of isoclines and as the period of the tiles along a leg is 3, all the tiles of the period appear on the successive rows crossed by the legs and the aperiodic part is used only with the isoclines 1, 6, 11 and 16. And so, we have three groups of vertical patterns, independent of our marking, for each side of a leg: 4 patterns coming from the aperiodic part, 12 patterns for the rows of the mantilla and 48 patterns for the passive zones.

Now, for the horizontal signals, the situation is very different: the tiles which support them are on any row of the mantilla, which makes 4 cases and all tiles of the mantilla are then possible,  $s.F$  being included when we have to do with a silent seed. This makes  $4 \times 34 = 136$  patterns. Most often, these patterns have to be multiplied by the number of various superpositions which we use to define the prototiles.

In what follows, we shall have to deal with various ways of meetings

between vertical and horizontal signals. Most often, the horizontal signals involve a basis. The next formulas indicate which signals may accompany a basis.

Indeed. Consider a basis  $\beta$ . We have a first distinction according to the colour: we know that only blue-0 basis may be accompanied by a yellow signal and that they are never accompanied by a green one which travels on the isoclines 5 and 15.

Next, a basis may or not be accompanied by a horizontal signal. If this is the case, there may be a yellow signal, an upper horizontal signal of a blue or red colour and there may also be a lower horizontal signal. We know that when an upper horizontal signal has the same colour as the basis we say that the basis is covered. At last, we also know that a basis may receive a scent or not.

What we above discussed introduces the following terms:

$$\begin{aligned}\epsilon_y &= \mathbf{1}_{\{\text{yellow row}\}}, \\ \epsilon_c &= \mathbf{1}_{\{\text{covered basis}\}}, \\ \epsilon_s &= \mathbf{1}_{\{\text{scent received}\}}, \\ \epsilon_a &= \mathbf{1}_{\{\text{accompanying horizontal signal}\}}.\end{aligned}$$

And so, we have the following representation for a blue-0 basis, using additional variables  $a$ ,  $b$  and  $c$  with values in  $\{0, 1\}$ :

$$\begin{aligned}(B_{b_0}) \quad & Bb_0\tau + \epsilon_a \cdot (\mathbf{1}_{\{\tau=\varphi\}} \cdot (a.Hb\xi_1l + \bar{a}.Jbl) + \epsilon_c \cdot (b.Hb\xi_2u + \bar{b}.Jbu) \\ & + \epsilon_y.Hy + \bar{\epsilon}_y \cdot (c.Hr\xi_3u + \bar{c}.Jru) + \epsilon_s.S0\nu f), \\ & \text{with } \epsilon_c \Rightarrow \bar{\epsilon}_s, a, b, c \in \{0, 1\} \text{ and } (a+b)(b+c)(c+a) > 0, \\ & \text{with also the conditions } \bar{\epsilon}_c \Rightarrow b \text{ and } \tau = t \Rightarrow c.\end{aligned}$$

First, we keep the possibility of a basis alone: this may happen in amplitudes of red trilaterals in the butterfly model.

When there is an accompanying signal, the formula takes into account that a blue-0 basis cannot be a mid-distance row and so, we again get that a blue-0 basis is never accompanied by a green signal. Now, if the basis receives the scent, as we consider a tile of a basis which is not a vertex, it can only terminate the branch which arrives to it. Also, a scent can reach an open basis only, whence the condition  $\epsilon_c=1 \Rightarrow \epsilon_s=0$ . Now, when the basis has an accompanying horizontal signal, either blue or red, it may also be the mark of a join tile. Such a case may also occur for the lower horizontal signal. However, as upper and lower joining signals obey different conditions, we do not permit that the same tile could be used to join more than two lateralities of the same kind of signal: it must be for a single colour and a single position. This is why we have the condition  $(\alpha+\beta).(\beta+\gamma)(\gamma+\alpha) > 0$ .

For conveniency, in order that the latter formula be true, we impose the conditions  $b = 1$  when  $\epsilon_c = 0$  and  $c = 1$  when  $\tau = t$ .

A tree-like representation of the formula may help to count the number of cases: each possibility gives rise to a different tile, see figure 29. The nodes represent the conditions. The left-hand side deals with the value 0 and the right-hand side with the value 1. For the nodes labelled by  $\tau$ , the left-hand side corresponds to the value  $\tau = t$ , *i.e.* the case of the triangles, and the right-hand side corresponds to  $\tau = \varphi$ , *i.e.* the case of the phantoms.

In figure 29, on the right-hand side, we can see two different  $\epsilon_c$  trees. The leftmost one corresponds to the blue sub-trees of the left-hand side of figure 29, where the number 23 is indicated. This number counts the leaves of the tree. Indeed, this  $\epsilon_c$ -tree has four  $\epsilon_y$ -trees. Those which depend on the node  $b$  are in the branch  $\epsilon_c = 1$  of the  $\epsilon_c$ -tree. Accordingly, necessarily,  $\epsilon_s = 0$  and so, in this case, the  $\epsilon_s$ -trees have one leaf exactly. Now, in the  $\epsilon_y$ -tree which is on the left-hand side of the  $b$ -tree, which means that  $b = 0$ , necessarily,  $c = 1$  and so, one  $\epsilon_s$ -tree is missing in this  $\epsilon_y$ -tree which has 3 leaves. The other  $\epsilon_y$ -trees in the right-hand side sub-tree of  $b$  have 4 leaves. Now, in the  $\epsilon_y$ -tree which is in the left-hand side of  $\epsilon_c$ , we have  $a = b = 1$ , and all the  $\epsilon_s$ -trees have 3 leaves as, in this  $\epsilon_y$ -tree, as  $\epsilon_c = 0$ , there is no constraint on  $\epsilon_s$ . And so we have 12 leaves. And now, it is easy to check that the corresponding  $\epsilon_c$ -tree has 23 leaves.

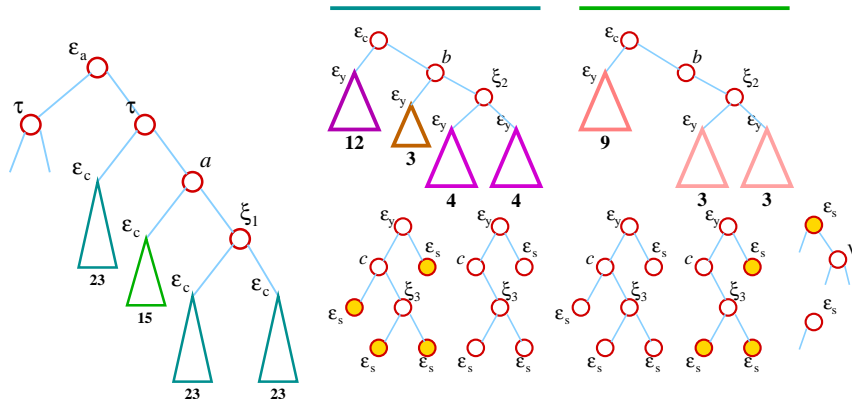


**Figure 29** The counting for formula  $(B_{b_0})$ . Remember the conventions: for an  $\epsilon_i$ -node, or an  $x$ -node,  $x \in \{a, b, c\}$ , we have 0 to the left and 1 to the right; for  $\tau$ -nodes,  $t$  to the left and  $\varphi$  to the right. The figure also indicate the number of leaves in the involved  $\epsilon_c$ -trees and explicits the counting inside  $\epsilon_c$ -,  $\epsilon_y$ - and  $\epsilon_s$ -trees.

Now, on the left-hand side of the node  $a$ , we have an  $\epsilon_c$ -tree which has only 15 leaves. This comes from the fact that, as  $a = 0$ , we must have  $b = c = 1$ . This rules out the  $\epsilon_y$ -tree which is on the left-hand side of  $b$ , and in all the remaining  $\epsilon_y$ -trees, we have only three  $\epsilon_s$ -tree. As previously, on the right-hand side of  $\epsilon_c$ , all the  $\epsilon_s$ -trees have one leaf only while they all have three leaves in the left-hand side of  $\epsilon_c$ . Hence, the total number of 15 leaves.

There are four  $\epsilon_c$ -trees and, from the above analysis, we know that three of them have 23 leaves and one of them has 15 leaves. Accordingly, we have 86 possible patterns with the two ones without accompanying signal.

Now, let us look at how many prototiles we obtain. As already mentioned, a horizontal signal travels on the rows of the mantilla and, on each of them it may be any of the 34 possible tiles of the mantilla. Now, blue-0 signals travel only on isoclines 0 or 10: isocline 0 for the case  $\tau = \varphi$  and isocline 10 for the case  $\tau = t$ . Accordingly, the difference between the isoclines is already marked by the basis. And so, we only have to take into account that on each isocline, we may have all the possible patterns of the mantilla. And so, we find that formula  $(B_{b_0})$  defines 2924 prototiles.

At last, for a later use of the formula, we shall denote it by  $B_{b_0}(\tau, \xi_i, \epsilon_i, x)$ . When a parameter  $\omega$  will be fixed, we shall write  $B_{b_0}(\tau, \xi_i, \epsilon_i, x)[\omega := \alpha]$ , where  $\alpha$  is the value, given to  $\omega$ .

We have a similar treatment for simple blue and red bases, where we replace  $\epsilon_y$  by  $\epsilon_m = \mathbf{1}_{\text{mid-distance row}}$ . Also, as a simple blue basis is always accompanied by a horizontal signal we do not use the condition  $\epsilon_a$  of formula  $(B_{b_0})$ .

$$(B_{b_n, r}) \quad B\gamma\tau + \mathbf{1}_{\{\tau=\varphi\}} \cdot (a.H\gamma\xi_1l + \bar{a}.J\gamma l) + \epsilon_c \cdot (b.H\gamma\xi_2u + \bar{b}.J\gamma u) \\ + \epsilon_m \cdot (Hg + \mathbf{1}_{\{\gamma=b_n\}}.Hy) + \bar{\epsilon}_m \cdot (c.H\bar{\gamma}\xi_3u + \bar{c}.J\bar{\gamma}u) \\ + \epsilon_4.S0\nu f, \\ \text{with } \epsilon_s \Rightarrow \epsilon_m \text{ and } \epsilon_c \Rightarrow \bar{\epsilon}_s, \text{ and with } a, b, c \in \{0, 1\}, \text{ together} \\ \text{with the conditions } (a + b)(b + c)(c + a) > 0, \bar{\epsilon}_c \Rightarrow b \text{ and} \\ \tau = t \Rightarrow c.$$

Indeed, we have to remember that when a tile receives the scent, it is the mid-distance row of some trilateral and so, it must emit the green signal. This is why the condition  $\epsilon_s \Rightarrow \epsilon_m$  is appended to the formula. Note that, in particular, if  $\epsilon_s = 0$ , we may also have a green signal: this is to extend the signal inside the whole trilateral for which this signal lies on the mid-distance row. Now, if the basis is covered, it cannot receive the scent, as in the case of a blue-0 basis. We have the same signification for  $a$ ,  $b$  and  $c$  as in formula  $(B_{b_0})$  and with the same conditions.

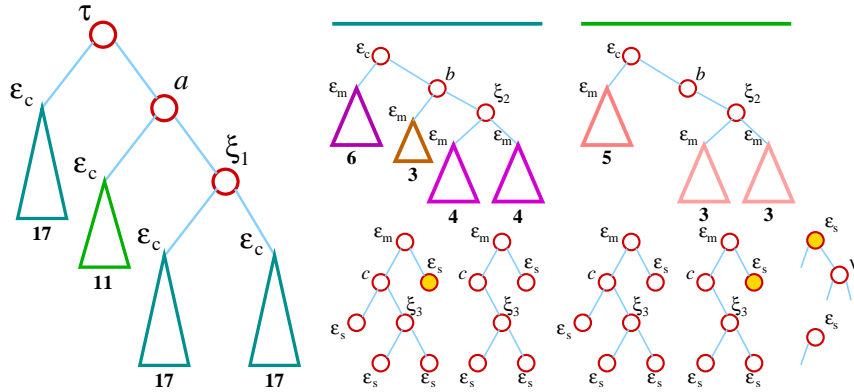


**Figure 30** The counting for formula  $(B_{b_n, r})$ . Remember the conventions: for an  $\epsilon_\alpha$ -node, 0 to the left, 1 to the right; for  $\tau$ -nodes,  $t$  to the left and  $\varphi$  to the right. Note here the  $\nu$ -node:  $\nu$  has two possible values:  $b$  or  $w$ . The figure also indicate the number of leaves in the involved,  $\epsilon_c$ -,  $\epsilon_m$  and  $\epsilon_s$ -trees.

The formula can also be represented in a tree-like form, see figure 30, which is very near figure 29. Now, in the counting, we have two conditions this time on the  $\epsilon_i$ 's. We again have 4  $\epsilon_c$ -nodes, each one ruling over 4  $\epsilon_s$ -trees. We deal with the condition  $\epsilon_c \Rightarrow \overline{\epsilon_s}$  as we did in the case of formula  $(B_{b_0})$ . This gives the same number of leaves as we have found in for formula  $(B_{b_0})$ . Now the condition  $\epsilon_s \Rightarrow \epsilon_m$  means that if  $\epsilon_m = 0$ , then  $\epsilon_s = 0$ . This exactly cancels six leaves in the  $\epsilon_m$ -trees with respect to the  $\epsilon_c$ -trees in the sub-tree where  $\epsilon_c = 0$  in the case when  $a = b = 1$  and it cancels four leaves in these trees when  $a = 0$ . This can be seen on the right-hand side part of figure 30, where we develop the  $\epsilon_m$ - and  $\epsilon_c$ -trees. As a consequence, here an  $\epsilon_c$ -tree has only 17 leaves instead of 23 in the case of  $(B_{b_0})$  when the conditions on  $a$ ,  $b$  and  $c$  change nothing. The exact counting is indicated in the figure. We have 62 patterns for each colour, so that the total number of patterns is 124.

The counting of the prototiles is simpler: we know that these bases travel on isoclines 5, used only by red signals and 15 used by simple blue and also red signals. And so, we have  $34 \times 3 \times 62 = 6324$  prototiles.

As for formula  $(B_{b_0})$ , the formula will later be used under the form  $B_{b_n, r}(\gamma, \tau, \xi_i, \epsilon_i, x)$  and use the same notation as for  $(B_{b_0})$  when we have to fix parameters.

Remark that the join pattern for the two lateralities of a horizontal signal can be used with a basis only. Hence, for the other tiles, we no more need this pattern. This means that  $a = b = c = 1$  in both  $(B_{b_0})$  and  $(B_{b_n, r})$

when they are used in a superposition with another pattern. Accordingly, we shall omit  $x$  in the notation of these formulas when we shall use them.

Let us now start our study with the vertices. Clearly, they are not exactly of the form  $V\gamma\tau + B\gamma\bar{\tau}$ , because, when horizontal signals of the colour  $\gamma$  occur, they appear with both lateralities. And so, we cannot easily use the general formulas for the basis. Accordingly, for the vertex and also for the mid-point tile we proceed in the same direct way.

If  $\tau = t$ , then the vertices emit lower horizontal signals of the same colour as the legs. In this case, we append the term  $\mu_L(H\gamma ll) + \mu_R(H\gamma rl)$ . Blue-0 signals being excepted, a vertex is always inside a triangle, moreover, of the opposite colour. More precisely, a vertex of a trilateral of the generation  $n+1$  occurs on the mid-distance row of a triangle of the generation  $n$ . Accordingly, it is always accompanied by a green signal. Now, the vertex of a simple blue trilateral arises on the mid-distance row of a red triangle of the previous generation. Now, such a row is free in the red triangle, and so, it is accompanied by a yellow signal. However, the vertex of a red trilateral occurs on the mid-distance line of a blue-0 or a simple blue triangle, where it is a free row, but it is not marked with a yellow signal.

Now, we come to the case of a blue-0 vertex. If it is on an isocline 0, which means that the basis is that of a phantom, as  $\tau = t$ , we may have that the basis is open and we may also have that it is covered. It also has a yellow signal if it is on the free row of a red triangle. Otherwise, it has an upper horizontal red signal: it is not on a free row of a red triangle or it is, but at this place and, in this latitude, the red triangle is missing. In this latter case, as the vertex is inbetween two consecutive red triangles, it has an upper horizontal red signal. Recall that as the tile is a vertex, it cannot be a join tile.

If the vertex is on an isocline 10, this corresponds to the case when  $\tau = \varphi$ , the basis is never covered, as it is a basis of a triangle. Now, the vertex is inside a red triangle or a red phantom, both of the generation 1. If it is inside a red triangle  $T$ , the basis is on a free row of  $T$  and so, it has a yellow signal. If it is inside a red phantom, it may be on the free row of a bigger triangle. Or it may be not or, as previously, it is on the free row of a missing red triangle.

At last, there is a scent connected with the vertex. The scent is on a branch if the  $\gamma \neq b_0$ . When  $\gamma = b_0$  and  $\tau = t$ , the scent is starting if the basis is covered but it may be on a branch or not in the other cases.

And so, we have the situations described by formula (V), below.

$$\begin{aligned}
(V) \quad & V\gamma\tau + B\gamma\bar{\tau} + \mathbf{1}_{\{\tau=t\}}(\mu_L(H\gamma ll) + \mu_R(H\gamma rl)) \\
& + \mathbf{1}_{\{\gamma \neq b_0\}}(Hg + \epsilon_s \cdot S0bc + \mathbf{1}_{\{\gamma=b_n\}} \cdot Hy) \\
& + \mathbf{1}_{\{\gamma=b_0\}}(\epsilon_y \cdot Hy + \bar{\epsilon}_y \cdot H\bar{\gamma}\xi_1 u \\
& \quad + \epsilon_s \cdot S0bc + \bar{\epsilon}_s \cdot (S0bs + \epsilon_c \cdot H\gamma\xi_2 u))
\end{aligned}$$

Note that here,  $\epsilon_c$  and  $\epsilon_s$  are independent as the occurrence of  $\epsilon_c = 1$  is connected with the starting of the scent.

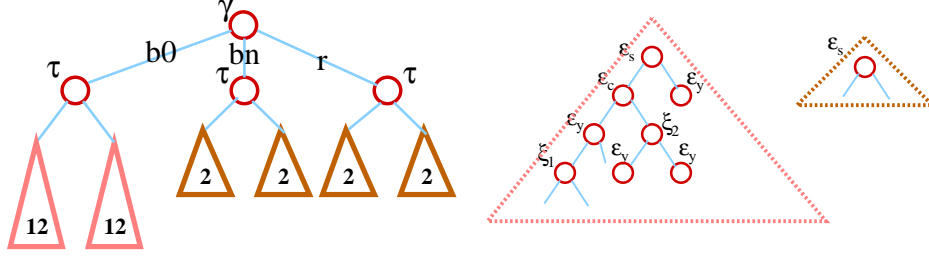


**Figure 31** The counting for formula (V). Note that the node  $\gamma$  has three sons. Indeed,  $\gamma$  has three possible values:  $b_0$ ,  $b_n$  and  $r$ .

The tree-like representation is given by figure 31, where the node  $\gamma$  has the degree 3, corresponding to the values  $b_0$ ,  $b_n$  and  $r$ , as indicated in the figure.

From the figure, it is clear that we have  $2 \times 12 + 4 \times 2 = 32$  cases for this pattern.

From this counting, we can find out the number of prototiles: each pattern goes with only the pattern  $s.F$  of the mantilla. Blue-0 vertices are on the isoclines 0 and 10, red ones on the isoclines 5 and 15 and simple blue on the isocline 15 only. Figure 31 allows to count the patterns according to the colours: And so this gives us  $24 + 4 \times 2 + 4 \times 1 = 36$  prototiles.

Now, we turn to the tiles which are at the mid-point of a leg. Also in this case, we cannot use the general formula for a basis. We have:

$$\begin{aligned}
(M) \quad & M\gamma\tau\xi + \mathbf{1}_{\{\tau=t\}} \cdot (B\bar{\gamma}\tau_1 + \mu_{\bar{\xi}}(Hg) + \mu_{\xi}(H\gamma\xi u) + \mathbf{1}_{\{\tau_1=\varphi\}} \cdot H\bar{\gamma}\xi_1 l \\
& \quad + \mathbf{1}_{\{\gamma=r\}} \cdot \mu_{\bar{\xi}}(Hy) + \epsilon_c \cdot H\bar{\gamma}\xi u) \\
& + \mathbf{1}_{\{\tau=\varphi\}} \cdot (B\gamma_1\tau_1 + Hg + \mathbf{1}_{\{\gamma_1=b_n\}} \cdot Hy + \mathbf{1}_{\{\tau_1=\varphi\}} \cdot H\gamma_1\xi_1 l \\
& \quad + \epsilon_c \cdot (\mathbf{1}_{\{\gamma_1 \neq \gamma\}} \cdot H\gamma_1\xi_2 u + \mathbf{1}_{\{\gamma_1=\gamma\}} \cdot H\gamma\xi u)) \\
& + \mathbf{1}_{\{\gamma=b_0\}} \cdot \bar{\epsilon}_c \cdot S0bf.
\end{aligned}$$

Note that a covered basis may be the mid-distance line of a trilateral: this is the case when a rather big trilateral is missing in a semi-infinite model, which happens from time to time. Note also that in a blue-0 trilateral, the first part of a leg is accompanied by the scent which stops at the mid-point as it cannot be a seed. In this case, the basis cannot be covered.

The tree-like representation of the formula is given by figure 32.

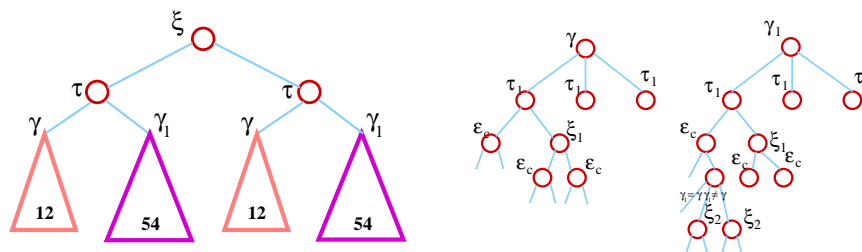


**Figure 32** *The counting for formula (M). Note that the nodes  $\gamma$  and  $\gamma_1$  have three sons. Indeed,  $\gamma$  and  $\gamma_1$  have three possible values:  $b_0$ ,  $b_n$  and  $r$ .*

The figure indicates that we have two sub-trees of the form  $\gamma$  which have 18 leaves and two sub-trees of the form  $\gamma_1$  each of them having  $3 \times 3 \times 6 = 54$  leaves. This makes 144 patterns. Again, we may notice that this time, the concerned tiles are on a row of the mantilla, thanks to the basis but also on a tree border, thanks to the leg. We shall discuss the number of prototiles according to the colour of the basis. From the figure, we can see that a blue-0 basis defines 36 cases for phantoms as the laterality is taken into account by considering a single border. For triangles, we have only 12 cases. As each case is on a separate isocline, 10 for triangles and 0 for phantoms, and as a border defines 3 tiles of the mantilla we have 144 prototiles. The red bases also define 36 cases for phantoms and 12 for triangles. But as two isoclines are possible, this makes 288 prototiles. At last, with a simple blue basis which travels only on an isocline 15 we get 144 prototiles and so, the mid-point tiles are defined by 576 prototiles.

Now, we come to the most intricate situation: when the first part of a leg meets horizontal signals: it is always a basis which is accompanied by one, two or three horizontal signals as we have seen in while proving formulas  $(B_{b_0})$  and  $(B_{b_n, r})$ . We shall have the opportunity to use these formulas, here too.

Following the algorithm of section 4.2.2, we shall successively examine the case of the first part of a leg and then the case of the second part. In the former situation, due to the important number of cases, we shall consider two sub-cases: the case when the basis belongs to a phantom and the case when it belongs to a triangle. Note that in the case of a phantom, the basis is either open or covered and it remains the same after the crossing. In the case of a basis from a triangle, the basis is necessarily covered when it has



the same colour as the legs. There is just one case when the basis is not covered: when the basis of a triangle  $T$  meets the leg of a trilateral which is issued from the mid-distance row of  $T$ . We say that this basis belongs to the generating triangle of the considered legs. As the meeting with open bases of phantoms occurs before the meeting of the basis of the generating triangle, we shall first consider the case of bases of phantoms and then, the case of bases of triangles.

We shall make use of formulas  $(B_{b_0})$  and  $(B_{b_n,r})$  as many times as possible. Note that the formulas cannot be used when a red leg of a triangle meets a free row: The signal  $\mu_\xi(Hr\xi u) + \mu_{\bar{\xi}}(Hy)$  does not occur in the patterns described by the formulas  $(B_{b_0})$  and  $(B_{b_n,r})$ . Now, this case occurs in both the sub-cases we consider.

And so, we first assume that the leg meets a basis of a phantom. This can be described by the following formula, where, in the occurrences of formulas  $(B_{b_0})$  or  $(B_{b_n,r})$ , the variable  $\tau$  of the formula is replaced by  $\varphi$ . Note that the occurrence of the variable  $\gamma$  of such a formula is replaced by  $\gamma_1$ . Also, we remark that when  $\gamma_1 = \gamma$ , the condition of agreement between the laterality of the basis and that of the leg requires that  $\xi_2 = \xi$  in both  $(B_{b_0})$  and  $(B_{b_n,r})$ , the other direction parameters being free. Similarly, the same conditions requires that  $\xi_1 = \xi$  in  $(B_{b_0})$  and in  $(B_{b_n,r})$  while  $\xi_2$  and  $\xi_3$  are free when  $\gamma_1 \neq \gamma$ . We also recall that  $a = b = c = 1$ , as there cannot be a join tile on a leg. At last, as the green signal meets the leg of a trilateral only at its mid-point, we have  $\epsilon_m = 0$  for formula  $(B_{b_n,r})$ .

We remark that in the part of the formula devoted to the meeting with of a blue-0 basis with the leg of a red triangle, the formula rules out the possibility of an upper horizontal blue signal together with a yellow signal. Let us prove this point.

**Lemma 22** *Consider the case when a blue-0 basis of a phantom meets the first part of the leg of a red triangle. Then, if the corresponding row is free, the basis is open in the red triangle.*

*Proof of lemma 22.* Let  $\rho$  be the basis of a blue-0 phantom  $P$ . If the basis is open, then the leg is emitted inside  $P$ , namely on its mid-distance row. Accordingly, we deal with a red triangle  $T$  of the generation 1. In this situation,  $\rho$  is on the first row inside the triangle and so, it is free. This yellow signal is accompanied by the lower horizontal blue signal which accompanies  $\rho$  as a basis of a phantom. The laterality of this latter signal is independent of the laterality of the leg: it is inbetween two vertices of blue-0 triangles and, *a priori*, we do not know where is the join tile with respect to the leg of  $T$ .

Let us look at the case when the basis is covered. Again denote by  $T$  the red triangle whose leg is met by  $\rho$  in its first half. As  $P$  is inside  $T$ , it belongs to a tower of phantoms which is closed by a triangle  $T_1$  which is inside  $T$ . Moreover, we know that  $\rho$  is also on the mid-distance row of  $T_1$ . Now, as  $\rho$  is blue, necessarily,  $T_1$  is red and, consequently, we are done. Indeed,  $\rho$  is free inside  $T_1$ , as it travels on its mid-distance row. Hence,  $\rho$  is not free outside  $T_1$  and, accordingly,  $\rho$  is covered by an upper horizontal red signal. ■

From the lemma, we can write the formula as follows:

$$\begin{aligned}
& L\gamma\tau u\xi + \mathbf{1}_{\{\gamma_1=\gamma\}} \cdot \\
& \left( \mathbf{1}_{\{\gamma_1=b_0\}} \cdot B_{b_0}(\tau_1, \xi_i, \epsilon_i)[\tau_1:=\varphi, \xi_2:=\xi] \right. \\
& + \mathbf{1}_{\{\gamma_1 \neq b_0\}} \cdot B_{b_n, r}(\gamma_1, \tau_1, \xi_i, \epsilon_i)[\tau_1:=\varphi, \xi_2:=\xi, \epsilon_m:=0] \\
& + \mathbf{1}_{\{\gamma_1 \neq \gamma\}} \cdot \\
& \left( \mathbf{1}_{\{\gamma_1=b_0\}} \cdot (\mathbf{1}_{\{\tau=\varphi\}} \cdot B_{b_0}(\tau_1, \xi_i, \epsilon_i)[\tau_1:=\varphi, \xi_3:=\xi] \right. \\
& \quad + \mathbf{1}_{\{\tau=t\}} \cdot (\epsilon_y \cdot (\mu_\xi(Hr\xi u) + \mu_{\bar{\xi}}(Hy) + SObf) \\
& \quad \quad \quad \left. + \bar{\epsilon}_y \cdot (Hr\xi u + H\gamma_1\xi_1 u) + H\gamma_1\xi_2 l) \right. \\
& \left. + \mathbf{1}_{\{\gamma_1 \neq b_0\}} \cdot B_{b_n, r}(\gamma_1, \tau_1, \xi_i, \epsilon_i)[\tau_1:=\varphi, \xi_3:=\xi, \epsilon_m:=0] \right),
\end{aligned}$$

with the condition  $\epsilon_s \Rightarrow \epsilon_m$  for both occurrences of  $(B_{b_n, r})$  and the condition  $\epsilon_c \Rightarrow \bar{\epsilon}_s$  for all occurrences of formulas  $(B_{b_0})$  and  $(B_{b_n, r})$ .

Note that the condition  $\epsilon_c \Rightarrow \bar{\epsilon}_s$  is implemented in figure 29 and that both conditions  $\epsilon_c \Rightarrow \bar{\epsilon}_s$  and  $\epsilon_s \Rightarrow \epsilon_m$  are implemented in figure 30.

First, consider the case when  $\gamma_1 = \gamma$ . We know that this entails  $\xi_2 = \xi$ , as an upper signal which crosses a leg of its colour must have the same laterality as the leg. And so, this means that  $\xi_2$  is fixed. Accordingly, looking at figure 29, we find that when  $\gamma_1 = b_0$ ,  $\tau_1 = \varphi$ ,  $\xi_2$  is fixed and  $a = b = c = 1$ , there are 25 patterns. As  $\tau$  and  $\xi$  are free, we have  $25 \times 4 = 100$  patterns.

When,  $\gamma_1 \neq b_0$ , we have to consider formula  $(B_{b_n, r})$ . We consider that  $\gamma_1$  is fixed, and we have that  $\tau_1 = \varphi$ ,  $\xi_2 = \xi$ ,  $a = b = c = 1$  and  $\epsilon_m = 0$ . This defines 8 patterns. As  $\gamma_1$  can take two values, there are 16 patterns. And  $\tau$  and  $\xi$  are free. Accordingly, we have  $16 \times 4 = 64$  patterns.

Accordingly, the case  $\gamma_1 = \gamma$  defines 164 patterns,  $\gamma$  being fixed by  $\gamma_1$ , taking into account all the possible values of  $\tau$  and  $\xi$ . These patterns split into 100 ones with a blue-0 basis, 32 ones with a simple blue basis and also 32 ones with a red basis.

In the case  $\gamma_1 \neq \gamma$ , the condition of the compatibility with the laterality of the leg entails that  $\xi_3 = \xi$ . And so,  $\xi_3$  being fixed, we have three cases depending on  $\gamma_1$ .

Now, in the case when  $\gamma_1 = b_0$ , we have two cases depending on  $\tau$ , assuming  $\xi$  fixed. The case of  $\gamma_1 = b_0$  gives us 21 cases when  $\tau = \varphi$  and, looking at the above formula, it is 6 when  $\tau = t$ ,  $\xi$  being fixed. This gives us 27 cases and, taking into account that  $\xi$  has two possible values, we obtain 54 patterns.

When  $\gamma_1 \neq b_0$ , we have 32 patterns, 8 cases with  $\gamma_1 = b_n$  and 8 cases with  $\gamma_1 = r$  and we have  $\xi$  and  $\tau$  free which means that this gives us  $16 \times 4 = 64$  patterns.

And so, in the case  $\gamma_1 \neq \gamma$ , we have found 118 patterns. Accordingly, the meeting of legs with bases of phantoms gives us 282 patterns. Remind that, by colours, we have 154 patterns with a blue-0 basis, 64 with a simple blue one and 64 with a red one.

Now, let us look at the corresponding prototiles. Again, We shall discuss by the colour of the basis. From the above analysis, the blue-0 cases represent 154 patterns which are all on the isocline 0 as we deal with phantoms. And so this defines  $3 \times 154 = 462$  prototiles. Now, the red bases represent 16 cases,  $\xi$  and  $\tau$  being fixed, which means 64 patterns, using 2 isoclines and so we have  $64 \times 2 \times 3 = 384$  prototiles. At last, the simple blue define also 64 patterns which are to be found on isoclines 15 only. This defines  $64 \times 3 = 192$  prototiles. And so, in this case we have 1038 prototiles.

Our next case is the meeting of a leg with a basis of a triangle. This case involves a bit less sub-cases but it is still important. Here also we have three important sub-cases: there is exactly one case of an open basis, it is the generating triangle of the legs; then we have covered bases and, among them, we have possible free rows when the legs belong to a red triangle which generates a yellow signal one side of the leg and an upper horizontal red signal on the other side. Formulas  $(B_{b_0})$  and  $(B_{b_n})$  are used for situations where the meeting with the leg just entails the superposition of the leg with the basis. We have:

$$\begin{aligned}
& L\gamma\tau u\xi + \mathbf{1}_{\{\gamma_1=\gamma\}} \cdot \\
& \quad \left( \mathbf{1}_{\{\gamma_1=b_0\}} \cdot B_{b_0}(\tau_1, \xi_i, \epsilon_i)[\tau_1:=t, \xi_2:=\xi, \epsilon_{c,s}:=1, 0] \right. \\
& \quad + \mathbf{1}_{\{\gamma_1 \neq b_0\}} \cdot B_{bn,r}(\gamma_1, \tau_1, \xi_i, \epsilon_i)[\tau_1:=t, \xi_2:=\xi, \epsilon_{c,s,m}:=1, 0, 0] \left. \right) \\
& \quad + \mathbf{1}_{\{\gamma_1 \neq \gamma\}} \cdot \\
& \quad \left( \mathbf{1}_{\{\gamma_1=b_0\}} \cdot \left( \mathbf{1}_{\{\tau=\varphi\}} \cdot B_{b_0}(\tau_1, \xi_i, \epsilon_i)[\tau_1:=t, \xi_3:=\xi] \right. \right. \\
& \quad \quad \left. \left. + \mathbf{1}_{\{\tau=t\}} \cdot (B\gamma_1 t + \epsilon_c \cdot H\gamma_1 \xi u + \epsilon_y \cdot (\mu_\xi(H\gamma \xi u) \right. \right. \\
& \quad \quad \quad \left. \left. + \mu_{\bar{\xi}}(Hy) + \epsilon_s \cdot S0bf) + \bar{\epsilon}_y \cdot H\gamma \xi u) \right) \right. \\
& \quad \left. + \mathbf{1}_{\{\gamma_1 \neq b_0\}} \cdot B_{bn,r}(\gamma_1, \tau_1, \xi_i, \epsilon_i)[\tau_1:=t, \xi_3:=\xi, \epsilon_m = 0] \right),
\end{aligned}$$

with the condition  $\epsilon_s \Rightarrow \epsilon_m$  for both occurrences of  $(B_{b_n,r})$  and the condition  $\epsilon_c \Rightarrow \overline{\epsilon_s}$  for all occurrences of formulas  $(B_{b_0})$  and  $(B_{b_n,r})$ .

Indeed, consider the case when  $\gamma_1 = \gamma$ .

As the leg and the basis have the same colour, this also contains the case when  $\gamma_1 = b_0$ , the meeting with the leg leads to a simple superposition of the already present signals. Hence, formulas  $(B_{b_0})$  and  $(B_{b_n,r})$  apply.

Now, consider the case when  $\gamma_1 \neq \gamma$ .

If  $\gamma_1 = b_0$ , the leg is red. If the leg belongs to a phantom, we have a simple superposition and so, we apply formula  $(B_{b_0})$ . If the leg belongs to a triangle, then, in any case, it may be either covered or not. Also, either it is a free row, and then we have a yellow signal on one side of the leg and an upper horizontal red signal on the other side, or it is not a free row, which means that an upper horizontal red signal crosses the leg, a signal with the same laterality as the leg. When it is in a free row, if it is inside a blue-0 triangle, then the basis may also receive the scent emitted by the vertex which gives rise to the legs met by the basis.

If  $\gamma_1 \neq b_0$ , we note that  $\gamma = \overline{\gamma_1}$ . If the basis is not covered, it meets a trilateral of the opposite colour and, as we have a superposition, the leg does not entail a covering of the basis. And this is conformal to the algorithm. If the basis is covered, we have the same situation: as we have a superposition, the covering signal is not removed by the leg, as required by the algorithm.

Let us count how many patterns the formula defines.

When  $\gamma_1 = \gamma$ , taking into account the values of  $\epsilon_c$  and  $\epsilon_s$ , we have 3 patterns for formula  $(B_{b_0})$ ,  $\tau$  and  $\xi$  being free. We have 2 patterns for each value of  $\gamma_1$  for formula  $(B_{b_n,r})$ . Accordingly, we have 28 patterns when  $\gamma_1 = \gamma$ . We have 12 patterns with a blue-0 basis, 8 patterns with a simple blue basis and also 8 patterns with a red basis.

When  $\gamma_1 \neq \gamma$ , we have 3 cases for each possible colour in formula  $(B_{b_n,r})$ ,  $\tau$  and  $\xi$  being fixed, which means 12 patterns for each colour. In the case when  $\gamma_1 = b_0$ , we have 11 cases for a phantom and 6 cases for a triangle, but  $\xi$  is not fixed. Accordingly, we have 34 cases. And so, when  $\gamma_1 \neq \gamma$ , we have  $12 \times 2 + 17 \times 2 = 58$  patterns, 34 patterns with a blue-0 basis, 12 ones with a simple blue basis and 12 one with a red basis.

And so, we find a total number of 86 patterns in this case: 46 of them with a blue-0 basis, 20 of them with a simple blue basis and 20 of them with a red basis.

Let us now count how many prototiles this gives us: again, we sort them by the colour of the basis. We have noticed that we have 46 patterns with a blue-0 basis. As this happens on the border of a tree, we have 138 prototiles.

For a red basis, we have 20 patterns and we have the same number for simple blue bases. Now, the red bases may travel on isoclines 5 and 15 which makes  $20 \times 2 \times 3 = 120$  prototiles. Now, as simple blue signals occur on isoclines 15 only, they induce 60 prototiles only. And so, we have 318 prototiles for this case.

Now, we arrive to the second part of the legs. This time, we can again use formulas  $(B_{b_0})$  and  $(B_{b_n,r})$ . As the legs must not undo the covering signal which is now present, and, here, we have  $\epsilon_c = 1$ , which entails  $\epsilon_s = 0$ . We have a simple superposition of the leg with the basis, except when we have a red triangle: in this case, if the basis is on a free row, which is necessarily on a signal of a blue-0 basis, then we append new signals: yellow signal on one side and an upper horizontal red one on the other side. Note that as we are on the second part of the legs, there cannot be a scent signal and so, we always have  $\epsilon_s = 0$ , as already noticed, so that  $\epsilon_c \Rightarrow \overline{\epsilon_s}$  is always true. Note that also in the case of a blue-0 basis  $\epsilon_s = 0$ , as we are on a tile of the border of a tree. Now, as  $\epsilon_s = 0$  and  $\epsilon_m = 0$  in the occurrences of formula  $(B_{b_n,r})$ , the condition  $\epsilon_s \Rightarrow \epsilon_m$  is satisfied.

When  $\gamma_1 = \gamma$ , figure 29 gives us  $\xi_2$  fixed,  $\epsilon_c = 1$ , as the basis is covered and  $\epsilon_s = 0$  as, accordingly, there is no scent. The counting using formula  $(B_{b_0})$  gives us 9 cases, as, this time,  $\tau_1$  is free, and the counting using formula  $(B_{b_n,r})$  gives us 6 cases for each colour, for the same reason. Note that  $\tau$  and  $\xi$  are free. Consequently, this defines 36 cases for blue-0 bases, 24 cases for simple blue bases and also 24 cases for red bases. And so, the case  $\gamma_1 = \gamma$  provides us with 84 patterns.

$$\begin{aligned}
& L\gamma\tau l\xi + \mathbf{1}_{\{\gamma_1=\gamma\}} \cdot \\
& \quad \left( \mathbf{1}_{\{\gamma_1=b_0\}} \cdot B_{b_0}(\tau_1, \xi_i, \epsilon_i)[\xi_2:=\xi, \epsilon_{c,s}:=1, 0] \right. \\
& \quad + \mathbf{1}_{\{\gamma_1 \neq b_0\}} \cdot B_{b_n,r}(\gamma_1, \tau_1, \xi_i, \epsilon_i)[\xi_2:=\xi, \epsilon_{c,s,m}:=1, 0, 0] \\
& \quad + \mathbf{1}_{\{\gamma_1 \neq \gamma\}} \cdot \\
& \quad \left( \mathbf{1}_{\{\gamma_1=b_0\}} \cdot (B_{b_0}\tau_1 + Hb\xi_1u + \mathbf{1}_{\{\tau_1=\varphi\}} \cdot Hb\xi_2l \right. \\
& \quad \quad \left. + \mathbf{1}_{\{\tau=t\}} \cdot \right. \\
& \quad \quad \left. (\epsilon_y \cdot (\mu_{\overline{\xi}}(Hy) + \mu_{\xi}(Hr\xi u)) + \overline{\epsilon_y} \cdot Hr\xi u) \right) \\
& \quad \left. + \mathbf{1}_{\{\gamma_1 \neq b_0\}} \cdot B_{b_n,r}(\gamma_1, \tau_1, \xi_i)[\xi_3:=\xi, \epsilon_{c,s,m}:=1, 0, 0] \right),
\end{aligned}$$

When  $\gamma_1 \neq \gamma$ , we cannot use formula  $(B_{b_0})$  in the case  $\gamma_1 = b_0$ : in the case of a red triangle, the half of a yellow signal must accompany the basis. Figure 33 allows us to deal with this case. It can easily be checked that then, there are 18 cases. Note that here, the possible values of  $\tau$  are taken

into account in figure 33. And so we have  $18 \times 2 = 36$  patterns. Now, when  $\gamma_1 \neq b_0$ , we can use formula  $(B_{b_n, r})$ . With the conditions  $\epsilon_c = 1$  and  $\epsilon_s = 0$  which also satisfy the conditions  $\epsilon_s \Rightarrow \epsilon_m$  and  $\epsilon_c \Rightarrow \bar{\epsilon}_s$ , it is not difficult to check that we have 6 cases, for each colour  $b_n$  or  $r$ . But as  $\tau$  and  $\xi$  are free, this gives us 24 patterns for each colour. And so, the case  $\gamma_1 \neq \gamma$  defines 84 patterns.

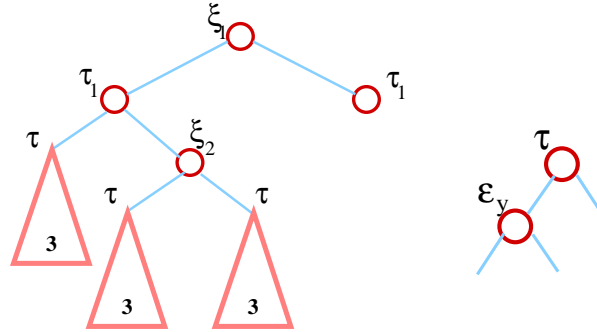


**Figure 33** The counting for the case of the second part of the legs when  $\gamma_1 = b_0$ .

Accordingly, we find 168 cases for the crossing of the second half of the legs by a covered basis. These patterns are split into 72 ones with a blue-0 basis, 48 ones with a simple blue basis and also 48 ones with a red basis.

Let us look at the number of the corresponding prototiles. When the basis is blue-0, we have  $36 + 36 = 72$  patterns. As there is exactly one isocline attached to each kind of trilaterals, triangle and phantoms, this gives us  $3 \times 72 = 216$  prototiles. The case when  $\gamma_1$  is red defines 48 patterns and it makes use of 2 isoclines: 5 and 15. Accordingly this defines  $48 \times 2 \times 3 = 288$  prototiles. At last, the case when  $\gamma_1$  is simple blue defines also 48 patterns. Now, as a simple blue basis travels on isoclines 15 only, we have 144 prototiles. Accordingly, this gives us 648 prototiles.

We arrive to the last situation in the study of the legs: the constitution of the corners which are built on the patterns  $C\gamma\tau\xi$ . We have the following formula:

$$\begin{aligned}
 C\gamma\tau\xi &+ \mathbf{1}_{\{\tau=\varphi\}} \cdot H\gamma\xi_1 l + \mu_\xi(H\gamma\xi u) \\
 &+ \mathbf{1}_{\{\gamma_1 \neq b_0\}} \cdot H\bar{\gamma}\xi_2 u \\
 &+ \mathbf{1}_{\{\gamma_1 = b_0\}} \cdot \epsilon_a \cdot (\epsilon_y \cdot Hy + \bar{\epsilon}_y \cdot H\bar{\gamma}\xi_2 u).
 \end{aligned}$$

Indeed, a corner meets a basis with the same colour and of the same type: triangle or phantom. In case of a phantom, it is accompanied by a

lower horizontal signal of its colour. Also, a corner always dispatch an upper horizontal signal of its colour outside the trilateral to which it belongs. This explains the first line of the formula. In the case when we have a simple blue or a red basis, the basis is accompanied by an upper horizontal signal of the opposite colour which is generated by the triangle which has given rise to the basis of the formula. In the case of a blue-0 basis, if it is inside a red triangle, either it is accompanied by a yellow signal, in the case of a free row, or it is accompanied by an upper horizontal red signal. In the butterfly model, it may happen that the corner falls inside a phantom which is not contained in a red triangle and, in this case, it may happen that the blue-0 basis is not accompanied by any horizontal signal. Figure 34 allows us to count the cases of the formula. It clearly appears that we have 48 patterns.

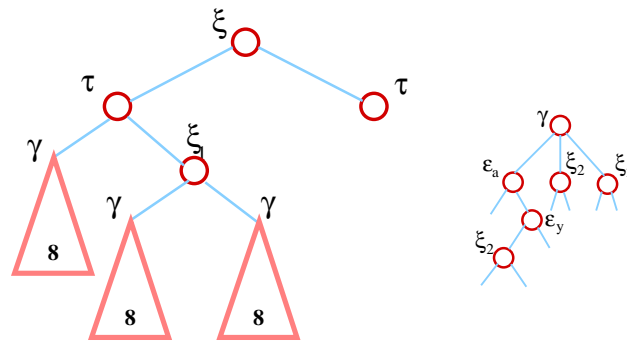


**Figure 34** *The counting for the case of a corner.*

Now, this counting also allows us to count the corresponding prototiles. The case of a blue-0 corner defines 24 patterns. And so we get  $24 \times 3 = 72$  prototiles. For a red corner, we get only 12 of them, but as red signals travel on isoclines 5 and 15, both for triangles and for phantoms, we have  $12 \times 2 \times 3 = 72$  prototiles too. For a simple blue corner, we also get only 12 patterns but as they travel on isoclines 15 only, this provides us with  $12 \times 3 = 36$  prototiles. All together, this makes 180 prototiles.

To conclude with the patterns and the prototiles they generate, we have to remember that we have still a few patterns which occur in the passive zones of the mantilla. It is the patterns of the legs alone: first and second half,  $L\gamma\tau\xi\pi$ . It is also the patterns of the scent: *Sivc*. At last, the blank pattern, *i.e.* the tiles which only have the isocline and mantilla patterns have also to be taken into the counting. Now, the passive legs define  $24 \times 16 \times 3 = 1152$  prototiles. A priori, the passive scent defines

$2 \times 16 \times 34 = 1088$  prototiles. However, a careful examination by computer, shows that there are much less prototiles. All 34 tiles of the mantilla occur within the first five isoclines of a tree of the mantilla. However, they do not all appear on each isocline. As we have to take into account the isoclines which occur on the isoclines 1-4 only, we have the following distribution:

isocline	1	2	3	4		5
mantilla patterns	3	5	10	18	36	22

As this is repeated four times with other numbers, we have  $36 \times 4 = 144$  patterns attached to the scent.

Note that the isocline 5 defines only 22 patterns, the pattern of a seed being included. This means that in the counting of  $(B_{b_0})$  and  $(B_{b_n,r})$  formulas, we have over-estimated the cases when a scent is received. This concerns only tiles with  $\epsilon_s = 1$ . There are 30 of them in the case of blue-0 bases and 12 in the other cases. For these particular tiles we have to count 21 possible patterns and not all the 34 ones. Accordingly the number of prototiles is reduced from 2924 to 2534 for blue-0 bases and from 6324 to 6012 for the others.

At last, the blank tile defines  $16 \times 34 = 544$  prototiles.

Now, if we sum up all the prototiles we have found in this study, we obtain 13,182 prototiles. Note that the total number of patterns we have defined is 997.

To better check the counting, we resume the formulas and the information about the patterns, the isoclines and the tiles of the mantilla in tables 5 and 6. We perform the checking of the counting in table 7.

Now we turn to the proof that this set of prototiles forces the tiling:

**Lemma 23** *The set of prototiles defined by tables 5, and 6 force the construction of the tiling of the interwoven triangles in the hyperbolic plane.*

First, remember that the proof of lemma 20 indicates that the set of tiles which we constructed for the Eulidean case forces the tiling which was described there, up to the position of the vertices. Second, the algorithm of section 4.2.2 gives an exact description of what is obtained.

Accordingly, we have to check that the tiles of tables 5 and 6 do not introduce disturbances in the proof of lemma 20 and that the connections between trilaterals of the same latitude is forced by the tiles in the way



case of	formula
blue-0 bases ( $B_{b_0}$ )	$Bb_0\tau + \epsilon_a \cdot (\mathbf{1}_{\{\tau=\varphi\}} \cdot (a.Hb\xi_1l + \bar{a}.Jbl)$ $+ \epsilon_c \cdot (b.Hb\xi_2u + \bar{b}.Jbu)$ $+ \epsilon_y \cdot Hy + \bar{\epsilon}_y \cdot (c.Hr\xi_3u + \bar{c}.Jru) + \epsilon_s \cdot S0\nu f),$ <p>with <math>\epsilon_c \Rightarrow \bar{\epsilon}_s</math>, <math>a, b, c \in \{0, 1\}</math> and the conditions <math>(a+b)(b+c)(c+a) &gt; 0</math>, <math>\bar{\epsilon}_c \Rightarrow b</math> and <math>\tau = t \Rightarrow c</math>. denoted <math>B_{b_0}(\gamma, \tau, \xi_i, \epsilon_i, x)</math></p>
simple blue and red bases ( $B_{b_n, r}$ )	$B\gamma\tau + \mathbf{1}_{\{\tau=\varphi\}} \cdot (a.H\gamma\xi_1l + \bar{a}.J\gamma l)$ $+ \epsilon_c \cdot (b.H\gamma\xi_2u + \bar{b}.J\gamma u)$ $+ \epsilon_m \cdot (Hg + \mathbf{1}_{\{\gamma=b_n\}} \cdot Hy)$ $+ \bar{\epsilon}_m \cdot (c.H\bar{\gamma}\xi_3u + \bar{c}.J\bar{\gamma}u) + \epsilon_4 \cdot S0\nu f,$ <p>with <math>\epsilon_s \Rightarrow \epsilon_m</math> and <math>\epsilon_c \Rightarrow \bar{\epsilon}_s</math>, <math>a, b, c \in \{0, 1\}</math>, and the conditions <math>(a+b)(b+c)(c+a) &gt; 0</math>, <math>\bar{\epsilon}_c \Rightarrow b</math> and <math>\tau = t \Rightarrow c</math>. denoted <math>B_{b_n, r}(\gamma, \tau, \xi_i, \epsilon_i, x)</math></p>
vertices ( $V$ )	$V\gamma\tau + B\gamma\bar{\tau} + \mathbf{1}_{\{\tau=t\}} (\mu_L(H\gamma ll) + \mu_R(H\gamma rl))$ $+ \mathbf{1}_{\{\gamma \neq b_0\}} (Hg + \epsilon_s \cdot S0bc + \mathbf{1}_{\{\gamma=b_n\}} \cdot Hy)$ $+ \mathbf{1}_{\{\gamma=b_0\}} (\epsilon_y \cdot Hy + \bar{\epsilon}_y \cdot H\bar{\gamma}\xi_1u + \epsilon_s \cdot S0bc$ $+ \bar{\epsilon}_s \cdot (S0bs + \epsilon_c \cdot H\gamma\xi_2u))$
mid-points ( $M$ )	$M\gamma\tau\xi + \mathbf{1}_{\{\tau=t\}} \cdot (B\bar{\gamma}\tau_1 + \mu_{\bar{\xi}}(Hg) + \mu_{\xi}(H\gamma\xi u)$ $+ \mathbf{1}_{\{\tau_1=\varphi\}} \cdot H\bar{\gamma}\xi_1l + \mathbf{1}_{\{\gamma=r\}} \cdot \mu_{\bar{\xi}}(Hy) + \epsilon_c \cdot H\bar{\gamma}\xi u)$ $+ \mathbf{1}_{\{\tau=\varphi\}} \cdot (B\gamma_1\tau_1 + Hg + \mathbf{1}_{\{\gamma_1=b_n\}} \cdot Hy$ $+ \mathbf{1}_{\{\tau_1=\varphi\}} \cdot H\gamma_1\xi_1l$ $+ \epsilon_c \cdot (\mathbf{1}_{\{\gamma_1 \neq \gamma\}} \cdot H\gamma_1\xi_2u + \mathbf{1}_{\{\gamma_1=\gamma\}} \cdot H\gamma\xi u))$ $+ \mathbf{1}_{\{\gamma=b_0\}} \cdot \bar{\epsilon}_c \cdot S0bf.$
legs: first half, crossing phan- tom bases ( $L_u\varphi$ )	$L\gamma\tau u\xi + \mathbf{1}_{\{\gamma_1=\gamma\}} \cdot$ $(\mathbf{1}_{\{\gamma_1=b_0\}} \cdot B_{b_0}(\tau_1, \xi_i, \epsilon_i)[\tau_1:=\varphi, \xi_2:=\xi]$ $+ \mathbf{1}_{\{\gamma_1 \neq b_0\}} \cdot B_{b_n, r}(\gamma_1, \tau_1, \xi_i, \epsilon_i)[\tau_1:=\varphi, \xi_2:=\xi, \epsilon_m:=0]$ $+ \mathbf{1}_{\{\gamma_1 \neq \gamma\}} \cdot$ $(\mathbf{1}_{\{\gamma_1=b_0\}} \cdot (\mathbf{1}_{\{\tau=\varphi\}} \cdot B_{b_0}(\tau_1, \xi_i, \epsilon_i)[\tau_1:=\varphi, \xi_3:=\xi]$ $+ \mathbf{1}_{\{\tau=t\}} \cdot (\epsilon_y \cdot (\mu_{\xi}(Hr\xi u) + \mu_{\bar{\xi}}(Hy)$ $+ S0bf) + \bar{\epsilon}_y \cdot (Hr\xi u + H\gamma_1\xi_1u)$ $+ H\gamma_1\xi_2l)$ $+ \mathbf{1}_{\{\gamma_1 \neq b_0\}} \cdot B_{b_n, r}(\gamma_1, \tau_1, \xi_i, \epsilon_i)[\tau_1:=\varphi, \xi_3:=\xi, \epsilon_m:=0])$

**Table 5** Table of the formulas describing the prototiles, first part.

case of	formula
legs: first half, crossing tri- angle bases  ( $L_u t$ )	$L\gamma\tau u\xi + \mathbf{1}_{\{\gamma_1=\gamma\}} \cdot$ $\left( \mathbf{1}_{\{\gamma_1=b_0\}} \cdot B_{b_0}(\tau_1, \xi_i, \epsilon_i)[\tau_1:=t, \xi_2:=\xi, \epsilon_{c,s}:=1, 0] \right.$ $+ \mathbf{1}_{\{\gamma_1 \neq b_0\}} \cdot B_{bn,r}(\gamma_1, \tau_1, \xi_i, \epsilon_i)[\tau_1:=t, \xi_2:=\xi,$ $\left. \epsilon_{c,s,m}:=1, 0, 0] \right)$ $+ \mathbf{1}_{\{\gamma_1 \neq \gamma\}} \cdot$ $\left( \mathbf{1}_{\{\gamma_1=b_0\}} \cdot \left( \mathbf{1}_{\{\tau=\varphi\}} \cdot B_{b_0}(\tau_1, \xi_i, \epsilon_i)[\tau_1:=t, \xi_3:=\xi] \right. \right.$ $+ \mathbf{1}_{\{\tau=t\}} \cdot (B\gamma_1 t + \epsilon_c \cdot H\gamma_1 \xi u$ $+ \epsilon_y \cdot (\mu_\xi(H\gamma\xi u) + \mu_{\bar{\xi}}(Hy)$ $\left. \left. + \epsilon_s \cdot SObf) + \bar{\epsilon}_y \cdot H\gamma\xi u) \right)$ $+ \mathbf{1}_{\{\gamma_1 \neq b_0\}} \cdot B_{bn,r}(\gamma_1, \tau_1, \xi_i, \epsilon_i)[\tau_1:=t, \xi_3:=\xi, \epsilon_m:=0] \right),$
legs: second half  ( $L_\ell$ )	$L\gamma\tau l\xi + \mathbf{1}_{\{\gamma_1=\gamma\}} \cdot$ $\left( \mathbf{1}_{\{\gamma_1=b_0\}} \cdot B_{b_0}(\tau_1, \xi_i, \epsilon_i)[\xi_2:=\xi, \epsilon_{c,s}:=1, 0] \right.$ $+ \mathbf{1}_{\{\gamma_1 \neq b_0\}} \cdot B_{bn,r}(\gamma_1, \tau_1, \xi_i, \epsilon_i)[\xi_2:=\xi, \epsilon_{c,s,m}:=1, 0, 0] \left. \right)$ $+ \mathbf{1}_{\{\gamma_1 \neq \gamma\}} \cdot$ $\left( \mathbf{1}_{\{\gamma_1=b_0\}} \cdot (Bb_0\tau_1 + Hb\xi_1 u + \mathbf{1}_{\{\tau_1=\varphi\}} \cdot Hb\xi_2 l \right.$ $+ \mathbf{1}_{\{\tau=t\}} \cdot$ $\left. (\epsilon_y \cdot (\mu_{\bar{\xi}}(Hy) + \mu_\xi(Hr\xi u)) \right.$ $\left. + \bar{\epsilon}_y \cdot Hr\xi u) \right)$ $+ \mathbf{1}_{\{\gamma_1 \neq b_0\}} \cdot B_{bn,r}(\gamma_1, \tau_1, \xi_i)[\xi_3:=\xi, \epsilon_{c,s,m}:=1, 0, 0] \right),$
corners  ( $C$ )	$C\gamma\tau\xi + \mathbf{1}_{\{\tau=\varphi\}} \cdot H\gamma\xi_1 l + \mu_\xi(H\gamma\xi u)$ $+ \mathbf{1}_{\{\gamma_1 \neq b_0\}} \cdot H\bar{\gamma}\xi_2 u$ $+ \mathbf{1}_{\{\gamma_1=b_0\}} \cdot \epsilon_a \cdot (\epsilon_y \cdot Hy + \bar{\epsilon}_y \cdot H\bar{\gamma}\xi_2 u).$
passive legs  ( $L_{pz}$ )	$L\gamma\tau\xi\pi$
passive scent  ( $S_{pz}$ )	$Sivc$
blank  ( $W$ )	$W$

**Table 6** Table of the formulas describing the prototiles, second part.

formula	colour	patterns	isoclines	mantilla	prototiles
$(B_{b_0})$	blue-0	86	phantoms: 0 triangles: 10	34	2534
$(B_{b_n,r})$	simple blue red	62 62	15 5, 15	34	6012
$(V)$	blue-0 simple blue red	24 4 4	0, 10 15 5, 15	1	36
$(M)$	blue-0 simple blue red	48 48 48	0, 10 15 5, 15	3	576
$(L_u\varphi)$	blue-0 simple blue red	154 64 648	0, 10 15 5, 15	3	1038
$(L_ut)$	blue-0 simple blue red	46 20 20	10 15 5, 15	3	318
$(L_\ell)$	blue-0 simple blue red	72 48 48	10 15 5, 15	3	648
$(C)$	blue-0 simple blue red	24 12 12	10 15 5, 15	3	180
$(L_{pz})$	any	24	1-4, 6-9, 11-14, 16-19	3	1152
$(S_{pz})$	any	2	'1-4'	34	144
$(W)$	any	1	1-4, 6-9, 11-14, 16-19	34	544
total		997			13,132

**Table 7** *The counting of the tiles.*

described by the mentioned algorithm. Also, as the construction is growing, it necessarily splits into two parts: one part consists in extending the number of trilaterals belonging to already constructed generations in new areas of the same latitudes and to extend the number of latitudes of this generation which contain actually constructed trilaterals. The second part consists in creating trilaterals of new generations. In doing in this way, we shall always consider that a new signal must not undo what was done before: otherwise, as the previous steps are forced without contradiction, the new signal would introduce a contradiction. This does not mean that nothing changes. In fact, from the algorithm, we know that a red triangle is no more touched when the trilaterals of the next generation which it creates are completed. This is not the case for a phantom for what is its mid-distance row: the basis signal which is present at a step  $k$  may be changed at a later step  $n$  because the smallest triangle which contains this phantom namely occurs at this step and it is of the same colour of the basis, which is not accepted by  $M$ -tiles.

Also, for blue triangles, when they are contained or partially contained in a red triangle, they may be crossed by yellow or upper horizontal red signals which were not yet present. The situation is the same as for a phantom: once this happens, we are again inside a red triangle  $T$  and it no more changes when the trilaterals of the next generation generated by  $T$  are completed.

Now, let us look at the important points.

The introduction of horizontal blue signal does not bring in a contradiction. It simply makes it easier to construct blue trilaterals. And so, as far as we are inside a triateral, the construction goes on as indicated by lemma 20 and the algorithm of section 4.2.2. There is also no change for the detection of the free rows in a red triangle. What is detected is the presence of a horizontal red signal in any position: either upper or low, see tables 5 and 6.

The important change in the construction is the detection of the basis which cannot be confused with the previous point as, this time, a horizontal basis signal of the same colour as that of the leg must be present. The rule which we introduced in section 4.2.2 is that a basis which meets its leg cannot have an upper horizontal signal of the same colour say  $\gamma$ . Imagine that such a tile  $\tau$  was put on the concerned isocline, between the points which will be reached by the legs which define an interval  $S$  of the isocline. As there is no triangle of the colour  $\gamma$  in  $S$ , the tile  $\tau$  forces a horizontal

$\gamma$  signal which, necessarily, is unilateral: the same laterality runs over  $S$ . Now, the legs require different lateralities. So the signal matches at one side but not at the other. So, we need two signals and a joining tile, but it is easy to see that a joining tile should bear signals  $\mu_L(H\gamma ul) + \mu_R(H\gamma ur)$ , a combination which is ruled out in the tiles of the tables.

The same argument prevents a leg of a later generation to capture a basis of a previous generation, already transformed into a synchronization signal. As the leg and the considered basis have the same colour  $\gamma$  there are tiles performing the crossing with signals  $H\gamma u\xi$  and tiles without it. If we put a tile without the signals, we are in contradiction with the side of the basis on which a corner sends the horizontal  $\gamma$  signal, as this corner is older than the legs. If the leg crosses a basis with the lower signal only, putting an upper signal also entails a contradiction: from the table, the leg can put the upper signal only on its both sides. As there is no triangle on this row, the introduced signal will match with one legs of the phantom but not the other, as already noticed.

Let us now check that the situation between trilaterals of the same latitude is forced by the tiles.

By construction, the basis of these trilaterals is a common signal which runs along the concerned isocline without interruption, from left to right across the whole hyperbolic plane. From what we have already seen, the situation inside the trilaterals is forced by the tiles. Now, outside, the corners emit a signal which goes on the direction indicated by the laterality of the corner. Between two consecutive corners which do not belong to the same trilateral, again defining an interval  $S$ , we have necessarily a right-hand side upper horizontal signal coming from the left and a left-hand side upper horizontal signal coming from the right. Now, there are  $B$ -tiles with the mark  $\mu_L(H\gamma ur) + \mu_R(H\gamma ul)$  which allows to join both signals. This signal may occur only once as can easily be seen and so, it can be placed anywhere between possible later legs which could come to intersect  $S$ , see figure 23. Now, this can come not later than a fixed delay depending on the length of  $S$ . And so, if we place the joining tile somewhere in  $S$ , we might have to put it at another point of  $S$  at most finitely many often.

Accordingly, the tiles of tables 5 and 6 force the procedure of joining corners from outside indicated in the algorithm of section 4.2.2.

Now, we have to relax the hypothesis on the choice of the first tile. Indeed, let us start with any tile from the set of prototiles defined by tables 5 and 6. Let us temporary forget the marks connected with the trilaterals, so that we only look at the tile of the mantilla and the isocline numbers. This tile allows to construct a part of the mantilla in which, necessarily from

lemma 5, we shall find a seed on the isocline 0. Now, we can start the above construction from this new tile and, at some time, it will be possible to place the tile which was first taken. And so, lemma 23 is proved. ■

Now, our preparation is completed. But before turning to the description of the computing areas, let us look at a point which will again appear in the proof of the main theorem.

Indeed, the construction allows to realize all possible models of the abstract brackets. In particular, let us have a look at the butterfly model. In this case, there is a row of the mantilla, call it 0, which contains an infinite green signal. In fact, this row is on an isocline 15, and the line is the centre of the latitudes of infinitely many infinite towers of phantoms. Now, by the structure of the tiles, such a green line is never left alone. It is always accompanied by a basis. In this case, the basis never finds its legs and it never finds corners neither. If it is a basis of a phantom, it gives rise to infinitely many triangles which are infinite: this is clear from lemmas 18 and lemma 19, as legs created inside  $T$  will be stopped by a triangle whose vertex appears inside  $T$ . If the basis is red, we have infinitely many infinite red triangles in which an infinite computation may take place in the case when the simulated Turing machine does not halt.

Now, if the basis which accompanies the infinite green signal is a basis of a triangle, and of a red triangle, then it is possible, but not forced by the tiles, that there are infinite yellow signals on infinitely many rows: those which separate the latitudes of contiguous red triangles, see lemma 11. Again, we shall look again at this possibility in the part devoted to the proof of the main theorem.

### 4.3 The new harps

At this moment, we have constructed what corresponds to the **skeleton** in the proofs of Berger and Robinson. Now, we are ready for the complete description of the computing areas.

The computing areas of our construction are the red triangles, whatever the generation. Accordingly, we forget the blue trilaterals, the red phantoms and the synchronization signals outside the basis of the red triangles.

Remember that in [9], we have considered the harps as implementations of a space time diagram of a Turing machine, as indicated in section 2.3. The horizontal paths for the Turing head will be the free rows of the considered red triangle. What we now need is to describe the verticals. In order to not confuse them with the legs of the trilaterals which we also called verticals up to now, we shall call **perpendiculars** the new object which we now define

which will play the rôle of a vertical in a space-time diagram: each one of our perpendiculars will contain the history of a given square of the Turing tape of the simulated machine.

For that purpose, we notice that the red triangles are set in trees of the mantilla whose borders do not meet. Now, the trees of the mantilla belong themselves to sectors of the mantilla and, from [9], we know that the borders of a sector do not meet the borders of a tree of the mantilla rooted in the centre of the head of the sector. We shall call **perpendicular** any ray which starts from the border of a tree and which follows the border of a sector. Accordingly, perpendiculars never meet a leg of a trilateral.

Consider a red triangle  $T$ . We shall consider that the tiles which are at the intersection of its right-hand side leg and its left-hand side leg with a free row are the squares of the Turing tape which we consider as bi-infinite. Fix a square 0 on the Turing tape, which we may consider as the initial position of the head. We associate this square of the Turing tape to the vertex of  $T$ . We may view the right-hand side leg as the squares with a positive address and the left-hand side one as the squares with a negative address. Note also that we shall assume, without loss of generality, that the instructions of the Turing machine always indicate an actual move: either to right or to left.

Now, the evolution in time of the squares will be performed by the perpendicular which can be drawn from the place of the considered square on the border of the triangle. It takes the nearest border of a sector inside the triangle. We simply notice that, due to the period 3 of the tile pattern on both the left-hand side and the right-hand side border of a tree of the mantilla, we may find an **8**-centre within two or three isoclines below the free row and, from this centre, the signal will follow the ray of **8**-centres, repeating the same period of three tiles. This is easy to perform: the pictures of figure 35 illustrate the implementation of the perpendiculars.

The new tiles needed for that are: tiles of the border of a tree, one or two intermediate tiles and then the tiles along a ray passing through **8**-centres. The tiles for the tree border are all the tiles which occur in a period: the tiles  $b.11 \circ 2$ ,  $b.G_r$  and  $b.1 \circ 15$  for the right-hand side border and the tiles  $b.6 \circ 77$ ,  $b.G_\ell$  and  $b.37 \circ 7$  for the left-hand side border, as already noted. As the period consists of 3 tiles and as the periodicity of the active isoclines is 5, all the tiles are involved in a big enough triangle. The path followed by the state/square signal is indicated by table 8. For each tile, we give the paternal coordinate of the entry- and exit points. For the tile of the border of a tree where the signal starts, we only indicate the exit point.

From the right-hand side part of figure 35, we can see that the concerned signal starts from the centre of a tile and goes to the mid-point of an edge 4

or 5. Later, the signal reaches an **8**-centre either through one or through two tiles. Once the **8**-centre is reached, a period is repeated which is indicated in the last three rows of the first column.

At last, inside  $T$ , a perpendicular never meets a leg of a triangle nor a basis of triangles which are inside  $T$ . The perpendicular will eventually meet the basis of  $T$  and only it.

The computing signal runs along yellow rows and the just defined perpendiculars. It always conveys a state of the machine and it also indicates the direction of the motion of the head, using lateral signals, following the same patterns as those used for horizontal blue and red signals. The signal has the form  $T\sigma\xi$  with  $\xi = r$  when the signal moves to the right and  $\xi = l$  when it moves to the left. The meaning of  $\sigma$  is defined a bit later.

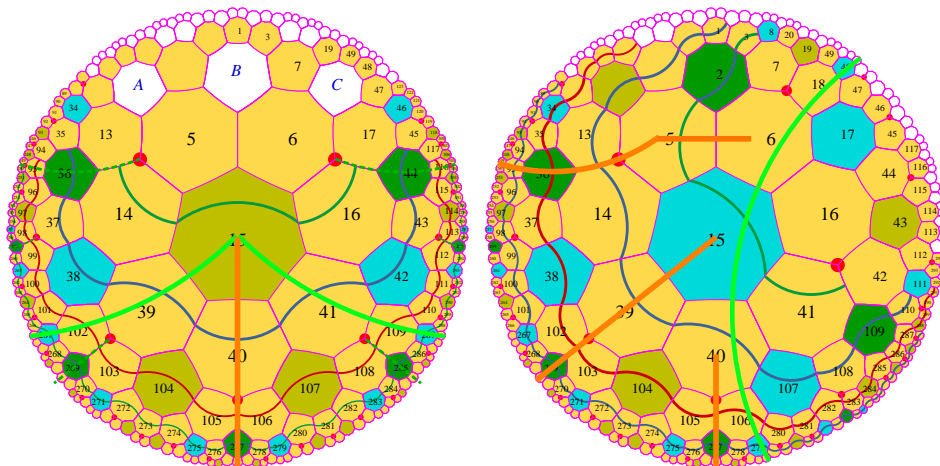


**Figure 35** *The perpendicular starting from a point of the border of a triangle which represents a square of the Turing tape.*

*On the left-hand side: the case of the vertex. On the right-hand side, the three other cases for the right-hand side border are displayed on the same figure.*

When it meets a perpendicular, which always indicates the current content of a square of the Turing tape a new instruction is performed and we have two cases. Either the move of the head is left unchanged by the instruction, or it is changed. In the first case, the signal goes on on the row without changing its laterality, unless the meeting with the perpendicular occurs at a tile which is on the border of a tree. In this latter case, the signal behaves as if the new move takes the opposite direction with respect to the former move: it goes down along the perpendicular. After the meeting, if the signal has to go down, it indicates the new content of the square, the



new state of the head and the new direction it will have to take. When the signal reaches the next yellow row, the content continues to go down along the perpendicular and the state goes on its way this time along the row, in the direction indicated by its own signalization. In this way, the next perpendicular which will be met will be the expected one: it will hold the content of the concerned square of the Turing tape.

$b.11\circ 2\ 4$	$b.G_r\ 5$	$b.1\circ 15\ 5$	$b.6\circ 77\ 5$	$b.G_\ell\ 5$	$b.37\circ 7\ 4$
$w.1\overline{22}\circ\ 1-5$	$w.47\ \circ\ 7\ 1-4$	$w.2\circ 77\ 1-6$	$w.\overline{66}7\circ\ 1-3$	$w.1\circ 14\ 1-4$	$b.6\circ 77\ 1-6$
$w.2\circ 77\ 1-6$	$w.6\circ 77\ 1-6$	<b>8</b> 7-4	$b.\overline{5}\circ 77\ 1-6$	$w.2\circ 77\ 1-6$	<b>8</b> 7-4
<b>8</b> 7-4	<b>8</b> 7-4		<b>8</b> 7-4	<b>8</b> 7-4	
$w.1\overline{47}\circ\ 1-4$					
$w.2\circ 77\ 1-6$					

**Table 8** *The paths for the perpendiculars. Once a 8-centre is reached, a period of three tiles is repeated: the period is indicated by the last three rows of the first column.*

Note that our general scheme differs a bit from that of [9]. With respect to that scheme, the present introduces a delay in the transfer of the new state. In case of a change in the direction of the motion of the head, the signal first follows the perpendicular, accompanying the new content of the square and then, when it finds the next yellow row, it goes on the row in the direction indicated by its signal. This is why we provide new tiles for the computation signals which are displayed by figure 37 and their use in accordance with the previous construction signals is precisely described by table 9. The figure indicates the signals in the square format for the convenience of the reader. Below, in figure 36, we first give the names of the new signals: they are of the form  $T\sigma[\xi]$ , as already mentioned. Here  $\xi \in \{l, r\}$  indicates the laterality and  $\sigma \in \{i, b, s, t, m, e, c, u, hu, hc\}$  indicates the nature of the operation performed by the tile. Thus,  $i$  indicates the start of the signal which only matches with the vertex of a red triangle. Next,  $b$  indicates a border tile:  $Tbi$  stands for an initialization of the corresponding Turing square,  $Tbl\xi$  indicates the two possible cases when the computing signal arrives at the left-hand side leg, while  $Tbr\xi$  does the same for the right-hand side leg. These tiles execute an instruction. Then,  $s$  and  $t$  simply convey the information:  $s$  for the state of the head of the Turing machine when it is conveyed by a yellow row,  $t$  for the content of the square when

it is conveyed by a perpendicular. The letters  $m$  and  $e$  refer to performing an instruction:  $m$  indicates the moment when a state signal meets a square cell. In fact, a yellow row crosses a perpendicular. At the intersection, we have a tile  $Tm\xi$ , depending on the motion of the head. The tile executes the instruction corresponding to the symbol conveyed by the perpendicular and the state conveyed by the row. As output, the tile indicates the new content of the tape, the new state of the head and the direction of the next motion of the head.

There are two cases, depending on whether the new direction is different or not from the current one. If it is not different, this is indicated by the tiles  $Tu\xi$  which also perform the instruction. If it is different, the tiles  $Tm\xi$  execute the instruction. Both the new state, the new content and the new direction are conveyed by the perpendicular through the tiles  $Tc\xi$ . When the perpendicular meets the next yellow row, the state and the content are separated by the tiles  $Te\xi$ . Afterwards, the tiles  $Ts\xi$  and  $Tt$  convey the new information.

$Ti$	$Tsl$	$Tsr$	$Tt$	$Tbi$			
$Tbll$	$Tblr$	$Tbrl$	$Tbrr$	$Tml$	$Tmr$	$Tul$	$Tur$
$Tel$	$Ter$	$Tcl$	$Tcr$				
$Tdl$	$Tdr$	$Thul$	$Thur$	$Thcl$	$Thcr$		

**Figure 36** *The names of the computing meta-tiles.*

At last, but not least, the tiles  $Td\xi$ ,  $Thu\xi$  and  $Thc\xi$  manage the interruption and the halting case.

The interruption case is defined by the tiles  $Td\xi$  which are used when the computing signal, being on a perpendicular, meets the basis of the red triangle where the computation is performed. As the corresponding signal may convey a left-hand side or a right-hand side new direction, we have two tiles:  $Tdl$  and  $Tdr$ .

The halting case is managed by the tiles  $Thu\xi$  and  $Thc\xi$ . The halting state appears in a tile which performs an instruction:  $Tm\xi$  or  $Tu\xi$ , depending on whether the new direction of the move of the machine head is different or not from that of the current move. In both cases, we consider that the halting state is black. Now, after a tile  $Tm\xi$ , a tile  $Tc\xi$  comes and, after a tile  $Tu\xi$ , it is a tile  $Ts\xi$ . We decide that no tile of this kind bears a black sign for the state. The only tiles with a black sign for the states are the tiles  $Thu\xi$  which match with the tiles  $Tu\xi$  and the tiles  $Thc\xi$  which match with the tiles  $Tm\xi$  only. Now, no other tiles may match with the tiles  $Thu\xi$  and  $Thc\xi$  which, accordingly cause the tiling to stop. Note that for the tiles

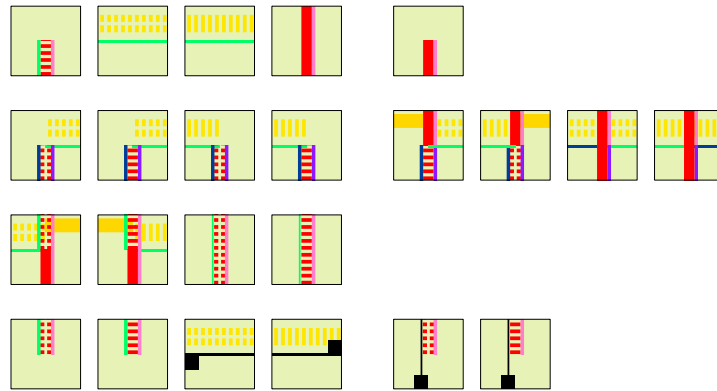
*Thcξ* and *Thuξ* it is important that the tiles can be neither rotated nor reflected.

Figure 37 illustrates these tiles, giving them in the order given above. Now, the implementation of the harp is completed.

We have just to count how many tiles are appended by those of figure 37. Note that these tiles are different from those of the skeleton. Indeed, the tiles of the figure are not an abbreviated representation of prototiles, but an abbreviate representation of *variables* for prototiles, let us call them **meta-tiles**. And so, they should be counted separately.

To facilitate the counting, we introduce a table in the same way as the ones we introduced to list the tiles needed by the skeleton, see table 9.

*e.* computing tiles:



**Figure 37** *The computing tiles.*

The counting is based on the following simple considerations. For a vertical signal, only the ten tiles the mantilla given in table 8 can be used. However, all the isoclines are involved, both active and passive ones.

Now, only the period of a vertical is concerned with all the values of the isoclines. The aperiodic part, which starts on a row of the mantilla, the corresponding tile being counted with the type of a horizontal signal, has three possible values for the isocline. Moreover, for each starting point of the vertical, the aperiodic part has at most two tiles. And so, as four tiles have an aperiodic part of two tiles and two ones have an aperiodic part of a single tile, this makes 10 cases. Accordingly, for a vertical signal, the number of tiles, regardless of the marking used for the counting is  $10 \times 3 + 3 \times 20 = 90$ .

On the other hand, horizontal signals travel on active isoclines only and, moreover, on the part of those which contain a yellow signal. This rules out

the isoclines 5. Accordingly, in this case we have only three possible values for the isoclines but we may meet all the tiles of the mantilla, which makes 102 cases, regardless of the marking used for the concerned computing tiles.

Now, we have again to look at tables 5 and 6 in order to count how many patterns, exactly, bear yellow signal. This involves the tiles defined by both formulas  $(B_{b_0})$  and  $(B_{b_n,r})$ , but also most of the other formulas as a yellow row may contain vertices of triangles or phantoms, as the yellow row also touches the legs of the triangle in which they lie. Also, a yellow row may cross the corners of another trilateral.

First, we shall look at the situation of 'pure' bases, *i.e.* the situation described by formulas  $(B_{b_0})$  and  $(B_{b_n,r})$ .

It is not difficult to see that with formula  $(B_{b_0})$  we have 23 cases, exactly: we have  $\epsilon_a = \epsilon_y = 1$ , we note that  $a$ ,  $b$  and  $c$  may be either 0 or 1, independently. We have the same counting for formula  $(B_{b_n,r})$  in which, necessarily, the colour of the basis must be  $b_n$ :  $\epsilon_0 = \epsilon_2 = 1$ . Let us denote by  $B_{yellow}$  the cases when formulas  $(B_{b_0})$  and  $(B_{b_n,r})$  yield a tile with a yellow signal. Then, the isoclines 0 and 10 are associated with the possible values of  $\tau$  in formula  $(B_{b_0})$ : the isoclines 0 with  $\tau = \varphi$  and the isocline 10 with  $\tau = t$ . Now, as we have 34 possible values for the mantilla signs, this gives us  $34 \times 46 = 1564$  patterns which can be combined with each tile of figure 37 to define a meta-tile. Now, the tiles of figure 36 which are on a yellow row are:  $Ts\xi$  and  $Thu\xi$ . Accordingly, this defines  $4 \times 1564 = 6256$  meta-tiles. All the other marks are on a perpendicular.

Now, let us look at the vertices. We notice that red vertices are ruled out, but the other colours, blue-0 and simple blue give us 12 cases: when  $\epsilon_y = 1$ , the contribution of formula  $(V)$  consists of 8 nodes, see figure 31, and the contribution of  $\gamma = b_n$  gives us 4 nodes. This gives 12 patterns. This gives indeed 12 prototiles, as a vertex goes only with  $s.F$ -tiles and with isoclines 0 and 10 for blue-0 and isoclines 15 for simple blue. The concerned counting marks are the same as previously, as an  $s.F$  tile does not occur on a leg: it may be a root but if it is a silent seed, it is not on a leg. Also, it cannot be on a perpendicular. Now, if a seed occurs on a yellow row, this may happen, it may convey a Turing signal and start a computation: there is no contradiction, as tiles  $Ti$  may combine with  $Ts\xi$  as well as with  $Thu\xi$ . Accordingly, this gives us  $2 \times 5 \times 12 = 120$  meta-tiles.

Then, we come to the case of a corner of a blue-0 trilateral. Looking at figure 34, we can see that the yellow mark occurs when  $\gamma = b_0$  and  $\epsilon_a = \epsilon_y = 1$ . We find 6 patterns. The isoclines are 0 or 10 and it is a tile on a leg of a trilateral. Accordingly there are  $3 \times 6 = 18$  prototiles. Note that such a tile cannot be on a perpendicular as it is on the border of a tree.

And so, taking the marks of tiles  $Ts\xi$  and  $Thu\xi$ , this gives us  $4 \times 18 = 72$  meta-tiles.

We also have to consider the case of a mid-distance row in a red triangle. On this row, several trilaterals are crossed at the mid-point of their legs by the simple blue basis which is accompanied by both a green and a yellow signal. Formula  $(M)$  gives us the expected situations with  $\tau = \varphi$ ,  $\gamma_1 = b_n$  and  $\epsilon_c = 0$  as the basis is not covered in our case, which is attested by the presence of the green signal. Figure 32 indicates that there are 18 patterns which are concerned in a  $\gamma_1$ -tree and so, we have 36 patterns. This defines 108 prototiles, as an  $(M)$ -tiles is on a vertical, and 432 meta-tiles, as the concerned computing tiles are  $Ts\xi$  and  $Thu\xi$ .

Another situation which is met by a yellow signal is the crossing of various legs. For a purely horizontal computing signal,  $Ts\xi$  and  $Thu\xi$ , all situations described by formulas  $(L_u\varphi)$ ,  $(L_ut)$  and  $(L_\ell)$  can be met, except the crossing of the leg of a red triangle: this defines the end of the horizontal signal.

First, we look at the first half of a leg.

In formula  $(L_u\varphi)$ , the yellow signal appears in several situations. Using formulas  $(B_{b_0})$  and  $(B_{b_n,r})$  only, we find 238 patterns. The isocline is fixed, as the basis belongs to a phantom, and as we are on a border, we have 3 tiles of the mantilla. This selects 714 prototiles. Combined with the 4 possible tiles,  $Ts\xi$  and  $Thu\xi$ , we have 2856 meta-tiles.

In formula  $(L_ut)$ , the yellow signal also appears in several situations. The counting based on the same principles as previously, going this time on the left-hand side of  $\tau$ -nodes, we get 60 patterns. Accordingly, this defines 180 prototiles and this gives us 720 meta-tiles.

Next, we look at the second half of the legs.

In formula  $(L_\ell)$ , the yellow signal again in several occasions, but this time the basis is always covered. This defines 100 patterns, hence 300 prototiles and then, 1200 meta-tiles.

Now, we arrive to the ends of a yellow row. However, ends are the starting point of a perpendicular. As we considered only 'pure' horizontal computing signs. We have counted all of them.

Accordingly, the total number of meta-tiles which we have for a pure horizontal computing signal is 11,486.

Now, we turn to the counting of the meta-tiles which involve perpendiculars. We start this counting with the ends of the yellow rows.

Necessarily, we have tiles of the border of a tree for what is the mantilla

and we also have the tiles  $Tbi$  and  $Tb\xi_1\xi_2$  for the counting marks. We have now the different situations on the border of a tree. We know that we are concerned with red triangles only and so,  $\tau = t$  and  $\gamma = r$ .

Let us start with the case when the yellow row is at a mid-point tile. The conditions  $\tau = t$  and  $\gamma = r$  in formula (M) provide us with 12 cases, exactly. There may be 2 isoclines: 5 or 15 and 3 tiles, as this happens on a leg. This indicates 72 prototiles. Now, for this case, we have the counting patterns  $Tbi$ ,  $Tb\xi_1\xi_2$  as already mentioned. There are five of them. Now, note that in a tile  $Tb\xi_1\xi_2$ ,  $\xi_1$  much match with the laterality of the tile defined by formula (M). Accordingly, we have  $3 \times 72 = 216$  meta-tiles. Note that in the other cases connected with the ends of a row, we shall have the same condition on  $\xi_1$  which must match with the laterality of the leg.

Next, we look at the first half of a leg.

In formula ( $L_u\varphi$ ), the end of a yellow signal appears in the case when  $\gamma = r$ ,  $\gamma_1 = b_0$ ,  $\tau = t$ , and, of course,  $\epsilon_y = 1$ , we have two cases, taking into account that  $\xi$  is free. This gives us 6 prototiles and 18 meta-tiles, as the concerned computing tiles are  $Tbi$  and  $Tb\xi_1\xi_2$  with  $\xi_1$  fixed by the leg, which defines 3 cases only.

In formula ( $L_ut$ ), we have a similar condition but a few more cases: 4 of them, with  $\xi$  fixed, which means 8 patterns. This gives us 24 prototiles and 72 meta-tiles.

Next, we look at the second half of the legs.

In formula ( $L_\ell$ ), the yellow signal occurs in two cases only, taking into account that  $\xi$  has two values. This defines 2 patterns, hence 6 prototiles and then, 18 meta-tiles.

Accordingly, this part of the counting signals needs 324 meta-tiles.

Next, we deal with the other situations: first, the conveying of the content of a square of the tape or the content of such a square together with the other instruction information: the new state and the new direction of the head. The second part of our counting will deal with the meeting of a perpendicular with a yellow row. Again, this situation splits into two cases: the computing signal is on the yellow row and meets the content of the new scanned square, which means that an instruction is applied. The other situation is the opposite case: when the computing signal is on a perpendicular and it meets a free yellow row on which it will go on in order to find the new square to be scanned.

And so, let us look at the first situation: conveying the content of a square of the tape. This involves a perpendicular and the tiles  $Ti$ ,  $Tt$ ,  $Tc\xi$ ,  $Td\xi$  and  $Thc\xi$ . From the beginning of our study, as we know that

type	formula	patterns	#
$B_{yellow}$ tiles : 'pure' basis	$a.Ts\xi + \bar{a}.Thu\xi + b.(B_{b_0}) + \bar{b}.(B_{b_n})$	23+23	6256
corner	$a.Ts\xi + \bar{a}.Thu\xi + (C)$	12	72
mid-point	$a.Ts\xi + \bar{a}.Thu\xi + (M)$	36	432
legs:			
first half	$a.Ts\xi + \bar{a}.Thu\xi + b.(L_u\varphi) + \bar{b}.(L_ut)$	238+60	3576
second half	$a.Ts\xi + \bar{a}.Thu\xi + (L_\ell)$	100	1200
starting point of perpen- diculars:			
inside the yel- low row:			
vertex	$Ti + a.Ts\xi + b.Thu\xi + (V),$ $a + b \leq 1$	12	120
ends of yel- low rows:			
first half	$a.Tbi + \bar{a}.Tb\xi\xi_1 + b.(L_u\varphi) + \bar{b}.(L_ut)$	2 + 8	90
second half	$a.Tbi + \bar{a}.Tb\xi\xi_1 + (L_\ell)$	2	18
mid-point	$a.Tbi + \bar{a}.Tb\xi\xi_1 + (M)$	12	216
the tape content	$a.Ti + b.Tt + c.Tc\xi + d.Thc\xi$ $+ (P), \quad a + b + c + d = 1$	90	720
execution	$a.Tm\xi + \bar{a}.Tu\xi + \{B_{yellow} \cap (P)\}$	46	552
splitting the Turing output	$Te\xi + \{B_{yellow} \cap (P)\}$	46	276
stopping by meeting the basis	$Td\xi + Brt$	6	12

**Table 9** *The precise description of the computing tiles and their counting.*

90 prototiles may be involved by a perpendicular, we have  $8 \times 90 = 720$  meta-tiles. Note that we did not take into account the tiles  $Tbi$  which are already counted.

Next, we look at the situation when a yellow row with the computing signal meets a perpendicular. The concerned counting tiles are  $Tm\xi$  and  $Tu\xi$ . Now, this time, as the tile belongs to a perpendicular, we have to take into account the possible horizontal patterns of the tile. As a perpendicular does not meet a leg, this means that we have the patterns with a yellow signal which are defined by formulas  $(B_{b_0})$  and  $(B_{b_n,r})$ . Call them  $B_{yellow}$  patterns. From what we have seen above, we know that there are 46  $B_{yellow}$  patterns. As we know, the pattern defines the isocline and the tiles belong to the periodic part of a perpendicular: hence, 3 possible tiles, which means 138 prototiles. Accordingly, taking into account the computing tiles,  $Tm\xi$  and  $Tu\xi$ , this situation defines  $4 \times 138 = 552$  meta-tiles.

The same counting holds for the reverse situation, when, going down along a perpendicular, the computing signal meets a yellow row. The concerned tiles are  $Te\xi$ . And so, we have  $2 \times 138 = 276$  meta-tiles.

We have dealt with the halting of the Turing machine, which involves the computing signs  $Thu\xi$  and  $Thc\xi$ , but we did not yet deal with the case when the computation of the Turing machine is interrupted by meeting the basis of the red triangle where the computation holds. This happens with an open red basis which is accompanied by an upper horizontal blue signal: it is the signal generated by the blue triangle which generates the basis and the meeting happens outside this blue-triangle as a perpendicular never meets the leg of a triangle. The concerned computing tiles are  $Td\xi$  and the patterns are defined by  $Brt + Hb\xi_1$ , as the direction of the horizontal blue signal is independent of the direction of the next move of the Turing head conveyed by the perpendicular. Also note that there are two possible isoclines as the basis is red. Accordingly we have  $2 \times 3 = 6$  patterns, as there are only 3 possible tiles of the mantilla on a perpendicular, and we get  $2 \times 6 = 12$  meta-tiles.

Summing up all these cases, we find out 13,540 meta-tiles.

The counting is summed up in table 9, below.

#### 4.4 The proof

The proof follows the same pattern as Berger's and Robinson's proofs. In the case when the simulated Turing machine does not halt, whatever the size of the computing areas, these region can be tiled.

In the case when the simulated Turing machine halts, we have to consider the possibility of starting the construction from any tile.

As in Berger's and Robinson's case, we can first consider the tiles omitting the computing signs as well as those which eventually concern the in-



terwoven triangles. And so, we first know in which part of the mantilla we are. Moreover, the isocline number tells us also where we are. This means that within a ball of radius at most 20, we find an active seed of the generation 0. We shall find also what is needed to start the generation 0 and the generation 1 on any length. Accordingly, from lemma 23 and the algorithm 4.2.2, the construction of the interwoven triangles is step by step forced. Now, from the properties of the interwoven triangles, as all of them occur at an appropriate latitude at least once, this provides computing areas with a size, as long as desired. Consequently, we shall find an area where the construction will be stucked by the halting of the Turing machine.

It remains to come back to the case of the butterfly model for which we have noted a few particularities after the proof of lemma 23. The case when a red basis occurs on the line 0 of the butterfly model is of interest for us. We noted that this case may happen and that it splits into two sub-case: we have a basis of a phantom or a basis of a triangle.

In the first case, as already noted, we have infinitely many infinite red triangles yielding infinite computations. If the simulated Turing machine halts, the construction of such triangles will be stopped at some point, possibly before other triangles, as they are bigger. If the simulated Turing machine does not halt, then the construction of such triangles go on endlessly and it does not interfere with the finite triangles which they contain. And so, in this case, the tiling can be completed.

In the second case, when the basis is that of a triangle, we have infinitely many phantoms below, which bring in nothing from the point of view of the computation. But, as noted, the presence of the basis, may involve, above, infinitely many infinite yellow rows, running across the hyperbolic plane, from left to right on this row. As these rows do not meet legs of the red triangle associated to this infinite basis, if they contain states, we may think that they are not connected between them. However, we may place verticals, as what is needed is a ray of  $\mathbf{8}$ -centres and so, a computation may takes place with no starting point.

First, note that such a phenomenon happens above the infinite basis. Accordingly, correct computations occur below in the finite triangles and so, if the halting occurs, it will be detected.

Now, if the simulated machine does not halt, as we just need to construct one solution, we may proceed to a few choices. We may rule out the butterfly model: this means that each time we choose the row of the triangles of a new generation, we perform the choice accordingly to the previous ones in order, for instance, to guarantee that each row of the mantilla corresponds to a point which is infinitely many times covered by the active intervals.

But we may also decide to construct the butterfly model only, in the case when the basis is that of a phantom. In this case this single construction provides us with a correct test: if the simulated machine does not halt, this provides us with a construction. If the simulated machine halts, the construction will be stucked and, from what we have seen before, we know that, starting from any tile, we shall find a big enough triangle in which the computation will halt, blocking the tiling.

And so, the main theorem is proved.

As a corollary, we can improve the construction of [9] to the following result:

**Corollary 2** *There is a finite set  $\mathcal{S}$  of tiles such that there is a non-recursive way to tile the hyperbolic plane with copies of  $\mathcal{S}$  but no recursive way.*

## Conclusion

I would like to conclude on two aspects of the construction.

The description of section 4, mainly the algorithm of section 4.2.2 and its preparation are in the style of signal drawn on the mantilla.

We have seen, in section 4.2.3, that this can be replaced by an algorithm in the style of [9] but we had to resign to the principle according to which once a tile is placed, it cannot be removed. We replaced it by a weaker version: it may be changed, but at most finitely many times. Indeed, we noticed that from time to time, later generations introduce something new in already settled domains without basically changing them. Note that this does not contradict the definition of the existence of at least one solution. Also note that the same phenomenon occurs with Robinson's construction in his proof.

I would like to indicate several things.

The first is that this solution is not unique, for sure. Of course we have continuously many realizations of the tiling: twice in some sense as there are continuously many realizations of the mantilla and continuously many models of the abstract brackets. I do not mean that. In fact there are possible variants of some points of the construction. As an example, it is possible that the yellow signal is useless. Perhaps horizontal blue signals not mixed with red ones are enough for our purpose. However, the yellow signal makes things easier and does not bring in too many tiles. Also, it simplifies things for the computation part of the proof. Another point is the use of the scent. Another variant could consist in using the perpendiculars as defined in section 4.3. We could restrict ourselves with the meeting of

the perpendicular issued from the root of the tree with the mid-distance row to define the green signal. In this case, we have to draw perpendicular also from the vertex of a phantom. And then we have to define again a selection principle. The solution of the scent seemed to us a bit simpler. Now, a more important question can be raised: after all, why to restrict the number of active seeds? Why not to decide that all seeds are active? In the present setting of the proof, the advantage of a rather strong restriction of the active seeds is that we better see what happens. In particular, the situation raised by missing trilaterals is more clearly handled. But, in fact, it is perhaps not needed to have strong restrictions. The basic principle of our construction could be stated as: *something exists because the objects of the previous generations which it contains are necessarily present*. And so, the restrictions can be relaxed as long as this principle is remains valid. Perhaps it is possible to remove any restriction.

The basic tiling can also be questioned: why the mantilla and not simply the underlying  $\{7, 3\}$  tiling or, the pentagrid, for instance?

The point is that in the mantilla, we have a way to define the computing verticals which is really very efficient: we know that the verticals which we defined, the **perpendiculars** defined in section 4.3, will never meet the legs of a triangle. Accordingly, dropping a vertical from any tile of the border of a tree  $T$  guarantees that the vertical will never meet a tree which is rooted inside  $T$ . It can be argued that the mantilla is not the single tiling where the isocline property occurs. In a simple Fibonacci carpet, this basic property also occurs. But there, things are not that simple: what to choose in order to construct the triangles and the verticals? We need Fibonacci trees. The way we defined them in the mantilla can of course be adapted here. Now, are we sure that the trees will keep the property that their legs do not intersect, as observed in the mantilla? This is not easy to prove and it cannot be at first glance. It needs further investigations. And now, how to define verticals? The suggested investigations have also to take this aspect in consideration.

It is plain that the huge number of tiles is due to the 20 degrees in the isoclines. But this is needed to fix the generations 0 and 1 because of lemma 5. Five is indeed the smallest distance from the root at which we can find other seeds. And so, to significantly reduce the number, it should be needed to change the basic tiling.

A last but not least point is what does the proof learn to us?

It seems to me that the main lesson of the proof is that the realm of absolute geometry is probably under-estimated. What shows the proof is that a construction which seems to be typically Euclidean is indeed not: it is purely combinatorial and it makes a very little use of the geometry, at

least we do not have to bother about parallels.

And it is interesting to notice that Robinson's question about the importance or not of non-periodic constructions in the case of the hyperbolic plane can be answered positively. In this proof, the tiling is not periodic: no shift can keep the tiling invariant.

## Acknowledgment

It is not usual that a technical report contains an acknowledgement section. Moreover, as the result has not been checked by other people than the author, it is a bit adventurous. However, I do so.

I would like very much to thank both Chaim Goodman-Strauss and Jarkko Kari again for pointing at my error in my previous attempt to prove the theorem. I would also like to thank Leonid Levin for indicating me his paper I quoted about the abstract brackets. I wish also to thank very much three colleagues, André Barbé, Serge Grigorieff and Tero Harju, and again Chaim Goodman-Strauss for their moral support.

## References

- [1] Berger R., The undecidability of the domino problem, *Memoirs of the American Mathematical Society*, **66**, (1966), 1-72.
- [2] Chelghoum K., Margenstern M., Martin B., Pecci I., Cellular automata in the hyperbolic plane: proposal for a new environment, *Lecture Notes in Computer Sciences*, **3305**, (2004), 678-687, proceedings of ACRI'2004, Amsterdam, October, 25-27, 2004.
- [3] Goodman-Strauss, Ch., A strongly aperiodic set of tiles in the hyperbolic plane, *Inventiones Mathematicae*, **159**(1), (2005), 119-132.
- [4] Hanf W., Nonrecursive tilings of the plane. I. *Journal of Symbolic Logic*, **39**, (1974), 283-285.
- [5] L.A. Levin, Aperiodic Tilings: Breaking Translational Symmetry, *The Computer Journal*, **48**(6), (2005), 642-645.
- [6] Margenstern M., Cellular Automata and Combinatoric Tilings in Hyperbolic Spaces, a survey, *Lecture Notes in Computer Sciences*, **2731**, (2003), 48-72.
- [7] Margenstern M., A new way to implement cellular automata on the penta- and heptagrids, *Journal of Cellular Automata* **1**, N°1, (2006), 1-24.

- [8] Margenstern M., About the domino problem in the hyperbolic plane from an algorithmic point of view, *iarXiv:cs.CG/0603093 v1*, (2006), 11p.
- [9] Margenstern M., About the domino problem in the hyperbolic plane from an algorithmic point of view, *Technical report*, 2006-101, *LITA, Université Paul Verlaine – Metz*, (2006), 100p., available at: [http://www.lita.sciences.univ-metz.fr/~margens/hyp\\_dominoes.ps.gz](http://www.lita.sciences.univ-metz.fr/~margens/hyp_dominoes.ps.gz)
- [10] Margulis G.A., Mozes S., Aperiodic tilings of the hyperbolic plane by convex polygons, *Israel Journal of Mathematics*, **107**, (1998), 319-325.
- [11] Myers D., Nonrecursive tilings of the plane. II. *Journal of Symbolic Logic*, **39**, (1974), 286-294.
- [12] Robinson R.M. Undecidability and nonperiodicity for tilings of the plane, *Inventiones Mathematicae*, **12**, (1971), 177-209.
- [13] Robinson R.M. Undecidable tiling problems in the hyperbolic plane. *Inventiones Mathematicae*, **44**, (1978), 259-264.
- [14] Wang H. Proving theorems by pattern recognition, *Bell System Tech. J.* vol. **40** (1961), 1-41.